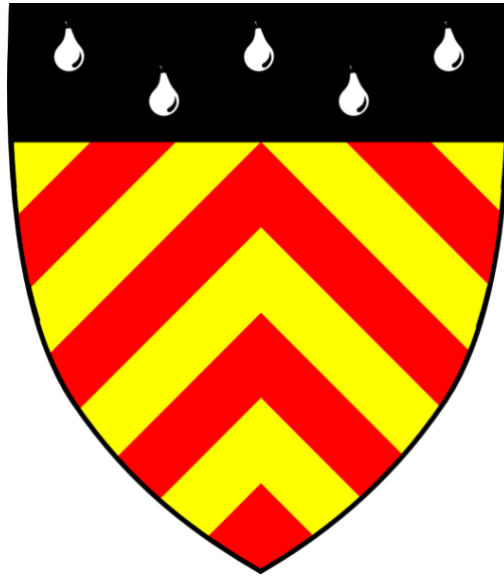


Tau pathology, microglia activation, and network dysfunction in Alzheimer's disease



Luca Passamonti

Clare Hall College

University of Cambridge

This dissertation is submitted for the degree of

Doctor of Philosophy

October 2019

Declaration

This thesis is the result of my own work and includes nothing which is the outcome of work done in collaboration except as declared in the Preface and specified in the text.

It is not substantially the same as any that I have submitted, or, is being concurrently submitted for a degree or diploma or other qualification at the University of Cambridge or any other University or similar institution except as declared in the Preface and specified in the text.

I further state that no substantial part of my thesis has already been submitted, or, is being concurrently submitted for any such degree, diploma or other qualification at the University of Cambridge or any other University or similar institution except as declared in the Preface and specified in the text.

The word count of 40,019 does not exceed the prescribed word limit for the relevant Degree Committee (60,000 words).

Abstract

Dr Luca Passamonti

Tau pathology, microglia activation, and network dysfunction in Alzheimer's disease

Tau pathology and neuroinflammation are key etio-pathogenetic mediators of Alzheimer's disease (AD). Network dysfunction has also been reported in AD and linked to cognitive impairment. However, it is unclear how tau pathology and neuroinflammation contribute to network dysfunction and cognitive deficit in AD.

I study these issues by combining: 1) positron emission tomography imaging using the [^{18}F -AV]-1451 tracer (measuring *in vivo* tau pathology) or [^{11}C]PK11195 ligand (indexing *in vivo* neuroinflammation), with 2) connectivity measures of resting-state functional magnetic resonance imaging.

I found increased [^{18}F -AV]-1451 binding (reflecting tau pathology) in AD patients, relative to controls, in the medial/lateral temporal and parietal cortices. In terms of functional connectivity, more strongly connected brain regions accrued more tau pathology. Increasing tau burden was also linked to progressive weakening of the connectivity across the same regions.

I also found increased [^{11}C]PK11195 binding (reflecting neuroinflammation) in the medial/lateral temporal and parietal cortices in AD patients, relative to controls. [^{11}C]PK11195 binding in the cuneus/precuneus correlated with episodic memory deficits in AD patients. This pattern of neuroinflammation was linked to large-scale network' dysfunction and cognitive deficit. AD patients with enhanced neuroinflammation showed more abnormal connectivity across the whole-brain. The expression of a stronger association between altered functional connectivity and high levels of neuroinflammation related to cognitive deficit in AD.

My studies have wide-ranging implications that include:

- 1) the validation of animal models of tau propagation in living patients with AD;
- 2) improvements in our understanding of the relationship between *in vivo* tau pathology and brain functioning;
- 3) evidence for a primary role of neuroinflammation in mediating network dysfunction in AD;
- 4) support to the notion that immune-therapeutic strategies targeting tau pathology and neuroinflammation may be useful in AD.

Preface

The patient and control data used throughout this thesis have been collected by myself and a team of researchers and clinicians at the Department of Clinical Neurosciences working in the context of the NIMROD study.

Chapter 2 summarises the relevant parts of the protocol of the NIMROD study. The NIMROD study is a collaboration led by Professors James B. Rowe and John O'Brien, with research assistant support from Dr Richard Bevan-Jones, Patricia Vazquez Rodriguez, and Mr Robert Arnold. I undertook part of the clinical investigations and assessments, especially those related to the AD and control group. This chapter has been published at BMJ Open (Bevan-Jones et al., 2017).

Chapter 3 includes tau ('AV') PET data obtained under the NIMROD research study collected by me, Mr Robert Arnold, Patricia Vazquez Rodriguez, and Dr Richard Bevan-Jones. The analysis, interpretation, and writing of this Chapter represent my own work which has been published in Passamonti et al., *Brain*, 2017 in collaboration with Patricia Vazquez Rodriguez (co-first author).

Chapter 4 includes the combination of the AV PET data described in Chapter 3 and the rsfMRI data obtained under the NIMROD research study collected by me, Mr Robert Arnold, Patricia Vazquez Rodriguez, and Dr Richard Bevan-Jones. My contribution to this Chapter (published in Cope et al., *Brain* 2018) includes the conception and design of the study, acquisition of data, and drafting of the manuscript.

Chapter 5 includes neuroinflammatory ('PK') PET data obtained under the NIMROD research study collected by me, Mr Robert Arnold, Patricia Vazquez Rodriguez, and Dr Richard Bevan-Jones. The analysis, interpretation, and writing represent my own work which has been published in Passamonti et

al., *Neurology*, 2018 in collaboration with Patricia Vazquez Rodriguez (co-first author).

Chapter 6 includes the combination of the PK PET data described in Chapter 5 and the rsfMRI data obtained under the NIMROD research study collected by me, Mr Robert Arnold, Patricia Vazquez Rodriguez, and Dr Richard Bevan-Jones. The analysis, interpretation, and writing of this Chapter represent my own work which has been published in Passamonti et al., *J Neurosci.*, 2019 in collaboration with Kamen Tsvetanov (co-first author).

Acknowledgements

I thank my Supervisor Professor James Rowe for giving me the opportunity to undertake this PhD project, and for his support and guidance during my initial and recent years in Cambridge.

Thank you to Professor John O'Brien for introducing me to the NIMROD study and for his valuable advice and help during my first year. Thank you also to Simon Jones for offering his expertise to guide my imaging analyses and to Patricia Vazquez Rodriguez for her appreciated support in helping in collecting the data of my PhD.

I also thank the volunteers who kindly participated in our research. Their willingness to engage in these studies is critical to advancing our understanding of neurodegenerative diseases. I thank the Biomedical Research Unit in Dementia for funding these studies and making my PhD possible.

Finally, thank you to my wife Pina, my sons Ciccio & Paolo, mum Giovanna, and dad Ubaldo for their constant and unconditional support and encouragement throughout my life.

Table of Contents

Declaration.....	3
Abstract.....	5
Preface.....	7
Acknowledgements.....	10
Abbreviations	16
Chapter 1 Introduction.....	19
1.1. Overview	19
1.2. Clinical description of Alzheimer's disease (AD).....	20
1.2.1. History of AD and mild cognitive impairment (MCI).....	20
1.2.2. Diagnostic criteria of AD and MCI.....	21
1.3. Genetics of AD.....	23
1.4. Molecular pathologies in AD.....	24
1.4.1. Tau pathology	24
1.4.2. Amyloid pathology.....	30
1.4.3. Microglia activation and neuroinflammation.....	32
1.5. Interim summary.....	33
1.6. Positron Emission Tomography (PET) in AD	34
1.6.1. PET to assess tau pathology in AD.....	34
1.6.2. PET to assess amyloid pathology	36
1.6.3. PET to assess microglia activation.....	37
1.7. Magnetic resonance imaging (MRI) in AD.....	38
1.7.1. Structural magnetic resonance imaging (MRI) in AD.....	38
1.7.2. Functional magnetic resonance imaging (MRI) in AD	39
1.8. Multi-modal neuroimaging in AD.....	41
1.9. Objectives of my thesis.....	42
Chapter 2 Study Participants & General Methodologies.....	43
2.1. Introduction	43
2.2. General description of the NIMROD study	45
2.3. Ethical Approval & Sponsorship	45
2.4. Locations.....	45
2.5. Recruitment.....	46
2.6. Inclusion & Exclusion criteria.....	47
2.7. NIMROD participants included in my PhD studies.....	47
2.8. Brain imaging visits	48
2.9. Power and Group Size Calculations.....	49
2.10. Neuropsychological and Behavioural Assessment Battery	49
2.11. PET acquisition protocol.....	50
2.11.1. [¹⁸ F]AV1451	51
2.11.2. [¹¹ C]PiB	51
2.11.3. [¹¹ C](R)-PK11195.....	51
2.12. PET data pre-processing	52
2.13. MRI acquisition protocol.....	54
2.14. MRI data pre-processing	56
2.14.1. Structural MRI analytical pipeline	56
2.14.2. Functional MRI analytical pipeline.....	56
Chapter 3 ¹⁸F-AV-1451 PET to assess <i>in vivo</i> tau pathology in Alzheimer's disease	59
3.1. Introduction	59
3.2. Main aims and hypotheses.....	61
3.3. Participants and Methods.....	61
3.3.1. Participants.....	61

3.3.2. PET imaging	62
3.3.2.1. PET pre-processing	62
3.3.2.2. PET statistical analyses	62
3.4. Results	63
3.4.1. Participants	63
3.4.2. [¹⁸ F]AV-1451 binding in Alzheimer's disease	64
3.4.3. [¹⁸ F]AV-1451 binding and AD cognitive deficit	67
3.5. Discussion	68
Chapter 4 Tau burden & network dysfunction in Alzheimer's disease	71
4.1. Introduction	71
4.1.1. Graph analysis to measure network function	72
4.1.2. Graph-measures of connectivity	73
4.2. Main hypotheses	76
4.3. Participants	76
4.4. rsfMRI data acquisition and pre-processing	76
4.5. rsfMRI connectivity analyses	77
4.6. Statistical analyses	78
4.7. Results	79
4.7.1. More Tau pathology in densely connected nodes	79
4.7.2. Reduced cortical connectivity strength in AD	80
4.7.3. Local connectivity reorganization relates to local tau pathology in AD	82
4.8. Discussion	85
Chapter 5 [¹¹C]PK11195 PET to assess microglia activation in Alzheimer's disease	89
5.1. Introduction	89
5.2. Main aim and hypotheses	91
5.3. Participants	91
5.4. PET protocol	93
5.5. PET findings	94
5.6. Discussion	97
Chapter 6 Microglia activation and network dysfunction in Alzheimer's disease	100
6.1. Introduction	100
6.2. Main hypotheses	102
6.3. Participants & Methods	103
6.3.1. Clinical and cognitive assessment	104
6.3.2. rsfMRI pipeline	104
6.3.3. PET acquisition and analysis pipeline	105
6.3.4. Statistical analyses	109
6.4. Results	110
6.4.1. Source-Based 'Inflammetry' (SBI)	110
6.4.2. Functional connectivity	113
6.4.3. Functional connectivity and neuroinflammation	114
6.4.4. Linking neuroinflammation and connectivity to cognitive deficit	114
6.5. Discussion	116
Chapter 7 General Discussion	119
7.1. Summary	119
7.2. Limitations	125
7.2.1. Demographic and clinical limitations	125
7.2.2. Technical limitations	126
7.2.3. Methodological limitations	128
7.2.3.1 PET methodological limitations	128
7.2.3.2 rsfMRI methodological limitations	129
7.3. Final discussion and future directions	130
7.4. Conclusion	135
Reference list	137

List of Figures

Figure 1: Midsagittal view of an Alzheimer's disease (AD) brain	27
Figure 2: Microscopic view of the hippocampus in AD.	27
Figure 3: Microscopic view of the hippocampus (CA1) in AD.....	28
Figure 4: Microscopic view of the parietal cortex in AD (tau pathology).	29
Figure 5: Microscopic view of the parietal cortex in AD (amyloid pathology).	31
Figure 6: Microscopic view (microglia activation) in AD.....	33
Figure 7: Flow chart showing participants' journey through the NIMROD study.	50
Figure 8: [¹⁸ F]AV-1451 findings in AD/MCI+ and controls (voxel-wise data).	65
Figure 9: [¹⁸ F]AV-1451 findings in AD/MCI+ and controls (ROI analyses).	66
Figure 10: [¹⁸ F]AV-1451 findings in AD, MCI+, and controls (ROI analyses).	67
Figure 11: Pictorial representation of graph-analysis connectivity metrics.	75
Figure 12: Relationship between tau pathology and weighted degree.	79
Figure 13: Relationship between tau pathology and local connectomic indices.....	81
Figure 14: The magnitude of disease-related change at each node.....	84
Figure 15: [¹¹ C]PK11195 findings in AD/MCI+ and controls (voxel-wise data).....	94
Figure 16: [¹¹ C]PK11195 findings in AD/MCI+ and controls (ROI analyses).....	95
Figure 17: [¹¹ C]PK11195 findings in AD, MCI+, and controls (ROI analyses).....	96
Figure 18: Pipeline analyses for the combined PET (microglia) and rsfMRI study.....	108
Figure 19: Source-based-'inflammation' (SBI) from [¹¹ C]PK11195 PET imaging.	111
Figure 20: Source-based-'inflammation' (SBI) derived independent components	112
Figure 21: Mean effects of functional connectivity data from rsfMRI.	113
Figure 22: Microglia activation, functional connectivity, and cognition in AD.....	115
Figure 23: Relation between tau burden and neuroinflammation in AD.	133

List of Tables

Table 1: The NIA and AA criteria (2011).	22
Table 2: NIMROD PET radiotracers and study groups.	52
Table 3: Participants' demographic and clinical details (tau PET study).	63
Table 4 Demographic & clinical details in AD, MCI+, and controls (tau PET study).....	64
Table 5: Participants' demographic and clinical details (microglia PET study).....	92
Table 6: Clinical details in AD, MCI+, and controls (microglia PET study).....	92
Table 7: Demographic and clinical data.	103

Abbreviations

AA	Alzheimer's Association
A β	Amyloid Beta
ACE-R	Addenbrooke's Cognitive Examination – Revised
AD	Alzheimer's Disease
ADL	Activities of Daily Living
ADRDA	Alzheimer's Disease and Related Disorders Association
ApoE	Apolipoprotein E
APP	Amyloid Precursor Protein
BOLD	Blood Oxygen Level Dependent
BP _{ND}	Non-displaceable Binding Potential
CANTAB	Cambridge Neuropsychological Test Automated Battery
CBD	Corticobasal Degeneration
CBS	Corticobasal Syndrome
CSF	Cerebro-Spinal Fluid
CUH	Cambridge University Hospitals
DeNDRoN	Dementias and Neurodegenerative Diseases Research Networks
DLB	Dementia with Lewy Bodies
DMN	Default Mode Network
FTD	Frontotemporal Dementia
fMRI	Functional Magnetic Resonance Imaging
GLM	General Linear Model
GWA	Genome Wide Association
HC	Healthy Controls
HSB	High Specific Binding
IWG	International Working Group
JDR	Join Dementia Research
lvPPA	Logopenic Variant Primary Progressive Aphasia
MAO-A	Monoamine Oxidase-A
MAO-B	Monoamine Oxidase-B
MAPT	Microtubule-Associated Protein Tau
MCI	Mild Cognitive Impairment
MCI ₊	Mild Cognitive Impairment with positive β -amyloid
MMSE	Mini Mental Stage Examination

MPRAGE	Magnetization-Prepared Rapid Acquisition Gradient-Echo
MRI	Magnetic Resonance Imaging
MTL	Medial Temporal Lobe
NFTs	Neurofibrillary Tangles
NIA	National Institute on Aging
NHS	National Institute Service
NIA	National Institute on Aging
NIMROD	Neuroimaging of Inflammation in Memory and Other Disorders
NINCDS	National Institute of Neurological and Communicative Disorders and Stroke
PCA	Posterior Cortical Atrophy
PET	Positron Emission Tomography
PHFs	Paired Helical Filaments
PIB	Pittsburgh Compound-B
PSEN1	Presenilin 1
PSEN2	Presenilin 2
PSP	Progressive Supranuclear Palsy
RAVLT	Rey Auditory Verbal Learning Test
ROIs	Regions of Interest
SD	Standard Deviation
SUVR	Standardized Uptake Value Ratio
TREM2	Triggering Receptor Expressed on Myeloid Cells 2
TSPO	Translocator Protein
WBIC	Wolfson Brain Imaging Centre

Chapter 1 | Introduction

1.1. Overview

My thesis examines how *in vivo* tau pathology and neuroinflammation relate to network dysfunction and cognitive deficit in Alzheimer's disease (AD), the most common neurodegenerative form of dementia. AD has a broad clinical phenotypic spectrum that include typical and atypical forms. However, both types of AD share key molecular pathologies including abnormal accumulation of tau aggregates, amyloid pathology, and chronic neuroinflammation.

My work focuses on the typical (i.e., amnesic) form of AD and I investigate the effects of tau pathology and neuroinflammation on network dysfunction and cognitive impairment in this form of AD. I combine positron emission tomography assessing *in vivo* tau pathology and neuroinflammation with resting-state functional imaging. This multi-modal approach offers better insights into the pathophysiology of a common neurodegenerative disorder such as AD.

Together, my studies highlight the need for better methods to evaluate the pathology of AD *in vivo*, and to reveal the critical links between pathological changes, functional alterations, and individual differences in cognitive performance. The combination of different neuroimaging techniques also raises important methodological issues which I examine in my thesis.

In this Chapter, I first set out the background of the clinical, genetic, and molecular aspects of AD. Second, I present the neuroimaging tools that enable the *in vivo* examination of tau pathology, neuroinflammation, and brain function in AD. Finally, I conclude this chapter with a summary of the objectives of my PhD.

1.2. Clinical description of Alzheimer's disease (AD)

1.2.1. History of AD and mild cognitive impairment (MCI)

The Alzheimer's disease (AD) was initially described by Dr Alois Alzheimer, who was the first to report the presence of severe pathological changes in the cerebral cortex of a 50-year-old lady who had died of a relatively rapid mental illness of unknown causes (Hippius & Neundörfer 2003). In his original description, Dr Alzheimer described a woman who suffered from memory deficits, language abnormalities, sleep problems, and mental symptoms that included paranoiac thoughts and bizarre behaviour. Since Dr Alzheimer's original description, and for several decades after, AD was regarded as a rare and young-onset form of dementia while the more common types of late-onset dementia was typically considered as "senile" (or age-related) dementia. It was only in the late 1970s' and early 1980s' that AD and its characteristic pathological changes were commonly recognized as the main cause of late-onset forms of dementia.

Historically, the concept of 'Mild Cognitive Impairment' (MCI) was introduced later than the initial description of AD. The notion of MCI was mainly developed to include the clinically less disabling forms of cognitive deficits that belong to the clinical spectrum of AD (Flicker *et al.* 1991). MCI was defined as a less severe type of cognitive impairment than the one present in AD. For example, MCI relates to problems in single cognitive domains (e.g., episodic memory) rather than on multiple cognitive aspects as in AD. The severity of the cognitive impairment in terms of patient lifestyle and everyday activities is another important aspect that distinguishes MCI from AD.

More recently, the definition of MCI has incorporated the presence of biomarkers of AD pathology. Specifically, biomarker evidence of tau and amyloid pathology in patients with MCI indicates that these MCI patients are more likely to progress and develop AD dementia relative to those MCI patients who are negative for these biomarkers (stable MCI) (Loewenstein *et al.* 2009). Some patients with stable forms of MCI can even revert to

normal cognition especially when the diagnosis of MCI is based on the results of a single, rather than multiple, neuropsychological tests (Loewenstein *et al.* 2009). These findings emphasize the importance of a deep neuropsychological phenotyping in patients with MCI, which should include assessment at least in two cognitive domains (Loewenstein *et al.* 2009). This is particularly relevant for clinical trials targeting AD pathology that aim at recruiting patients at early stages of AD or with MCI and high risk to develop AD (Loewenstein *et al.* 2009)

1.2.2. Diagnostic criteria of AD and MCI

AD is typically defined at the clinical level, although there have been significant changes in the clinical criteria used in the past. The most commonly used clinical criteria for the diagnosis of AD are those developed by the Alzheimer's Disease and Related Disorders Association (ADRDA) (McKhann *et al.* 2011a). These criteria classify AD in: 1) "probable AD", in which frank and severe cognitive impairments that include memory deficits and at least deficits in one other cognitive domain are recognized, or 2) "definite AD" which includes those cases that have received confirmation of AD diagnosis at the pathological level (McKhann *et al.* 2011a).

Previously, the International Working Group (IWG) led by Dubois and collaborators (Dubois *et al.* 2007b) had conceptualized the AD spectrum in three stages that depended on the combination of clinical symptoms and biomarker assessment. Three stages were recognized in the IWG criteria: 1) the clinically asymptomatic but biomarker-positive forms of AD; 2) the MCI and biomarker-positive forms of AD; 3) the frank forms of AD dementia.

The key elements of the IWG criteria are:

- i. It is possible to diagnose AD not only *post mortem* but also *in vivo* via the use of objective and reliable biomarkers.

- ii. The positivity of biomarkers enhances the confidence to detect AD-pathology before pathological confirmation and in early cases of MCI without frank forms of dementia.
- iii. AD pathology can be assessed even in patients with no cognitive or memory problems.
- iv. The integration of fluid biomarkers (e.g., A β , tau quantification in the CSF) and neuroimaging measures from different modalities (e.g., PET, MRI) has a role in anticipating the diagnosis of AD in pre-symptomatic cases and early forms of dementia.

After the IWG, the National Institute on Aging (NIA) and Alzheimer's Association (AA) have developed other criteria to define AD (Jack *et al.* 2011). Similar to the IWG criteria, the NIA/AA criteria include the use of biomarkers to detect early AD-pathology.

The NIA/AA criteria are summarized in **Table 1**.

Stages	Features
Preclinical AD	Before symptoms appear but initial changes are present in the default mode network (Nobili & Morbelli 2010).
MCI	Noticeable symptoms begin, and dementia is anticipated in three to four years (Albert <i>et al.</i> 2011a).
Dementia due to AD	Daily function is impaired (Thies <i>et al.</i> 2013).

Table 1: The NIA and AA criteria (2011).

Abbreviations: AD, Alzheimer's Disease; MCI, Mild Cognitive Impairment.

Although different, the IWG and NIA/AA share many elements in their recognition of the early emergence of AD-related pathological features before the onset of frank dementia. The three stages of AD conceptualized in both criteria acknowledge the pathological and phenotypic continuum that exists in AD.

However, the IWG criteria describe AD as a unique clinico-pathological entity that embraces all the clinical stages of AD while the NIA/AA criteria apply different diagnostic criteria to each of the three phases of AD. This means that the NIA/AA MCI criteria do not explicitly recognize a continuity with the AD clinical spectrum of disorders and do not incorporate the use of biomarkers in the diagnosis of MCI, although the biomarkers are considered supportive to the AD diagnosis due to the highly variable nature of the MCI clinical phenotypes (i.e., stable vs. progressive-MCI) (Jicha *et al.* 2006; Ganguli *et al.* 2011).

1.3. Genetics of AD

Although the majority of cases with AD (>90%) are sporadic and non-inheritable, the studies of the genetic risk factors have provided invaluable information regarding the etiology of AD (Prince & Jackson 2009), (van Duijn *et al.* 1994; Campion *et al.* 1999; Jarmolowicz *et al.* 2015), (Campion *et al.* 1999; Jarmolowicz *et al.* 2015). For example, genome-wide-association studies (GWAS) have revealed the critical importance of the apo-lipoprotein E (ApoE- ϵ 4 haplotype) as a key risk factor for AD (Deelen *et al.* 2011; Sebastiani *et al.* 2012).

More recently, a key etiological role for immune-related molecular pathways and neuroinflammation has been recognized in AD. For example, GWAS have identified genetic variants in the Triggering receptor expressed on myeloid cells 2 (TREM2), an immune-related gene expressed in microglia, as another important genetic risk factors for AD, is similar to the ApoE- ϵ 4 haplotype (Jonsson *et al.* 2013c; Neumann & Daly 2013). In addition, variations in other genotypes including the *SORL1* (sortilin-related

receptor) gene have been linked to risk to develop AD (Rogaeva *et al.* 2007; Guerreiro *et al.* 2013b; Jonsson *et al.* 2013a).

Overall, these studies have led to the identification of the genetic risk profile in AD and represent a scientific breakthrough, although they have not been able to explain the pathophysiological mechanisms that lead to the characteristic clinical symptoms in AD.

None of the patients included in my studies had familial forms of AD or were known to be positive for mutations in MAPT, APP, PSEN1, PSEN2, TREM2 or ApoE- ϵ 4 genes. In other words, the patients described in my thesis were not included neither excluded on the basis of genetic data.

1.4. Molecular pathologies in AD

1.4.1. Tau pathology

The normal Tau protein is typically expressed in neuronal cells and is essential for the correct function of their microtubules, a set of macromolecular elements that form the neuronal cytoskeleton (Weingarten *et al.* 1975). Chemical phosphorylation of the Tau protein is another important determinant of Tau physiological function, although the excessive phosphorylation of the neuronal Tau protein has also been consistently associated with AD-pathology and with the abnormal aggregation and accumulation of different Tau isoforms. Tau aggregation is a pathological 'hallmark' of AD and it is expressed by the presence of intra-neuronal filamentous tangles (Buée *et al.* 2000; Martin *et al.* 2011).

Several lines of research have provided robust evidence that the generation and propagation of 'toxic' Tau proteins represent a fundamental etio-pathogenetic mechanism not only in AD but also in other, non-AD, tauopathies or dementias (Spillantini *et al.* 1998; D'Souza & Schellenberg 2005; Goedert & Jakes 2005; Kaat *et al.* 2009; Martin *et al.* 2011). It is therefore of primary importance and interest to study tau pathology in early

cases of AD, in which pathological spread of tau can be potentially halted or slowed.

The microtubule-associated-protein (MAPT) gene, which is located on the chromosome 17q21 (Neve *et al.* 1986), codes for the human Tau protein. The MAPT gene can be transcribed into six different isoforms, from alternative splicing that include or not the gene exons 2, 3, and 10 (Avila *et al.* 2004; Andreadis 2005). The tau isoforms that contain the exon 10 result in a Tau protein that include four microtubule-binding repeats (tau 4R isoforms). In contrast, the tau isoforms that do not include the exon 10 result in Tau protein that contains three microtubule-binding repeats (tau 3R isoforms). The abnormal tau deposits in AD (i.e., in the neurofibrillary tangles) are typically formed by both the four (4R) and three (3R) Tau isoforms and by paired helical filaments of a diameter between 10-20 nm (Sisodia *et al.* 1990; Liu *et al.* 2001).

Another important aspect of tau pathology in AD regards the mechanisms by which the abnormal Tau proteins diffuse to various brain regions as the disease progresses. Animal research has provided converging evidence that local tau pathology can have 'infectious' properties especially in terms of its diffusion and spread of the disease from one area of the brain to another one. However, it has remained unclear whether the same mechanisms that regulate this pathological Tau 'spread' can be detected in humans. In Chapter 4, we combine network analyses, as assessed via resting-state functional imaging, with *in vivo* molecular imaging of tau pathology to study this critical pathophysiological mechanism in AD in humans.

From a pathological point of view, it is also clear that the progression of tau pathology in AD typically follows a consistent pattern of diffusion which has been used to define six 'Braak' stages of AD pathology (Braak & Braak 1991a). At stage I and II, Tau pathology is mainly detected in the trans-entorhinal and entorhinal cortex. At stage III and IV, different parts of the hippocampus (e.g., Cornu of Ammones 1, CA1) become affected by Tau

pathology (**Figure 1, Figure 2, Figure 3**). Finally, at stage V and VI, abundant and diffuse Tau pathology is observed in cortical areas including the temporal, parietal, and other posterior cortical regions (**Figure 4**). Each pathological 'Braak' stage of AD-related Tau pathology corresponds to a specific clinical stage. Patients in pathological stages V and VI typically meet the clinical criteria for AD diagnosis and are severely demented at the time of death. The cognitive impairment in patients with lower pathological Braak stages can range from asymptomatic to MCI (Braak & Braak 1991b; Price *et al.* 1991).

Abnormal Tau accumulation and diffusion have also been considered in the context of the other pathological hallmark of AD, i.e., the accumulation of amyloid- β , and to a newly recognized but critical etio-pathogenetic mediator of AD (i.e., neuroinflammation), which I will discuss in the next sections (Desikan *et al.* 2012; Jack & Holtzman 2013). Nevertheless, past pre-clinical research has clearly demonstrated that tau pathology *in itself* has deleterious effects on cell survival and synaptic function (Gómez-Isla *et al.* 1997; Beharry *et al.* 2014; Spires-Jones & Hyman 2014), and that Tau pathology, rather than amyloid- β pathology, is more strongly linked to cognitive impairments in AD and with the different phenotypes of the AD clinical spectrum (Arriagada *et al.* 1992a; Nelson *et al.* 2012; Rolstad *et al.* 2013).

For example, the extent and distribution of tau pathology *in vivo* correlates with distinct clinical variants of AD, including, for example, the posterior cortical atrophy (PCA) and logopenic variant of primary progressive aphasia (lvPPA). In these AD-related clinical syndromes, tau molecular imaging with the PET [^{18}F]AV1451 radioligand has been found to be associated to higher levels of hypometabolism and cognitive deficits than amyloid- β deposition, as assessed via the PiB PET tracer (Ossenkoppele *et al.* 2015a).



Figure 1: Midsagittal view of an Alzheimer's disease (AD) brain

The medial aspect of the left hemisphere shows moderate to severe atrophy of the neocortex and of the medial temporal lobe including the hippocampus. The weight of this brain was 1,180g (normal brain weight range: 1,300-1,400). Image kindly provided by Dr Kieren Allinson from the Cambridge Brain Bank.

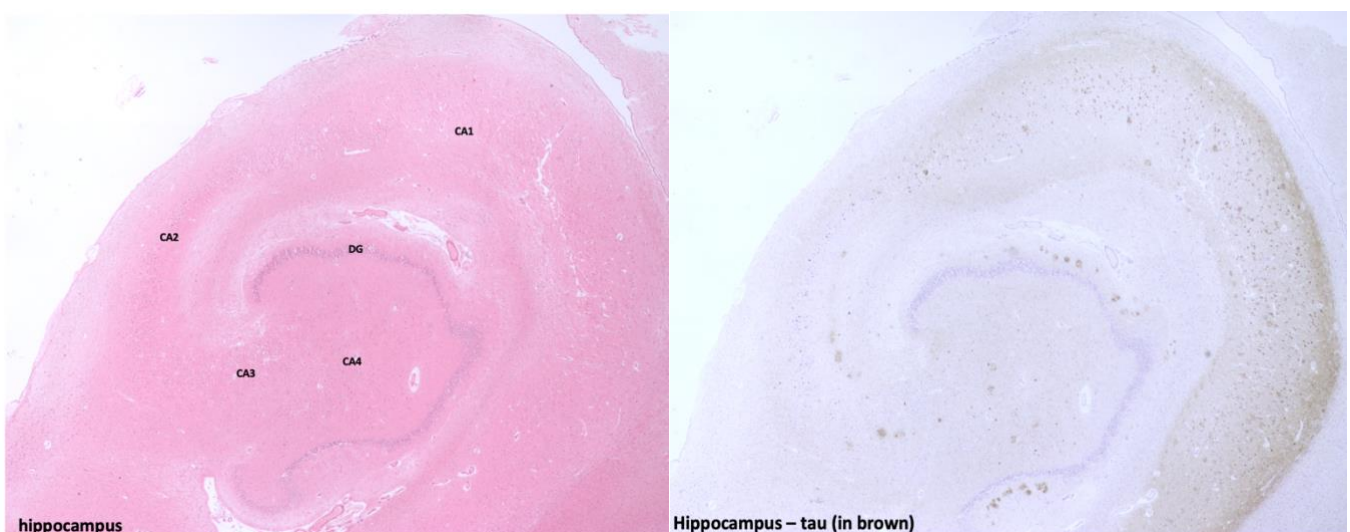
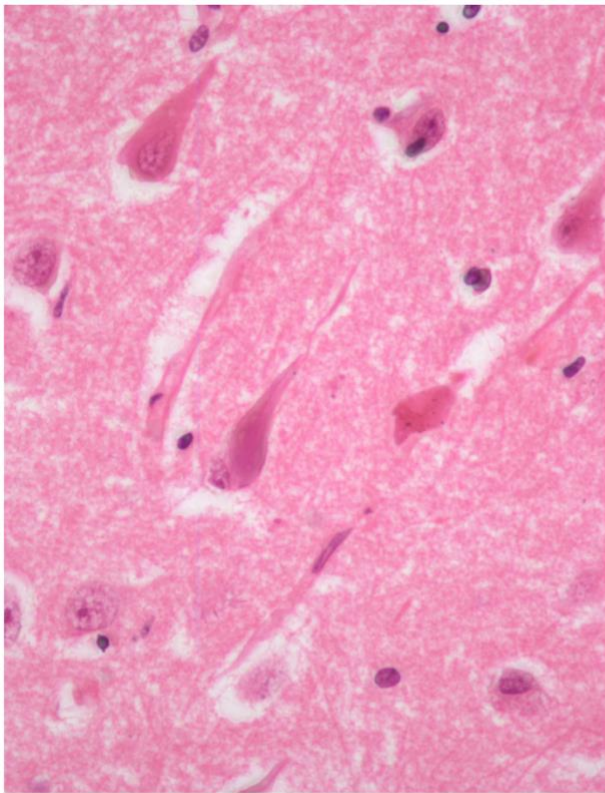


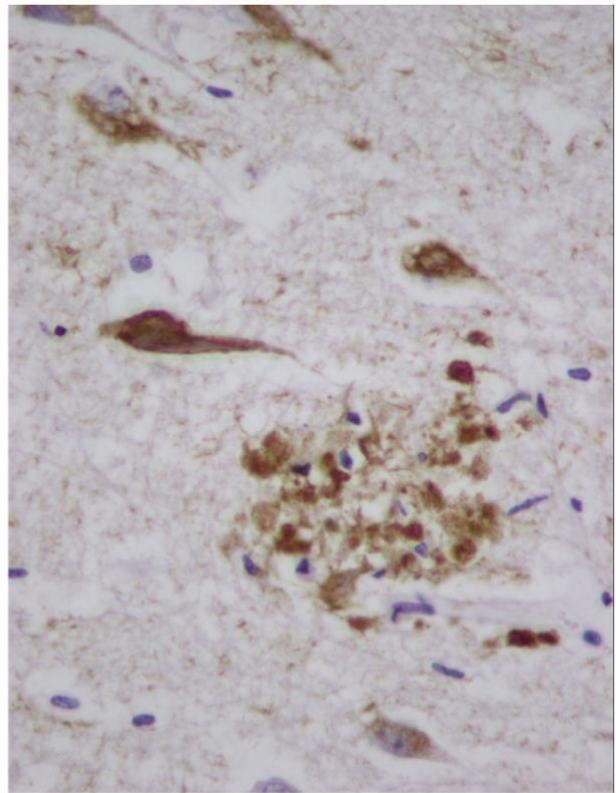
Figure 2: Microscopic view of the hippocampus in AD.

Left. Staining for different hippocampal sub-fields. CA; Cornus of Ammones, DG, Dentate Gyrus. **Right** Staining for tau pathology (in brown). Tau pathology is evident in different

hippocampal sub-fields especially CA1. Image kindly provided by Dr Kieren Allinson from the Cambridge Brain Bank.



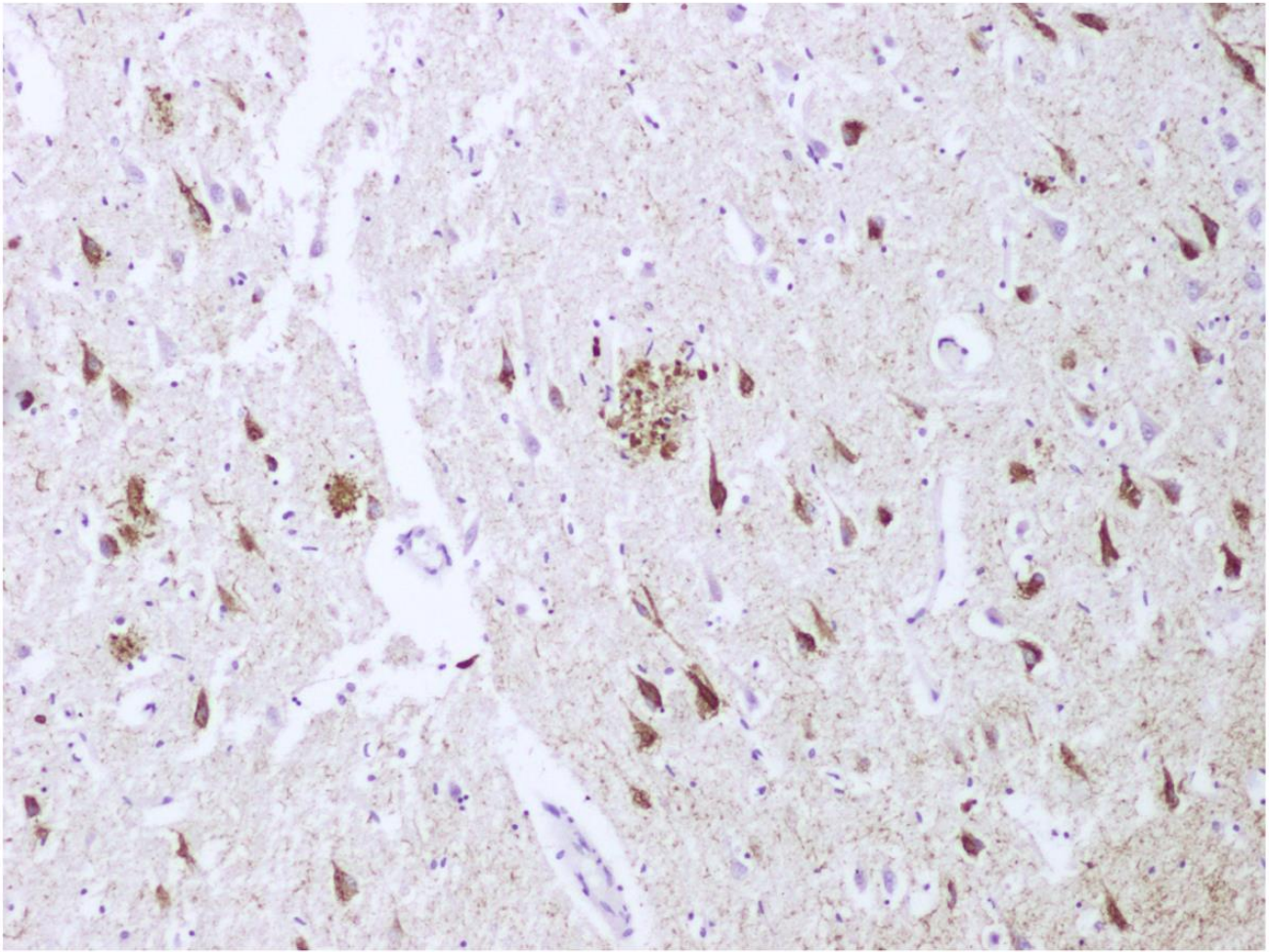
Hippocampus CA1



tau staining (brown)

Figure 3: Microscopic view of the hippocampus (CA1) in AD.

Left. Staining for hippocampal neurons in the CA1 sub-field. **Right,** Staining for tau pathology (in brown). Image kindly provided by Dr Kieren Allinson from the Cambridge Brain Bank.



Parietal cortex - tau

Figure 4: Microscopic view of the parietal cortex in AD (tau pathology).

Staining for tau pathology (in brown). Image kindly provided by Dr Kieren Allinson from the Cambridge Brain Bank.

1.4.2. Amyloid pathology

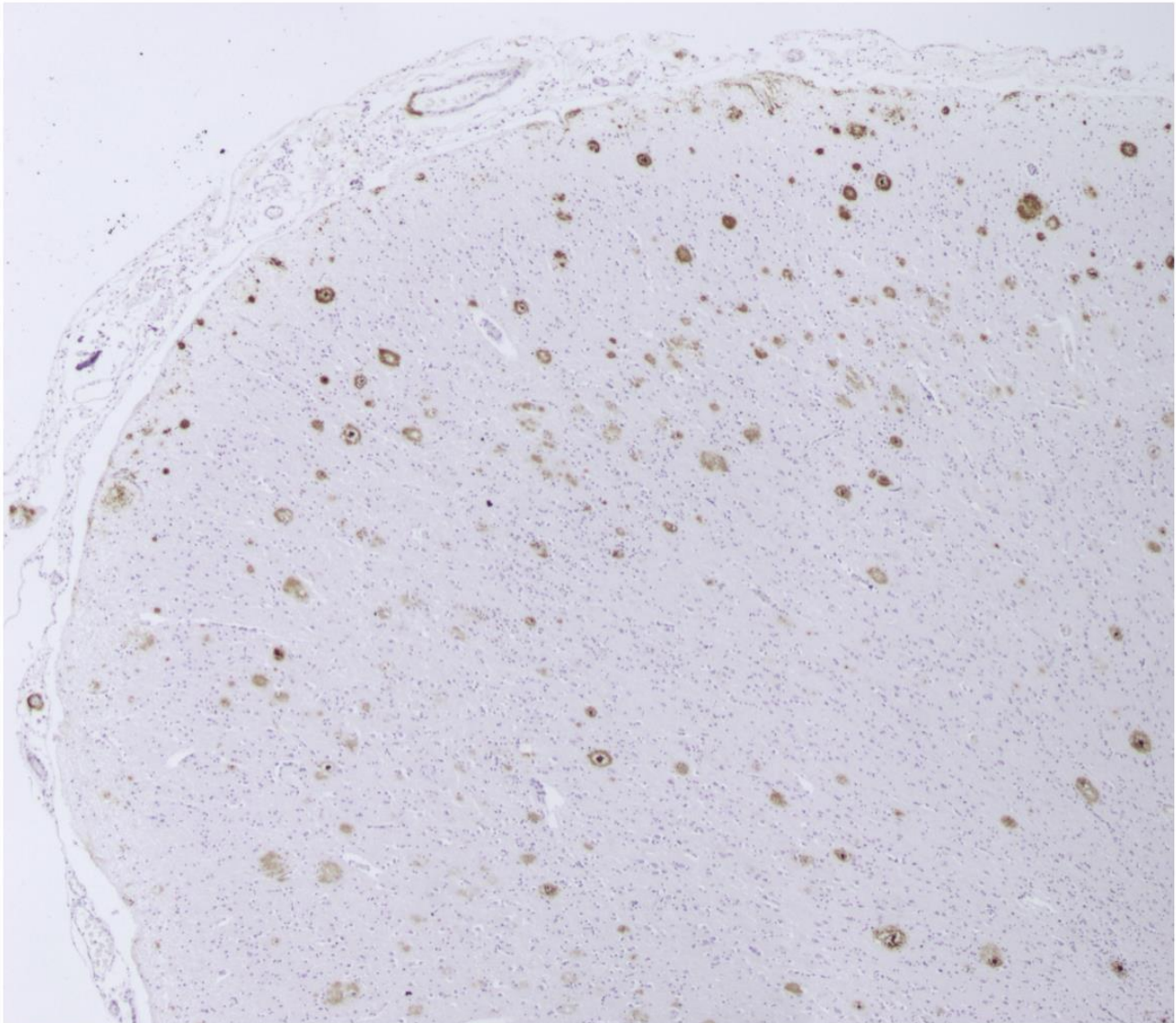
The role of pathological accumulation of β -amyloid in AD patients is a well-established etio-pathogenetic aspect of AD (**Figure 5**). This is known as the “amyloid cascade hypothesis”. This hypothesis has implicated the formation of β -amyloid fibrils ($A\beta$) as the main event that determines the tau hyperphosphorylation and the consequent development of neurofibrillary tangles (NFT), cell dysfunction, neuronal loss, and ultimately dementia (Beyreuther & Masters 1991; Hardy & Allsop 1991). However, this hypothesis remains controversial especially after the recent lack of success of some disease-modifying clinical trials selectively targeting amyloid pathology in AD.

Other studies have also consistently reported that it is the tau pathology, and not the amyloid burden *in itself*, that correlates with cognitive impairment, disease severity, and clinical phenotypic spectrum in AD (Arriagada *et al.* 1992b; Buchhave *et al.* 2012). Nevertheless, the biomarkers assessing amyloid pathology *in vivo* remain a fundamental diagnostic tool to discriminate the MCI patients who are likely to develop AD pathology over 2-5 years from those who do not develop AD (Reisberg *et al.* 1982; Flicker *et al.* 1993; Gauthier *et al.* 2006; Wisse *et al.* 2015).

My thesis does not examine the β -amyloid hypothesis in AD. However, I employ an amyloid imaging biomarker (PiB PET) to identify a group of patients in which their MCI is driven by AD-related amyloid pathology. I also include patients with clinically probable AD as defined by the ADRDA criteria. The use of amyloid biomarkers in this group of clinically probable AD was not thought to be necessary, especially considering: 1) the high sensitivity (up to 87%) of the ADRDA criteria in predicting *post mortem* AD pathology in clinically probable cases; 2) the high costs of PET scanning.

To summarize, only the MCI patients who were amyloid positive (MCI+) were included in my analyses. To assess amyloid pathology *in vivo*, we employed PiB PET imaging as this ligand has the longest history as a amyloid biomarker for clinical use (Mathis *et al.* 2002). Nevertheless, I

acknowledge that other, and potentially more accessible (as they include [^{18}F] rather than [^{11}C]), compounds are nowadays available (e.g., flutemetamol, florbetaben, florbetapir) (Villemagne *et al.* 2011; Thurfjell *et al.* 2012; Ong *et al.* 2013; Martinez *et al.* 2017).



Parietal cortex – amyloid (in brown)

Figure 5: Microscopic view of the parietal cortex in AD (amyloid pathology).

Staining for amyloid pathology (in brown). Image kindly provided by Dr Kieren Allinson from the Cambridge Brain Bank.

1.4.3. Microglia activation and neuroinflammation

Microglia activation and neuroinflammation are another key molecular contributor to the etio-pathogenesis of AD. Animal and human studies have provided robust evidence that microglia, the brain's principal innate immune system, show increased activation in AD and other neurodegenerative disorders (Fernandez-Botran *et al.* 2011a; Edison *et al.* 2013a; Schuitemaker *et al.* 2013a; Fan *et al.* 2015a; Stefaniak & O'Brien 2016a) (**Figure 6**). For instance, there is evidence that the microglia-mediated release of cytokines such as interleukin-1 β and TNF- β can accelerate neurodegeneration and synaptic loss in AD (Fernandez-Botran *et al.* 2011a). On the other hand, activated microglia has also been shown to promote phagocytosis and clearance of amyloid plaques (Wisniewski *et al.* 1991; Frackowiak *et al.* 1992).

In addition, genome wide associations studies (GWAS) in different neurodegenerative disorders including AD have revealed that variations in genes that contribute to immune signalling are important risk factors in AD (Villegas-Llerena *et al.* 2016). There is also epidemiological evidence showing that patients using non-steroidal anti-inflammatory drugs have a reduced risk to develop dementia and AD (Breitner & Zandi 2001; in t' Veld *et al.* 2001).

This raises the possibility of using immuno-therapeutic strategies for preventing the development of AD or even as disease modifying treatments. However, key issues need to be addressed before such strategies can be employed, including the confirmation of clinico-pathological correlations of neuroinflammation and the establishment of the potential utility of biomarkers for measuring neuroinflammation *in vivo*. Despite the importance of neuroinflammation, there is still insufficient information regarding the extent and regional distribution of microglial activation in AD, and its association with clinical markers of disease severity. I tackle these issues in my thesis and I also study the role of neuroinflammation and

microglia activation in mediating network dysfunction and variability in cognitive deficit in AD.

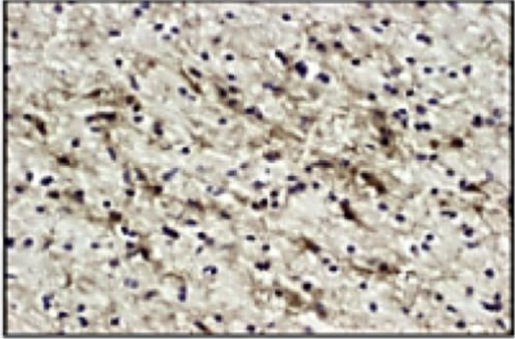
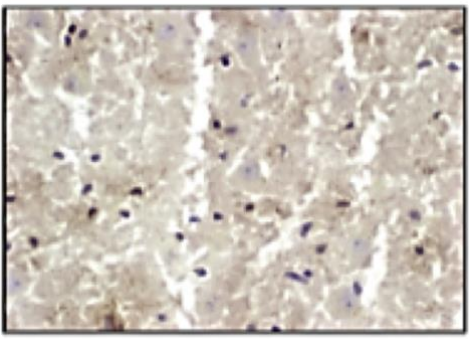
	Alzheimer’s disease (AD)	Healthy control
Hippocampus		

Figure 6: Microscopic view (microglia activation) in AD.

This figure aligns the HLA-DR staining (in brown, reflecting activated microglia) in one key region of interest (i.e., hippocampus) in an Alzheimer’s disease (AD) case (left), and a control of similar age (right). Activated microglia was mainly identified in the hippocampus of the AD case. In contrast, the control case did not show activated microglia staining in the same region. Image kindly provided by Dr Kieren Allinson from the Cambridge Brain Bank.

1.5. Interim summary

The characterization of AD at the clinical, genetic, and pathological level is still evolving, in part due to rapid developments in the biomarker research field. The recent introduction of the concept of asymptomatic AD with biomarker evidence emphasizes the need to develop better models that describe, in neurobiologically realistic terms, the complexity of AD pathophysiology. In other words, it is necessary to characterize with quantitative and objective measures how the molecular pathologies of AD lead to brain dysfunction and cognitive impairment.

This is the first critical step before developing biomarkers that can de-risk and empower future clinical trials in AD via improved outcome measures and mechanistically-informed stratification procedures.

1.6. Positron Emission Tomography (PET) in AD

Positron emission tomography (PET) is a diagnostic imaging modality that uses isotope-labelled molecular ligands to probe specific biomolecules of interest with both high specificity and affinity. When I started my thesis, there were only a few studies on tau pathology and neuroinflammation using PET imaging biomarkers *in vivo* in AD but nowadays the number of PET studies using tau imaging and neuroinflammation has greatly expanded.

In Chapter 3 and 5, I discuss in more detail the most recent PET studies assessing tau pathology and microglia activation. Nevertheless, to fulfil the potential of these PET ligands as biomarkers, we still need to answer several important questions, including: 1) the ability of these ligands to localize and quantify the underlying pathological process, with high specificity and sensitivity, 2) the ability of these tracers to relate to clinical features including severity of cognitive impairment, directly or via the mediation of network function, and 3) the ability of these PET markers to track disease progression longitudinally.

My thesis focuses on questions 1) and 2) and present data from PET tracers assessing *in vivo* tau pathology and neuroinflammation. In the following sections, I briefly introduce part of the literature on PET biomarkers assessing tau and amyloid pathology as well as neuroinflammation in AD.

1.6.1. PET to assess tau pathology in AD

[¹⁸F]AV1451 (formerly called [¹⁸F]T807) was one of the first PET radioligand introduced to study the tau pathology in AD and MCI *in vivo*. Chien et al. were the first to show that *in vivo* cortical [¹⁸F]AV1451 binding recapitulates the well-known distribution of tau pathology in AD, in which higher [¹⁸F]AV1451 uptake was related to increasing disease severity (Chien *et al.* 2014). More recently, Schöll's et al. have reported that patients with early-onset AD already display increased [¹⁸F]-AV-1451 uptake in several cortical regions, while enhanced [¹⁸F]-AV-1451 binding in medial

temporal lobe regions is only seen in late-onset AD (Schöll *et al.* 2017). Since these reports, there have been several other studies which have consistently reported increased [^{18}F]AV-1451 binding in MCI amyloid positive patients and in people with clinically probable AD including our studies reported in Chapter 3 and 4.

When the data collection for my thesis started, the [^{18}F]AV1451 PET tracer was one of the few available compounds. I will discuss this ligand in detail in Chapter 3 and 4. Since then, other tracer targeting tau pathology in AD have been developed, including [^{18}F]THK523, [^{18}F]THK5105, [^{18}F]THK5117, and [^{11}C]PBB3 which I briefly review here.

Studies of [^{18}F]THK523 in animal models indicated that this tracer selectively binds to tau pathology in AD brains. In addition, autoradiographic and histo-fluorescent data of THK523 hippocampal sections from human brain tissue have shown high affinity and selectivity of this ligand for tau pathology (Fodero-Tavoletti *et al.* 2011). However, the preclinical data also reported that the pharmacokinetics and binding characteristics of [^{18}F]THK523 do not meet the threshold required for PET tracers with high sensitivity and specificity.

More specifically, it was concluded that the [^{18}F]THK523 uptake in AD patients was too similar to that observed in healthy controls (V.L. *et al.* 2012). Successively, there have been further optimization of the [^{18}F]THK523, [^{18}F]THK5105, and [^{18}F]THK5117 tracers (Okamura *et al.* 2013a), but in all of these additional developments of the [^{18}F]THK tracers 'off-target' binding was noted especially to the monoamine oxidase-B enzyme (Hirvonen *et al.* 2009; Gulyás *et al.* 2011; Ng *et al.* 2017).

[^{11}C]PBB3 reversibly binds to neurofibrillary AD-related tau tangles with high affinity and selectivity (Maruyama *et al.* 2013b; Hashimoto *et al.* 2014). Moreover, accumulation of [^{11}C]PBB3 has been seen in the medial and lateral temporal cortices, and the frontal cortex—consistent with the

Braak staging of AD (Maruyama *et al.* 2013b). [^{11}C]PBB3 has also been recently tested in non-AD tauopathies including progressive supranuclear palsy (PSP) and corticobasal degeneration (CBD) (Sahara *et al.* 2017). In these tauopathies, a degree of specificity of this tracer was reported, at least when the [^{11}C]PBB3 binding in PSP and CBD was compared to that of healthy controls (Shimada *et al.* 2016). However, additional studies need to assess the specificity of this tracer in the differential diagnosis between AD and non-AD tauopathies.

1.6.2. PET to assess amyloid pathology

The ^{11}C PiB PET tracer has revolutionized the *in vivo* molecular imaging of AD and has allowed to track for the first time a critical pathological aspect of AD (i.e., abnormal amyloid deposition)(Klunk *et al.* 2004; Jack *et al.* 2008). As expected from *post mortem* research, patients with MCI and PiB evidence of amyloid pathology are more likely to convert to AD rather than PiB negative MCI patients (Forsberg *et al.* 2008)(Engler *et al.* 2006). The ability of the ^{11}C PiB PET tracer to identify AD pathology is elevated and reach around 96% of accuracy (Johnson *et al.* 2012).

Longitudinal studies using ^{11}C PiB PET have also revealed that people at high risk of developing AD due to genetic mutations show increased amyloid burden when assessed with ^{11}C PiB PET(Reiman *et al.* 2009)(Reiman *et al.* 2009). However, the ^{11}C PiB PET shows limited ability to characterize the phenotypic complexity of AD (O'Sullivan & Vann 2016). In other words, there is poor correlation between the ^{11}C PiB PET signal and the clinical spectrum of AD, in terms of localization of the phenotypic syndromes and in terms of regional deficits in glucose metabolism (O'Sullivan & Vann 2016). The amyloid burden that is quantified by the ^{11}C PiB PET tracer can be found in several brain regions, even those which might not have immediate relevance at the symptomatic level (O'Sullivan & Vann 2016). Consistently, the correlation between the amyloid burden detected via ^{11}C PiB PET tracer and glucose hypo-metabolism, brain atrophy, and disease progression is limited (O'Sullivan & Vann 2016).

1.6.3. PET to assess microglia activation

In vivo microglia activation in the brain can be assessed using PET imaging in conjunction with radio-ligands like [^{11}C]PK11195. The [^{11}C]PK11195 tracer binds to the mitochondrial translocator protein (TSPO) that is present in the activated microglia. Compounds such as [^{11}C]PK11195 are widely used biomarkers of microglia activation, although it is important to bear in mind that microglial activation represents only a part of the complex cascade of events that lead to neuroinflammation in AD and other disorders.

Amongst the first-generation TSPO tracer, [^{11}C]PK11195 has been also widely used to study microglial activation in several other neurologic disorders in which neuroinflammation play a central role. These include for example acute neurological conditions such as stroke (Price *et al.* 2006), multiple sclerosis (Banati *et al.* 2000), and other chronic neurodegenerative disorders like Parkinson's disease (Gerhard *et al.* 2006a), corticobasal degeneration (Gerhard *et al.* 2004), and Huntington's disease (Pavese *et al.* 2006). There is also a study in healthy elderly people showing that [^{11}C]PK11195 PET can demonstrate increased TSPO density in 'normal' brain aging (Kumar *et al.* 2012).

In AD, microglial activation detected through [^{11}C]PK11195 binding has been reported in the entorhinal, temporo-parietal, and other cortical regions that are typically affected by AD-related neurodegeneration in early stages. This suggests that neuroinflammation could be considered as an early factor in the pathogenesis of AD rather than merely reflecting a consequence of brain atrophy (Cagnin *et al.* 2001a; Okello *et al.* 2009a). In addition, *post mortem* studies have consistently shown increased microglia activation and cytokine release in the frontal cortex, parietal and occipital cortices in patients with AD pathology (Fernández-Botrán *et al.* 2011). Enhanced [^{11}C]PK11195 binding in several cortical and subcortical regions has also been found in patients with MCI (Cagnin *et al.* 2006).

1.7. Magnetic resonance imaging (MRI) in AD

Magnetic resonance imaging (MRI) is another standard imaging technique in both research and clinical assessment of patients with AD. For the purposes of my thesis, I describe the two main MRI modalities that enables: (a) the visualization of the disease-specific patterns of neurodegeneration and atrophy in AD (structural MRI, section 1.7.1), and (b) the study of the function of single brain regions and large-scale networks (functional MRI, section 1.7.2.). Together, as well as in conjunction with the PET imaging modalities described in section 1.6, these MRI indices offer important information that not only facilitates clinical diagnosis of AD, but also provide critical insights into its underlying pathophysiology (Iwata 2005; Berg *et al.* 2011).

1.7.1. Structural magnetic resonance imaging (MRI) in AD

This is one of the most commonly employed MRI modalities to assess the early and late neuroanatomical changes associated with MCI and AD and for predicting, via the use of sophisticated machine-learning algorithms, the disease course over time. In my thesis, structural MRI is only used in the context of PET and functional imaging analyses, although structural MRI data on the same AD patients described here have also been published separately (Mak *et al.* 2018). More specifically, in Mak *et al.* 2018, we have reported that cortical thinning in temporal cortices was related to tau pathology as assessed via the PET biomarker described in section 1.6.

Other studies have also found that structural MRI markers including hippocampal atrophy and enlarged ventricles differentiate patients with AD from MCI patients and from age-matched healthy controls (Nestor *et al.* 2008; Chou *et al.* 2009; Risacher *et al.* 2009, 2010) . Structural MRI can also be employed to predict the conversion from MCI to probable AD in 1 year (Calvini *et al.* 2009; Misra *et al.* 2009) or 3 years (Spasov *et al.* 2019).

In summary, several studies using structural MRI have converged to show that the rate of annual change in the whole-brain volume, hippocampal

atrophy, and ventricular enlargement are reliable predictors of AD pathology and its clinical progression (McEvoy *et al.* 2009; Morra *et al.* 2009; Evans *et al.* 2010; Ho *et al.* 2010).

1.7.2. Functional magnetic resonance imaging (MRI) in AD

Although the effect of neurodegeneration on the patterns of brain atrophy detected with structural MRI have provided important and useful information for the diagnosis and prognosis of AD, the effects of neurodegeneration on network connectivity remain elusive.

A better understanding of brain dysfunction in AD can have a more direct role in predicting response to both symptomatic and disease-modifying pharmacological therapies, as it is likely that the brain function is closer to the symptomatic level than the brain structure (Seeley *et al.* 2009; Pievani *et al.* 2011; Warren *et al.* 2012).

Recently, most of the functional imaging studies that have investigated the network function in AD have employed task-free or 'resting state' paradigms. This is because rsfMRI has several advantages in clinical settings, relative to classic task-based fMRI. These advantages include:

- 1) the minimization of cognitive training demands, which is critical in patients with AD;
- 2) the lack of confounding effects linked to practice effects across different fMRI sessions;
- 3) the possibility to examine 'all at once' (i.e., within the context of a single experimental session), several, although distinct, brain networks that would have otherwise required the use of many task-based fMRI sessions,
- 4) the possibility to derive, from rsfMRI data, reliable measures of brain connectivity that can be used in network approaches.

All in all, I exploited these methodological advantages of rsfMRI to develop more realistic models of the brain functioning in AD, in relation to key pathological aspects such as tau pathology and neuroinflammation.

Regarding the biological nature of the rsfMRI signal, this is thought to derive from the electro-physiological coherence among spontaneous neuronal oscillators, which may reflect the functional anatomy of distinct brain networks (Corbetta 2012). Critically, most of these 'resting-state' circuits also respond and create dynamic patterns of connectivity in response to specific task demands or during strictly manipulated experimental conditions.

This supports the validity and reliability of using rsfMRI measures for studying cognition in healthy people and in patients with neurological disorders including AD (Kitzbichler *et al.* 2011). There is indeed consistent evidence that rsfMRI connectivity patterns are significantly altered in AD (Badhwar *et al.* 2017), although only few studies (including ours) have assessed how these abnormal patterns of network function relate to different molecular pathologies in AD (Cope *et al.* 2018; Yokoi *et al.* 2018; Passamonti *et al.* 2019).

This concept of multi-modal imaging is now introduced in the next section 1.8.

1.8. Multi-modal neuroimaging in AD

A central aspect of the work described in my thesis regards the integration of different neuroimaging modalities. This raises a series of conceptual and methodological issues which I tackle in detail in Chapter 4 and 6. Briefly, one of the most important methodological issue is the necessity to integrate a large volume of different sources of information that are provided by distinct neuroimaging modalities. Hence, there is a need to reduce the complexity of the dataset and the necessity to minimize the number of statistical comparisons, especially when small sized populations are employed.

More broadly, it is also important to acknowledge that different definitions of multi-modal neuroimaging exist (Uludağ & Roebroek 2014). In this thesis, I use the term multi-modal neuroimaging to describe determinate analytical procedures that I have used to combine two or more neuroimaging datasets that have been acquired with different imaging modalities (i.e., fMRI and PET) in the same groups of participants.

This neuroimaging data integration has the main advantage of improving our knowledge of the (dys)function of large-scale brain networks in AD by exploiting the physical (i.e., MRI-sensitive) and physiological (i.e., related to AD biology) sensitivities provided by each neuroimaging modality in isolation.

This definition of multi-modal imaging is thus different from other definitions that for example refer to the fusion of imaging data obtained with the same physical instrument (e.g. combining perfusion- and diffusion-weighted MRI in stroke imaging) (Uludağ & Roebroek 2014).

1.9. Objectives of my thesis

The main aim of my PhD was to improve our knowledge of how tau pathology and neuroinflammation mediate brain dysfunction and cognitive deficit in AD. To achieve this end, I structured my work in five distinct, although related, objectives.

The first objective was to successfully recruit and clinically define the populations of patients with AD and MCI with biomarker positive evidence of amyloid pathology (MCI+) (Chapter 2).

Second, I wanted to successfully exploit the [^{18}F]AV1451 PET tracer to examine the extent and localization of *in vivo* tau pathology in AD/MCI+ patients and to assess the utility of this ligand as biomarker of tau pathology in AD (Chapter 3).

Third, I aimed at evaluating the impact of *in vivo* tau pathology on brain functional connectivity, using multi-modal integration of [^{18}F]AV1451 PET and rsfMRI data (Chapter 4).

My fourth objective was to examine the extent and localization of *in vivo* neuroinflammation in AD/MCI+ patients using the [^{11}C]PK11195 ligand (Chapter 5).

Fifth, I aimed at linking this PET marker of neuroinflammation to measures of large-scale connectivity and aggregated indices of cognitive deficit (Chapter 6).

Chapter 2 | Study Participants & General Methodologies

2.1. Introduction

My thesis is based on the dataset collected within the context of the Neuroimaging of Inflammation in Memory and Related Other Disorders (NIMROD) study. The NIMROD study is a deep phenotyping cohort study, the aims of which include:

- 1) the extent and patterns of *in vivo* tau deposition, as revealed by [¹⁸F]AV-1451 PET ligand, in AD and other neurodegenerative disorders relatively to age- and sex-matched controls;
- 2) the extent and patterns of *in vivo* neuroinflammation (as indexed via the [¹¹C]PK11195 PET radiotracer) in patients with AD and other neurodegenerative disorders, relatively to age-and sex-matched control participants;
- 3) how *in vivo* tau pathology and neuroinflammation in AD and other neurodegenerative disorders is linked to relevant clinical symptoms in each disorder (e.g., episodic memory deficits in AD);
- 4) the relationship between *in vivo* tau accumulation and microglia activation,
- 5) the peripheral markers of neuroinflammation (e.g., serum cytokines, T-cell subsets) in patients with AD and other neurodegenerative disorders;
- 6) the grey-matter and white-matter structural damage in AD and other neurodegenerative disorders in relation to *in vivo* tau accumulation and microglia activation;

7) the alterations in resting-state functional connectivity in AD and other neurodegenerative disorders in relation to *in vivo* tau pathology and neuroinflammation;

8) the relationship between *in vivo* tau pathology and neuroinflammation in predicting longitudinal changes in cognitive decline.

9) the relationship between *in vivo* tau pathology, neuroinflammation, and peripheral markers of inflammation

My PhD focuses on aims 1),2),3), and 7), although in Chapter 7 (Future directions section), I briefly present some preliminary data, by Su Li (one of my NIMROD colleague) regarding aim 8).

Achieving these aims has direct implications for treatment studies (both disease-modifying and symptomatic), healthcare planning and policy, and design of future researches in AD and in other neurodegenerative disorders. The NIMROD study comprises an extensive set of demographic, clinical, behavioural, PET, Magnetic Resonance Imaging (MRI) (both structural and functional), and serum data that can provide a long-term resource for studies evaluating the impact of *in vivo* tau deposition and neuroinflammation in AD and other disorders. Improved knowledge of disease etio-pathological mechanisms and their relationship with clinical markers may also provide a mean to validate preclinical models and inform future clinical studies.

The NIMROD study gained clinical and behavioural data from various sources of information including the carer, patient, and clinician ratings as well as via the use of objective (i.e., computerized) psychological tasks and brain imaging measures. Patient and carer questionnaires are typically employed in clinical assessments and trials, enabling evaluation of potential inconsistencies between carer and patient rating. Objective neuropsychological tests and brain imaging methods were used to create a

bridge between preclinical and clinical research, supporting the development of translational models.

In this chapter, I describe the methods of the NIMROD study in general, focusing on the cohort demographics, assessment tools, and brain imaging acquisition methods. The more specific analytical methods employed to examine the NIMROD data included in my thesis are discussed in each chapter.

2.2. General description of the NIMROD study

The NIMROD study protocol consists of a series of visit for brain imaging and behavioural evaluations as well as annual neuropsychological and neurological assessments over a period of 3 years (**Figure 7**). The baseline assessments are followed by one visit for MRI and then one, two or three visits for PET depending on the specific cohort examined.

2.3. Ethical Approval & Sponsorship

The NIMROD study was approved by the Cambridge Research Ethics Committee. The study was jointly sponsored by the University of Cambridge and Cambridge University Hospitals Foundation NHS Trust.

2.4. Locations

The investigators were based in the Herchel-Smith Building (HSB) at the University of Cambridge where regional National Health Service (NHS) clinics for AD and non-AD disorders (e.g., progressive supranuclear palsy (PSP), frontotemporal dementia (FTD), and corticobasal syndrome (CBS)) are held. PET and MRI scans were performed at the Wolfson Brain Imaging Centre (WBIC) at the University of Cambridge and at the PET-CT centre on the Cambridge Biomedical Campus (both of which are contiguous to the HSB). Neuropsychological and behavioural assessments were conducted at the Herchel Smith Building or in participants own homes.

2.5. Recruitment

Patients were recruited from the counties of Cambridgeshire, Lincolnshire, Bedfordshire, Norfolk, Suffolk, Hertfordshire and Essex, where participants were willing to travel to Cambridge for imaging studies. Recruitment relied on multi-source identification from primary, secondary and tertiary care, self-referral and relevant patient charities. Patients were recruited from regional specialist clinics for cognitive disorder clinics in neurology, old age psychiatry, and related services at Cambridge University Hospital (CUH) and other trusts within the regions described above. Direct referrals from neurological and psychiatric services were also accepted, with help from the National Institute for Health Research Clinical Research Network Dementias and Neurodegeneration Speciality (DeNDRoN) and the Join Dementia Research (JDR) web-based platform.

Control participants were recruited from regional healthy adults who have indicated a willingness to participate in dementia research via JDR or DeNDRoN. We also recruited healthy friends and non-blood-related family members of the patients who were interested and willing to participate in research. Potential participants identified as above who showed willingness to take part in the research are provided with information about the study in the form of a patient information sheet. Following a period of time (1 week) to consider the information, a follow-up phone call was made to inquire as to their interest in participation and to ask for further information to ensure they are eligible to take part. An appointment was then booked at the study premises or at participants' home to provide an opportunity to ask further questions and obtain formal written informed consent from the participant.

A personal consultee process was set up to assess the potential participation of patients who lacked mental capacity, in accordance with UK law. Firstly, their willingness to consider research participation at a level compatible with their cognitive abilities was evaluated. Secondly, a nominated individual was consulted, which included the spouse, holder of Lasting Power of

Attorney, IMCA, an appropriate next of kin or chosen personal consultee as outlined in the Mental Capacity Act (2005). All participants included in my thesis, including patient participants, had mental capacity.

2.6. Inclusion & Exclusion criteria

Inclusion and exclusion criteria differed depending on type of participant or on their clinical diagnosis. Potential participants were excluded if they had a concurrent major psychiatric illness (except if this is depression in the late-onset depression cohort) or if they had a clear contraindication to an MRI scan (such as a permanent pacemaker), were unable to tolerate an MRI (e.g., due to claustrophobia) or if they had a medical comorbidity that limited their ability to take part in the study (e.g. serious kidney disorders). Participants with previous head injury were also excluded. Potential participants were also excluded if they had atypical or focal parenchymal appearances on MRI which were not in keeping with their diagnosis (e.g., brain tumour or severe vascular disease). Systemic inflammatory diseases (e.g., lupus, rheumatoid arthritis, etc.) were also exclusion criteria as well as concurrent medications that might have affected the study assessments (e.g., chronic use of oral steroids).

2.7. NIMROD participants included in my PhD studies

1. Healthy control participants, defined as participants with MMSE scores >26 and with an absence of: (i) regular memory symptoms, (ii) signs or symptoms suggestive of dementia or (iii) unstable or significant medical illnesses.
2. Participants with AD who meet the diagnostic criteria for probable AD as defined by National Institute on Aging-Alzheimer's Association workgroups on diagnostic guidelines for AD (McKhann *et al.* 2011a).
3. Participants with mild cognitive impairment (MCI), defined as participants having an MMSE >24 but with memory impairment beyond that expected

for age and education which does not meet criteria for probable AD and is not explained by another diagnosis (Albert *et al.* 2011b). The MCI patients did also have biomarker evidence of amyloid pathology, as assessed via positron emission tomography (PiB PET ligand).

Once written and informed consent had been provided, participants performed a neuropsychological assessment using a test battery described in detail below. The neuropsychological battery was tailored to the cohort to which the participant belonged to. All participants also underwent an initial clinical assessment, including the collection of clinical and demographic information (including medication, smoking, alcohol and education histories).

The patients with AD pathology included in my studies were in their early stages of their disease trajectory, although the inclusion of patients with MCI and biomarker evidence of amyloid pathology expanded the phenotypic variability of the clinical spectrum to power the analyses assessing for individual differences in the episodic memory problems.

2.8. Brain imaging visits

Participants attended two or four times for brain imaging depending on their cohort. All participants had an MRI scan. Healthy control participants underwent one PET scan (either with [^{11}C]PK11195 or [^{18}F] AV-1451). MCI participants had three PET scans ([^{11}C]PK11195, [^{18}F] AV-1451 and [^{11}C]PiB) to respectively evaluate microglia activation, tau pathology and amyloid deposition. Participants in all other cohorts had two PET scans (for the DLB cohort it was [^{11}C]PK11195 and [^{11}C]PiB, while for AD, PSP and FTD cohorts it was [^{11}C]PK11195 and [^{18}F] AV-1451 PET scanning).

Venepuncture was carried out at the time of [^{11}C]PK11195 imaging in all participants to measure peripheral markers of inflammation. Each participant underwent repeat neuropsychological testing annually, for up to 3 years, to provide a longitudinal assessment of cognitive function.

2.9. Power and Group Size Calculations

A sample size of $n=15$ per each diagnostic cohort was estimated to enable the detection of a one standard deviation (SD) difference between groups with 80% power, with one SD being less than group differences in [^{11}C]PK11195 binding potential in previously published studies (e.g. Edison et al, 2012: patients mean 0.50 (SD 0.18), controls mean 0.30 (SD 0.08); Iannaccone et al (2012): patients mean for precuneus 0.19 (SD 0.08); controls 0.06 (SD 0.02)). Groups of $n=15$ also allowed detection of correlations of moderate strength (80% power for detected $r=0.45$ or greater). Groups sizes of $n=15$ can robustly detect other changes associated with dementia, such as the extent of atrophy on MRI and increased [^{11}C]PIB binding on PET imaging.

2.10. Neuropsychological and Behavioural Assessment Battery

Patients underwent a clinical assessment battery, including a semi-structured interview for clinical history, demographic data, and questionnaire-based as well as detailed neuropsychological assessments of cognitive and behavioural changes (**Figure 7**). The following principles were applied in selecting the NIMROD test battery: 1) to employ a variety of tests to examine the multi-faceted cognitive deficits of different neurodegenerative and dementia disorders, 2) to include clinically standard tests as well as experimental paradigms; 3) to include questionnaires to be completed by patients and carers to enable complementary perspectives; 4) to include both subjective symptom-based questionnaires and objective neuropsychological tests for both patients and controls, and 5) to use only measures that have been published and used with independent cohorts.

Clinical and neuropsychological assessments were carried out either at the same visit or on a day of attendance for imaging. Neuropsychological follow-up using the same battery of tests was undertaken annually for up to 3 years from the date of initial assessment.

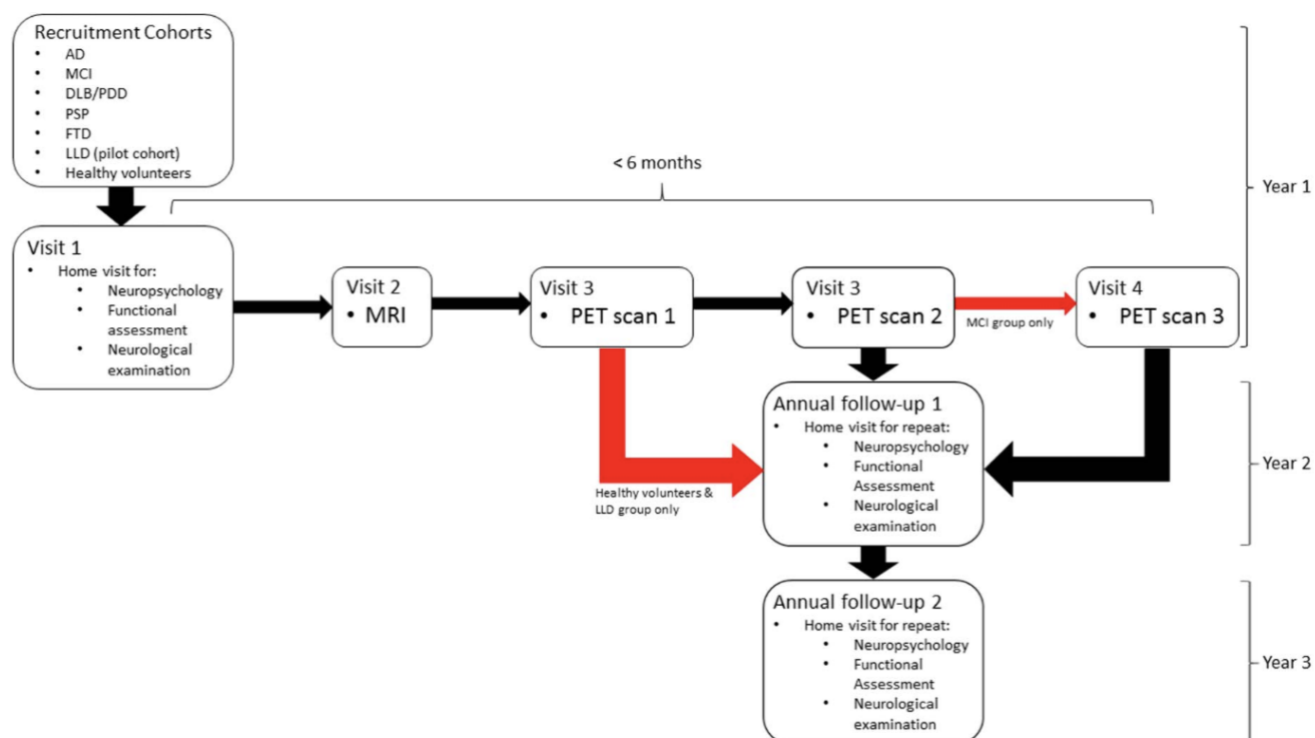


Figure 7: Flow chart showing participants' journey through the NIMROD study.

AD, Alzheimer's disease; MCI, mild cognitive impairment; DLB, dementia with Lewy bodies; PDD, Parkinson's disease dementia; PSP, progressive supranuclear palsy; FTD, frontotemporal dementia; LLD, late life depression; MRI, magnetic resonance imaging; PET, positron emission tomography.

2.11. PET acquisition protocol

PET scanning was performed either on a GE Advance PET scanner (GE Healthcare, Waukesha, WI) at the WBIC or in the GE Discovery 690 PET/CT scanner at Addenbrooke's hospital. The number of patients and controls across both scanners were equally distributed. A 15 minutes $^{68}\text{Ge}/^{68}\text{Ga}$ transmission scan was used for attenuation correction on the Advance, which was replaced by a low dose computed tomography (CT) scan on the Discovery 690. The emission protocols were the same on both scanners.

The radiotracers were produced at the WBIC Radiopharmaceutical Chemistry laboratories with high radiochemical purity (>95%). ^{18}F AV1451, ^{11}C (R)-PK11195 and ^{11}C PiB were produced using the GE PET trace cyclotron, a 16 MeV proton and 8 MeV deuteron accelerator. The

production of [^{18}F]AV1451 was based on the synthetic methods developed by Avid Radiopharmaceuticals and modified to use the GE TracerLab FX-FN synthesizer at WBIC. [^{11}C](R)-PK11195 were prepared using the 'Disposable' synthesis system or GE TRACER laboratory FX-C module. [^{11}C]PiB was prepared using the GE TRACER laboratory FX-C module. All PET radiotracers detailed information is displayed in **Table 2**.

2.11.1. [^{18}F]AV1451

[^{18}F]AV1451 radioligand was selected to evaluate the density of tau deposits. 370MBq of [^{18}F]AV1451 was injected intravenously over 30 seconds at the onset of a 90 minutes scan, with emission data subsequently reconstructed into 58 contiguous time frame (18x5, 6x15, 10x30, 7x60, 4x150 and 13x300 seconds) images for kinetic analysis with the simplified reference tissue model.

2.11.2. [^{11}C]PiB

[^{11}C]PiB PET specifically binds to fibrillar amyloid-beta plaques. It indicates the presence of AD pathology, and increases the likelihood that participants with MCI at baseline will clinically convert to AD over time (Okello *et al.* 2009b). 550MBq of [^{11}C]PiB were injected as a bolus followed by PET imaging from 40-70 minutes post-injection, providing imaging data suitable for subsequent standardised uptake value ratio (SUVR) analysis

2.11.3. [^{11}C](R)-PK11195

[^{11}C](R)-PK11195 radioligand aimed to measure the density of activated microglia as an indication of neuroinflammation. 500MBq [^{11}C](R)-PK11195 was injected intravenously over 30 seconds at the onset of a 75 minutes scan, with emission data subsequently reconstructed into 55 contiguous time frame (18x5, 6x15, 10x30, 7x60, 4x150 and 10x300 seconds) images for kinetic analysis with the simplified reference tissue model.

.

PET radiotracer type	[¹⁸F]AV1451	[¹¹C](R)-PK11195	[¹¹C]PiB
Radioligand specific activity at the end of synthesis (GBq/μmol)	> 216	> 85	> 150
PET radioligand injection dose (MBq)	370	500	550
PET duration (minutes)	90	75	45
Frame images	58	55	1
Cohorts	PSP, AD, MCI and healthy control	PSP, AD, MCI and healthy control	MCI
Measurement	Tau pathology	Activated microglia	Amyloid-β deposits

Table 2: NIMROD PET radiotracers and study groups.

Abbreviations: PET, Positron Emission Tomography; GBq, Gigabecquerel; MBq, Megabecquerel; PSP, Progressive Supranuclear Palsy; AD, Alzheimer's disease; MCI, Mild Cognitive Impairment.

More than one PET scan was required in patient groups to allow direct comparison between tau, amyloid, and inflammation. Two healthy control groups were recruited in order for them to prevent excessive radiation exposure; therefore one group took a [¹⁸F]AV1451 PET session and the other healthy cohort attended [¹¹C](R)-PK11195 PET scan instead.

2.12. PET data pre-processing

Each PET emission frame was reconstructed using the PROMIS 3-dimensional filtered back projection algorithm into a 128 x 128 matrix 30cm trans-axial field of view, with a trans-axial Hann filter cut-off at the Nyquist frequency (Kinahan & Rogers 1989a). Corrections were applied for random movements, dead time, normalization, scatter, attenuation, and sensitivity.

Each emission image series was realigned using SPM8 to correct for patient motion during data acquisition (www.fil.ion.ucl.ac.uk/spm/software/spm8)

and create a mean image. In cases of very large movement ($>10\text{mm}$ in translation or >10 degrees of rotation; this applied for 10% of the cases) the SPM co-registration function was used. Every dynamic frame after 1 minute post-injection was co-registered to the first minute frame. This process was repeated until the motion was corrected. The mean aligned PET image was rigidly co-registered to the MRI T1-weighted image using SPM8 and the inverse transformation applied to the modified Hammers atlas to put it in native PET space. Kinetic modelling was then performed on the motion-corrected time series in the cases of [^{18}F]AV1451 and [^{11}C](*R*)-PK11195. Reference regions were required for the kinetic modelling analysis.

For [^{18}F]AV1451, the reference region was defined in the superior grey-matter of the cerebellum using a 90% grey-matter threshold on the grey-matter probability map produced by SPM8 smoothed to PET resolution. The superior cerebellum was used as reference region as it is considered to have little or no tau pathology in AD/MCI+ (Okello *et al.* 2009c; Scholl *et al.* 2016a; Schwarz *et al.* 2016a). This was confirmed in our *post mortem* cases (see supplementary material published in (Passamonti *et al.* 2017b)).

In the case of [^{11}C](*R*)-PK11195, it is well known that it is difficult to identify a suitable reference region; therefore, supervised cluster analysis was used to determine the reference tissue time-activity curve (Yaquub *et al.* 2012). Supervised cluster analysis was designed to extract pure grey matter signal. Yaquub and colleagues (2012) demonstrated that the supervised cluster analysis with 4 kinetic classes (grey, white, blood and high specific binding (HSB)) performs better than 6 kinetic classes (grey, white, bone, soft tissue, blood and HSB). In order to extract the reference time activity curve (TAC), each voxel TAC of the scan was analyzed using the set of predefined kinetic classes to find the scaling coefficient of each kinetic class, so that the total TAC is equal to the sum of these scaled kinetic classes. A non-negative least squares algorithm was used for finding the scaling coefficients (Turkheimer *et al.* 2000). Scaling coefficients of each kinetic

class were stored in coefficient maps showing their spatial distribution. Finally, to extract the reference tissue TAC, the coefficient map from the (normal) grey-matter kinetic class was used to calculate the weighted average, as follows:

$$C_t^{ref}(t) = \left(\frac{\sum_{i=1}^N w_i^{grey} \times C_t^{voxel}(t)}{\sum_{i=1}^N w_i^{grey}} \right)$$

where, N is the number of voxels, C_t^{ref} the resulting reference tissue TAC, w_i^{grey} the grey scaling coefficient and C_t^{voxel} the voxel TAC.

[^{18}F]AV1451 and [^{11}C](R)-PK11195 non-displaceable binding (BP_{ND}) was determined for each Hammers atlas ROI using a basis function implementation of the simplified reference tissue model (SRTM) operating upon the dynamic Hammers atlas and reference tissue ROI data, both with and without CSF correction (Gunn *et al.* 1997). CSF partial volumes were calculated by division with the mean ROI probability (normalized to 1) of grey and white matter segments, each smoothed to PET resolution. To test whether correction for CSF affected the main results, we repeated all the [^{18}F]AV1451 and [^{11}C](R)-PK11195 PET analyses using data not corrected for CSF (see chapter 3 and 5).

[^{11}C]PiB data were quantified using standardized uptake value ratio (SUVR) by dividing the static image by mean radioactivity concentration of the reference tissue region defined by >90% of the superior cerebellum. [^{11}C]PiB data were treated as dichotomous measures (i.e., positive or negative MCI) and considered MCI positive if the average SUVR value across the cortical ROIs was > 1.52 (Hatashita & Yamasaki 2013).

2.13. MRI acquisition protocol

MRI scanning was carried out at the Wolfson Brain Imaging Centre (WBIC) using 3 T Siemens scanners. The following sequences were used during the scanning protocol:

1. Three-dimensional structural high-resolution T1-weighted sequence examining for structural brain abnormalities (176 slices of 1.0 mm thickness, first echo time (TE)=2.98 ms, repetition time (TR =2300 ms, flip angle=9°, acquisition matrix 256x240; voxel size=1x1x1 mm³).
2. Perfusion (pulsed arterial spin labelling) for blood flow (9 slices of 8.0 mm thickness, TE=13 ms, TR=2500 ms, acquisition matrix 64x64; voxel size=4x4x8 mm³, inversion time 1=700 ms, inversion time 2=1800 ms).
3. Diffusor tensor imaging (DTI) to obtain fractional anisotropy measures of white matter integrity and gross axonal organisation (63 slices of 2.0 mm thickness, 63 diffusion directions, TE= 106 ms, TR=11 700 ms, b-value 1=0 s/mm², b-value 2=1000 s/mm², acquisition matrix 96x96; voxel size=2x2x2 mm³).
4. Susceptibility-weighted imaging (SWI) to identify microhaemorrhages, venous blood and iron deposition (40 slices of 2.0 mm thickness, TE=20 ms, TR=35 ms, flip angle=17°, acquisition matrix 256x240; voxel size=1x1x2 mm³).
5. High-resolution hippocampal subfield sequences carried out in coronal T2 for smaller structural changes in the hippocampus (20 slices of 2.0 mm thickness, TR=6420 ms, flip angle=160°, acquisition matrix 512x408; voxel size=0.4x0.4x2 mm³).
6. Resting state functional MRI with pulse and breathing monitored to examine 'task-free' functional brain connectivity (34 slices of 3.8 mm thickness, TE=13 ms, TR=2430 ms, flip angle=90°, acquisition matrix 64x64; voxel size=3.8x3.8x3.8 mm³, duration 11 min and 5 s).
7. T2 Fluid Attenuated Inversion Recovery (FLAIR) for characterising periventricular lesions adjacent to the sulci and white matter lesions and

hyperintensities (75 slices of 2 mm thickness, TE=132 ms, TR=12 540 ms, flip angle=120°, acquisition matrix 256x256; voxel size=0.9x0.9x2 mm³).

All images were reviewed by a Consultant Radiologist at CUH to exclude unexpected brain abnormalities in participants. None of the participants recruited in the NIMROD study showed significant abnormalities.

2.14. MRI data pre-processing

2.14.1. Structural MRI analytical pipeline

The T1-weighted images were used to facilitate tissue class segmentation (grey- and white-matter, together with cerebro-spinal fluid; CSF), and to allow inverse normalisation of template space regions of interest (ROIs) defined by modified Hammers atlas to subject MRI space (Hammers *et al.* 2003). The left and right ROIs were combined in the AD and PSP clinical cohorts based on the fact that these diagnostic groups do not show any laterality of the clinical symptoms. The brainstem of the atlas was split into midbrain ($z \geq 22\text{mm}$), pons ($z < -22\text{mm}$) and medulla oblongata ($z = -49\text{mm}$). Each T1 image was non-rigidly registered to the ICBM2009a template brain using ANTS (<http://www.picsl.upenn.edu/ANTS/>) with default settings, and the inverse transform was applied to the modified Hammers atlas (resliced from MNI152 to ICBM2009a space) to bring the ROIs to subject MRI space.

2.14.2. Functional MRI analytical pipeline

The first six volumes were discarded to eliminate saturation effects and achieve steady-state magnetization. Pre-processing of resting-state data employed the Multi-Echo Independent Components Analysis (ME-ICA) pipeline, which uses independent component analysis to classify blood oxygenation dependant (BOLD) and non-BOLD signals based on the identification of linearly dependent and independent echo-time related components (<https://wiki.cam.ac.uk/bmuwiki/MEICA>) (Kundu *et al.* 2013a).

The ME-ICA pipeline provides an optimal approach to correct for movement-related and non-neuronal signals, and is therefore particularly suited to our study, in which systematic differences in head position might have been expected between groups. After ME-ICA, the data were smoothed with 6 mm full-width half maximum kernel.

The location of the key cortical regions in each network was identified by spatial independent component analysis (ICA) using the Group ICA of fMRI Toolbox (Calhoun *et al.* 2001a) in an independent dataset of 298 age-matched healthy individuals from the population-based cohort in the Cambridge Centre for Ageing and Neuroscience (Cam-CAN) (Shafto *et al.* 2014a). Details about pre-processing and node definition are published previously (Tsvetanov *et al.* 2016a). Four networks were identified by spatially matching to pre-existing templates (Shirer *et al.* 2012a). The default mode network contained five nodes: the ventromedial prefrontal cingulate cortex, dorsal and ventral posterior conjugate cortex, and right and left inferior parietal lobes. The fronto-parietal network was defined using bilateral superior frontal gyrus and angular gyrus. Subcortical nodes included nodes like the bilateral putamen and hippocampus. The node time-series were defined as the first principal component resulting from the singular value decomposition of voxels in a 8-mm radius sphere, which was centred on the peak voxel for each node (Tsvetanov *et al.* 2016a).

After extracting nodal time-series we sought to reduce the effects of noise confounds on functional connectivity effects of node time-series using a general linear model (Geerligs *et al.* 2017). This model included linear trends, expansions of realignment parameters, as well as average signal in the white-matter and cerebrospinal, including their derivative and quadratic regressors from the time-courses of each node (Satterthwaite *et al.* 2013).

The signals in the white-matter and cerebrospinal fluid were created by using the average across all voxels with corresponding tissue probability larger than 0.7 in associated tissue probability maps available in the SPM12

software (<http://www.fil.ion.ucl.ac.uk/spm/software/spm12/>). A band-pass filter (0.0078-0.1 Hz) was implemented by including a discrete cosine transform set in the general linear model, ensuring that nuisance regression and filtering were performed simultaneously (Hallquist *et al.* 2013; Lindquist *et al.* 2018).

The general linear model excluded the initial five volumes to allow for signal equilibration. The total head motion for each participant, which was used in subsequent between-subject analysis as a covariate of no interest (Geerligs *et al.* 2017), was quantified using the approach reported in Jenkinson and colleagues (Jenkinson *et al.* 2002a), i.e. the root mean square of volume-to-volume displacement. Finally, the functional connectivity between each pair of nodes was computed using Pearson's correlation on post-processed time-series.

Chapter 3 | ^{18}F -AV-1451 PET to assess *in vivo* tau pathology in Alzheimer's disease

3.1. Introduction

In this Chapter, I describe part of the results of my published study (Passamonti *et al.* 2017a), in which I sought to evaluate the utility of the ^{18}F -AV-1451 PET tracer in assessing tau pathology in Alzheimer's disease (AD).

In AD, oligomeric and aggregated neurofibrillary tau tangles are one the major determinant of synaptic/cell dysfunction and death (Goedert *et al.* 1988; Ballatore *et al.* 2007; De Calignon *et al.* 2012), notwithstanding the importance of β -amyloid in its 'toxic alliance' with pathological tau (Bloom 2014). The intensity and distribution of tau in AD also correlates with the clinical syndrome and severity and has been considered as one of the primary factors in the neuropathological staging of AD (Braak *et al.* 2006b; Murray *et al.* 2014; Ossenkoppele *et al.* 2015b). To be able to quantify the burden and distribution of tau pathology in living patients, or those at high risk of developing tau-related disorders is a major step forward in the development of disease modifying therapies targeting the tau protein.

Different PET radioligands have been developed to measure *in vivo* binding to aggregated tau, including PBB3 (Maruyama *et al.* 2013a), a series of 'THK' compounds (Okamura *et al.* 2013b), and [^{18}F]AV1451 (Chien *et al.* 2013; Xia *et al.* 2013). In autoradiographic studies with *post mortem* human brain tissues, the radiotracer [^{18}F]AV1451 colocalizes selectively with hyperphosphorylated tau over β -amyloid plaques (Marqu   *et al.* 2015), although off-target binding and lack of sensitivity to non-AD tau pathology has been described since they initial study by Chien and

colleagues (Marquie *et al.* 2015). In our NIMROD study we chose to use [¹⁸F]AV1451, which have had the most extensive evidence internationally at the time when the data of my thesis were collected. Subsequently, the severity of displacement of THK5351 by selegiline (acting on MAO-B), and lack of large scale data with PBB3, have had left [¹⁸F]AV1451 the lead compound despite its controversies, while second generation ligands are still developed and validated.

In patients with MCI and AD, there is higher [¹⁸F]AV1451 non-displaceable binding potential (BP_{ND}), a measure of specific binding, in parietal and temporal cortices relative to age-matched healthy controls (Okello *et al.* 2009b). Progressively increasing regional [¹⁸F]AV1451 binding in AD has also been associated with Braak staging of neurofibrillary tau pathology (Schöll *et al.* 2016; Schwarz *et al.* 2016b), while [¹⁸F]AV1451 PET binding patterns mirror the clinical and neuroanatomical variability in the AD spectrum (Ossenkoppele *et al.* 2016a).

Specifically, patients with the amnesic presentation of AD (as those included in my thesis) showed the highest [¹⁸F]AV1451 uptake in medial temporal lobe regions such as the hippocampus, amygdala, and parahippocampal cortex, while patients with the logopenic variant of AD displayed increased left hemispheric [¹⁸F]AV1451 binding, particularly in posterior temporoparietal areas implicated in linguistic processes (Ossenkoppele *et al.* 2016a). Performance on domain-specific neuropsychological tests was also associated with increased [¹⁸F]AV1451 uptake in brain regions involved in episodic memory, visuospatial skills, and language production or comprehension (Ossenkoppele *et al.* 2016a).

3.2. Main aims and hypotheses

The main aim of the study described in this chapter was to test two hypotheses:

1) that patients with AD and MCI+ show increased [^{18}F]AV-1451 binding in cortical and sub-cortical areas typically associated with AD pathology, including the medial temporal lobe as well as parietal and lateral temporal cortices (Serrano-Pozo *et al.* 2011).

2) that higher [^{18}F]AV-1451 in these brain regions positively relate to cognitive impairment as assessed via the Addenbrooke's Cognitive-Examination score-revised, MMSE, and Ray-Auditory Verbal Learning Test (RAVLT).

3.3. Participants and Methods

3.3.1. Participants

Nine patients meeting diagnostic criteria for probable AD (McKhann *et al.* 2011b), and six patients with MCI and biomarker evidence of AD (i.e., amyloid pathology) were included in this study. All participants with MCI had a positive Pittsburgh compound B (PiB) PET scan (assessing *in vivo* amyloid pathology).

Thirteen age- and sex-matched healthy controls with no history of major psychiatric or neurological illnesses, head injury or any other significant medical co-morbidity were also included to allow group-wise comparisons with the AD cohort.

All participants were aged over 50 years, had sufficient proficiency in English for cognitive testing and had no contraindications to magnetic resonance imaging (MRI).

3.3.2. PET imaging

3.3.2.1. PET pre-processing

Each emission frame was reconstructed using the PROMIS 3-dimensional filtered back projection algorithm into a 128x128 matrix 30cm trans-axial field of view, with a trans-axial Hann filter cut-off at the Nyquist frequency. Corrections were applied for randoms, dead time, normalization, scatter, attenuation, and sensitivity. Each emission image series was aligned using SPM8 to correct for patient motion during data acquisition (www.fil.ion.ucl.ac.uk/spm/software/spm8).

The mean aligned PET image, and hence the corresponding aligned dynamic PET image series, was rigidly registered to the T1-weighted image using SPM8 to extract values from both the Hammers atlas regions of interest (ROIs) and those in a reference tissue defined in the superior grey-matter of the cerebellum using a 90% grey-matter threshold on the grey-matter probability map produced by SPM8 smoothed to PET resolution. The superior cerebellum was used as reference region as it is considered to have little or no tau pathology in AD (Okello *et al.* 2009d). All ROI data, including the reference tissue values, were corrected for cerebrospinal fluid (CSF) partial volumes through division with the mean ROI probability (normalized to 1) of grey + white matter segments, each smoothed to PET resolution. To test whether correction for CSF affected the main results, we repeated all the [^{18}F]AV-1451 PET analyses using data not corrected for CSF.

3.3.2.2. PET statistical analyses

To compare [^{18}F]AV-1451 binding across groups (AD/MCI+ and controls), individual ROI binding values for [^{18}F]AV-1451 were used in a repeated-measures general linear model (GLM) to test for the main effect of ROI, main effect of group, and group x ROI interaction.

Age and education were included as covariates of no interest. For the AD/MCI+, I also tested for correlations between regional [^{18}F]AV-1451

binding and cognitive impairment using the ACE-R and MMSE scores with Pearson's correlation (with partial correlations accounting for variability in age and education).

3.4. Results

3.4.1. Participants

As expected, patients with AD and MCI+ demonstrated cognitive impairment compared to controls, as measured by the Addenbrookes' Cognitive Examination-Revised test (ACE-R), mini-mental status examination (MMSE), and Ray-Auditory Verbal Learning Test (RAVLT) (**Table 3**).

Demographic & Clinical data	AD / MCI+ (n=15)	Controls (n=13)	Group difference
Sex (males/females)	9/6	6/7	N/S
Age (years) (SD, range)	71.6 (\pm 8.7, 54-85)	67.2 (\pm 7.3, 55-80)	NS
Education (years) (SD, range)	13.8 (\pm 3.1, 10-19)	13.1 (\pm 1.7, 10-18)	NS
MMSE (SD, range)	25.5 (\pm 2.8, 18-28)	29.3 (\pm 0.7, 28-30)	F=4.90, P=0.012
ACE-R (SD, range)	75.9 (\pm 11.0, 51-89)	95.5 (\pm 3.0, 89-99)	F=10.3, P=0.0002
RAVLT (SD, range)	1.3 (\pm 1.4, 0-4)	10.7 (\pm 2.8, 4-16)	F=11.6, P<0.0001

Table 3: Participants' demographic and clinical details (tau PET study).

Participant details (mean, with standard deviation (SD) and range in parentheses) and group differences by one-way analysis of variance or chi-squared test. AD/MCI+: Alzheimer's disease/mild cognitive impairment (amyloid positive from Pittsburgh Compound-B, PiB, positron emission tomography scan); MMSE: Mini Mental State Examination; ACE-R: Addenbrookes' Cognitive Examination, Revised. N/S, not significant at P<0.05 (uncorrected).

Next, I examined the demographic and clinical characteristics of the patients with clinically probable AD, relative to MCI+ patients and controls.

Table 4 shows that clinically probable AD patients were similar to MCI+ patients in terms of demographic and clinical features.

Demographic & Clinical data	AD (n=9)	MCI+ (n=6)	Controls (n=13)	Group difference
Sex (males/females)	2/7	4/2	6/7	N/S
Age (years) (SD, range)	69.4 (\pm 10, 54-85)	72.2 (\pm 9.7, 58-83)	67.2 (\pm 7.3, 55-80)	NS
Education (years) (SD, range)	15.1 (\pm 3.2, 10-19)	13.0 (\pm 2.9, 10-18)	13.1 (\pm 1.7, 10-18)	NS
MMSE (SD, range)	25.1 (\pm 3.4, 18-28)	26.2 (\pm 1.1, 25-28)	29.3 (\pm 0.7, 28-30)	F=3.85, P=0.025
ACE-R (SD, range)	72.9 (\pm 11.7, 51-89)	80.3 (\pm 8.0, 66-87)	95.5 (\pm 3.0, 89-99)	F=8.7, P=0.004
RAVLT (SD, range)	0.9 (\pm 1.3, 0-4)	1.2 (\pm 1.2, 0-3)	10.7 (\pm 2.8, 4-16)	F=10.4, P<0.001

Table 4 Demographic & clinical details in AD, MCI+, and controls (tau PET study).

Participant details (mean, with standard deviation (SD) and range in parentheses) and group differences by one-way analysis of variance or chi-squared test. AD: clinically probable Alzheimer's disease; /MCI+: mild cognitive impairment (amyloid positive from Pittsburgh Compound-B, PiB, positron emission tomography scan); MMSE: Mini Mental State Examination; ACE-R: Addenbrookes' Cognitive Examination, Revised. N/S, not significant at $P < 0.05$ (uncorrected).

3.4.2. [^{18}F]AV-1451 binding in Alzheimer's disease

The mean [^{18}F]AV-1451 PET map in each group (**Figure 8**) and quantitative region of interest (ROI) analyses (**Figure 9**), indicated high [^{18}F]AV-1451 binding in the basal ganglia in both groups including controls.

In the repeated-measures GLM of regional binding, we found a significant main effect of group ($F=17.5$, $P=0.00001$), and a ROI x group interaction ($F=7.5$, $P<0.00001$), although there was no main effect of ROIs, even considering the binding values in the 'hot-spot' ROIs (basal ganglia including caudate, putamen, and pallidum) ($F=0.8$, $P=0.8$) (**Figure 9**).

The group and interaction effects were driven by higher [^{18}F]AV-1451 binding in the AD/MCI+ group relative to controls, in frontal, parietal, lateral temporal, and occipital cortices as well as in the hippocampus and other medial temporal lobe ROIs (post-hoc t-tests, T 's >2.2 , P 's <0.04) (**Figure 9**).

Next, I examined the [^{18}F]AV-1451 ROI binding in AD and MCI+ groups separately, relative to controls, with the caveat of the small sample size in each group of patients (AD=9, MCI+=6). Nevertheless, there were still group and interaction effects that were driven by higher [^{18}F]AV-1451 binding in the patients' groups relative to controls ($F=4.3$, $P<0.001$), although the difference between AD and MCI+ patients were not significant (post-hoc t-tests, T 's <1.3 , P 's >0.1) (**Figure 10**).

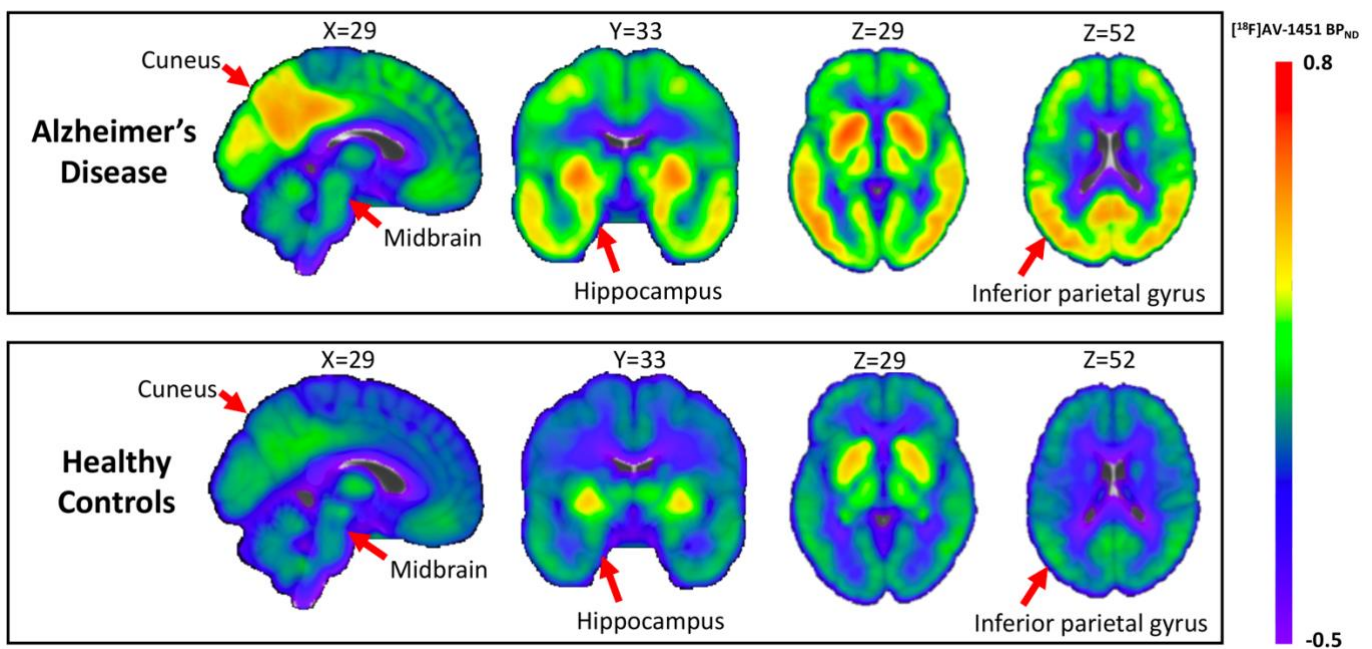


Figure 8: [^{18}F]AV-1451 findings in AD/MCI+ and controls (voxel-wise data).

Mean [^{18}F]AV-1451 positron emission tomography map in each group. Note the overall high [^{18}F]AV-1451 binding in the basal ganglia in both groups including controls. Patients with Alzheimer's disease (AD) pathology showed increased [^{18}F]AV-1451 binding in the medial temporal lobe regions and other cortical areas, relative to controls (see Figure 10 for quantitative analyses in each region of interest (ROI)).

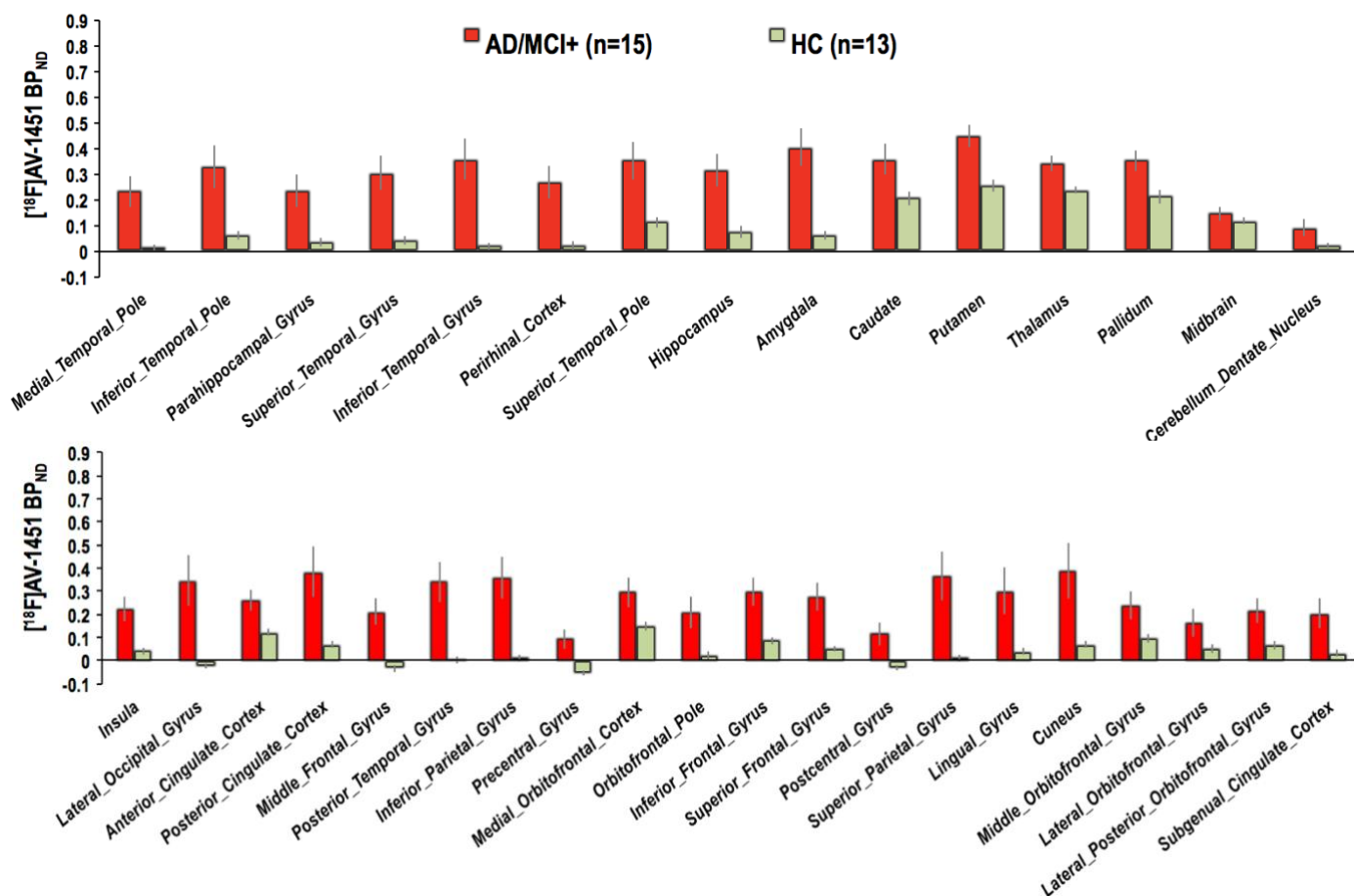


Figure 9: [18F]AV-1451 findings in AD/MCI+ and controls (ROI analyses).

Mean (\pm standard error) [18F]AV-1451 non-displaceable binding potential (BP_{ND}) in each region of interest (ROI) for the following participant groups: Alzheimer's disease (AD) and amyloid positive mild cognitive impairment (MCI+); healthy controls (HC). The [18F]AV-1451 BP_{ND} data showed in this figure are corrected for cerebrospinal fluid (CSF) volume.

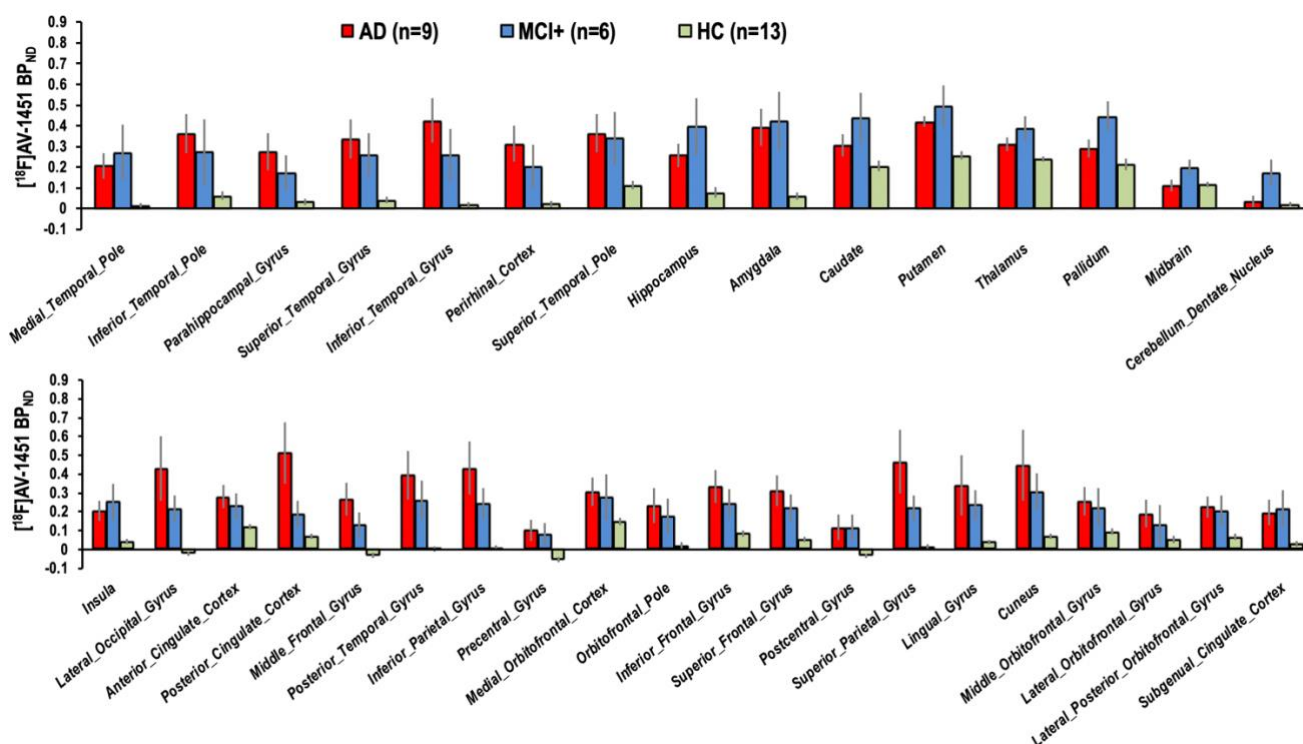


Figure 10: $[^{18}\text{F}]\text{AV-1451}$ findings in AD, MCI+, and controls (ROI analyses).

Mean (\pm standard error) $[^{18}\text{F}]\text{AV-1451}$ non-displaceable binding potential (BP_{ND}) in each region of interest (ROI) for the following participant groups: clinically probable Alzheimer's disease (AD), amyloid positive mild cognitive impairment (MCI+); healthy controls (HC). The $[^{18}\text{F}]\text{AV-1451}$ BP_{ND} data showed in this figure are corrected for cerebrospinal fluid (CSF) volume.

Repeating the same analyses using $[^{18}\text{F}]\text{AV-1451}$ binding values that were not corrected for CSF partial volume effects yielded similar results ($F=1.1$, $P=0.2$, for the main effect of ROIs; $F=16.7$, $P<0.00001$ for the main effect of group; and $F=6.3$, $P<0.00001$ for the group \times ROI interaction).

This analysis demonstrates that our main findings were robust against between-groups effects that might have been driven by differences in grey-matter atrophy between patients and controls.

3.4.3. $[^{18}\text{F}]\text{AV-1451}$ binding and AD cognitive deficit

Next, I tested whether the regional $[^{18}\text{F}]\text{AV-1451}$ binding related to cognitive deficit as assessed via the ACE-R, MMSE, and Rey-Auditory Verbal Learning (RAVLT) scores. In the AD/MCI+ group, there was no significant correlation between ACE-R, MMSE or RAVLT scores and $[^{18}\text{F}]\text{AV-1451}$

binding in any ROI (P 's>0.14). These null results were also found when the correlation analyses between ACE-R, MMSE or RAVLT scores and [^{18}F]AV-1451 binding was repeated for the clinically probable AD and the MCI+ groups, separately (P 's>0.23).

Repeating the correlation analyses when using the [^{18}F]AV-1451 binding values that were not corrected for CSF volume also yielded non-significant results (P 's>0.1).

3.5. Discussion

This study shows that PET imaging with the radiotracer ^{18}F -AV-1451 can reveal distinct patterns of tau pathology in AD and its prodromal state of MCI, in comparison to healthy controls. However, despite the potential of ^{18}F -AV-1451 as biomarker of tau pathology in AD, caution in the interpretation of its binding targets is indicated by our current and previous studies (Marquie *et al.* 2015). In particular, high levels of non-specific binding were detected in the basal ganglia of patients with AD as well healthy controls. Different unspecific targets for the ^{18}F -AV-1451 tracer have been proposed and these include neuromelanin, ferritin, other iron-related proteins or the MAO enzyme (Marquie *et al.* 2015).

However, some of these 'off-target' sites of ^{18}F -AV-1451 as the neuromelanin binding can only be expected in certain brain regions that contain neuromelanin (e.g., the substantia nigra). Neither the basal ganglia or the cortical mantle have neuromelanin deposits so the neuromelanin hypothesis of the ^{18}F -AV-1451 'off-target' binding cannot explain the high unspecific binding that we and others observed *in vivo* in the basal ganglia (see **Figure 9**).

An alternative explanation is that ^{18}F -AV-1451 unspecifically binds to the MAO-A enzyme that is significantly expressed in the basal ganglia (Ng *et al.* 2017), although displacement studies to test this hypothesis have not been conducted yet.

Over and above the clarification of its off-target binding properties, there is nowadays robust evidence from longitudinal studies that changes in [^{18}F]AV-1451 binding over time relate to progressive accumulation and spreading of tau pathology in AD as well as to cognitive decline. This reinforces the use of [^{18}F]AV-1451 PET as a clinically useful biomarker to track tau pathology and disease progression in AD (Harrison *et al.* 2019; Pontecorvo *et al.* 2019). At the time of the data collection for my thesis, a cross-sectional study like ours could not be used to infer such important longitudinal changes in tau pathology.

Nevertheless, our understanding of *in vivo* tau pathology and neuroinflammation in AD will greatly benefit from longitudinal and interventional studies. Some of these studies have already been conducted while others are underway. Amongst these, two prominent studies have clearly shown that *in vivo* tau accumulation (as assessed via [^{18}F]AV1451 PET imaging) increases over time as AD progresses (Harrison *et al.* 2019; Pontecorvo *et al.* 2019). Interestingly these PET-tracked tau changes in relation to disease severity follow the pathologically well-established Braak staging (Jack *et al.* 2018; Lowe *et al.* 2018). These are promising studies that reinforce the value of using [^{18}F]AV1451 PET as biomarker of AD and support its intrinsic ability to objectively assess the high individual difference in disease progression that is present in the AD clinical spectrum.

In contrast to previous studies (Johnson *et al.* 2016; Ossenkoppele *et al.* 2016b), our [^{18}F]AV-1451 data did not correlate with severity of cognitive impairment in the MMSE and ACE-R tests. Although there can be several reasons for null results, this may be due to lack of statistical power (type II error) or the use of clinical measures that were not sensitive enough to describe the full spectrum of clinical variability in AD.

Technical limitations should also be discussed. In particular, our PET analyses used 'partial volume' corrections that derived from the amount of cerebrospinal fluid (CSF) volume included in each ROI. Although this

attenuates the potential effect of AD-related brain atrophy, at the same time, this analytical procedure might induce an over-correction of the data that could in turn inflate the size of the statistical effects. To avoid the potential over-correction of the PET binding values, I have therefore re-run the analyses using the uncorrected PET data which reassuringly yielded to similar results in terms of the main effect of group and group x ROI interaction.

Interestingly, the brain regions in which I identified the most significant group differences in [^{18}F]AV-1451 binding in AD, relative to controls, were those predicted from the specific patterns of AD-related neuropathology. In particular, patients with clinical probable AD and amyloid positive MCI displayed increased [^{18}F]AV-1451 binding in a widely distributed group of sub-cortical and cortical regions that have been repeatedly implicated in the pathophysiology of AD (e.g., hippocampus, medial temporal lobe as well as parietal and lateral temporal cortices)(Braak & Braak 1995; Braak *et al.* 2006a).

In conclusion, the [^{18}F]AV-1451 tracer is a potentially useful PET ligand for clinical and non-clinical research in AD, despite its non-specific “off-target” binding which remains to be clarified and quantified. Overall, my and other studies support the use of [^{18}F]AV-1451 PET ligand for further research in AD and related neurodegenerative disorders.

Chapter 4 | Tau burden & network dysfunction in Alzheimer's disease

4.1. Introduction

In this chapter, I examine the relationship between *in vivo* tau pathology and brain functional connectivity by combining PET imaging with the ligand [¹⁸F]AV-1451 and graph theoretical measures derived from 'task-free' functional magnetic resonance imaging (fMRI) data.

In Alzheimer's disease (AD), neuropathology and atrophy are most marked in those brain regions that are densely connected, both at the structural (Crossley et al., 2014) and functional level (Dai et al., 2014). In other words, these densely connected regions are usually referred to as 'hubs' (Buckner et al., 2009). There are a number of hypotheses as to why hubs are vulnerable to neurodegeneration. First, pathological proteins may propagate trans-neuronally, in a prion-like manner (Prusiner, 1984; Baker et al., 1994; Goedert, 2015) such that highly connected regions are more likely to receive pathology from 'seed' regions affected in early stages of the disease (Zhou et al., 2012), leading to neurodegeneration that mirrors structural and functional brain connectivity (Raj et al., 2012, 2015; Abdelnour et al., 2014).

In addition, hubs might be selectively vulnerable to a given level of pathology, due to a lack of local trophic factors (Appel, 1981).

The trans-neuronal spread hypothesis predicts that regions that are more strongly interconnected would accrue more tau pathology. This would manifest as higher tau burden in nodes with larger weighted degree, which is a measure of the number and strength of functional connections involving each node.

However, if trophic support is an important factor in tau accumulation, this might manifest as a negative relationship between tau burden and connectivity measures; in other words, nodes with less tightly clustered connectivity patterns might have more vulnerable trophic supply.

In this study we examine, in the same subjects, the relationship between in vivo tau burden, as measured by the PET ligand 18F-AV-1451 BPND, and functional connectivity, as summarized by graph theoretic measures based on resting state (task-free) functional MRI.

I now introduce the graph analysis mathematical framework that has been used to quantify the brain connectivity measures employed in this study and to test the hypotheses stated in section 4.2.

4.1.1. Graph analysis to measure network function

In recent years, there has been a growing interest in describing the brain functioning by using theoretical frameworks that can formally model the complexity of the neural connectivity patterns. Within this context, mathematical approaches based on graph theory have been applied to measure the architecture ('topology') of the brain functional connectivity patterns (i.e., 'connectomic' approach) (Fornito & Bullmore, 2015).

This graph theoretical approach provides a series of key indices to quantify different aspects of the brain 'connectome' (Fornito & Bullmore, 2015). For instance, the network's capacity to 'route' information across its distinct elements ('nodes' or brain areas) can be estimated by computing the efficiency of the paths ('edges') linking these nodes (Boccaletti, Latora, Moreno, Chavez, & Hwang, 2006).

In other words, a network's efficiency is a quantitative representation of the average number of steps it would take for information to 'travel' across the network. Higher efficiency reflects fewer steps needed to route information from A to B. The standard graph metric of efficiency does not directly

indicate metabolic costs, time taken, network capacity, or data corruption, although these factors can be considered in more complex graphs. Measures of efficiency are most informative about integration within a network. Related measures can be applied at the global or local level (Rubinov & Sporns, 2010).

Graph analyses also enable one to quantify the degree of segregation within a network. For example, networks may comprise a set of modules, within which there is strong connectivity but between which there is selective connectivity (modularity). The clustering of small sets of nodes, and the degree to which two connected nodes are both connected to a third node, also confer particular properties to a network, that we shall see are relevant to the vulnerability and impact of neurodegeneration (i.e., global or local clustering coefficient).

Studying the connectome's relationship to *in vivo* tau pathology in dementia has thus the potential to test hypothesis of functional brain mechanisms underlying AD; and to quantify the effect of pathology the connectome. This study associates the molecular tau pathology in AD, as assessed via [¹⁸F]AV-1451 PET imaging, with functional connectivity patterns across large-scale networks, as measured via resting-state fMRI (rsfMRI).

4.1.2. Graph-measures of connectivity

A pictorial representation of the graph indices employed in this chapter is provided in **Figure 11**. Note the distinction between measures that relate to nodes and to edges, and the distinction between global network measures and local properties. The graph metrics that we assessed in this study were the following:

- 1) Weighted degree: the number and strength of functional connections involving each node.
- 2) Betweenness centrality: the number of shortest paths between any other

two nodes that pass through the node of interest. Nodes that are important for the transfer of information between other nodes have high betweenness centrality.

3) Closeness centrality: the inverse of the path length between a node and all other nodes in the graph. This is the node-wise equivalent of global efficiency, which is the inverse sum of all the shortest path lengths in the graph.

4) Local efficiency: the number of strong connections a node has with its neighbouring nodes. This reflects the robustness of local networks to disruption.

5) Eigen-centrality: this measure quantifies the functional influence of a node on every other node in the graph, by weighting the importance of each nodal connection based on the influence of the nodes with which they connect.

Nodal connectivity strength was assessed for comparison to weighted degree, to ensure that our results did not result from bias introduced by proportionate thresholding. This metric is related to weighted degree but includes information from all strengths of connection between every pair of nodes. As such, it is more subject to functional MRI signal-to-noise ratio limitations, and it is not a suitable metric for whole-brain, cross-sectional analysis across individuals, but it can be used to make a node-wise, group average assessment analogous to that for weighted degree.

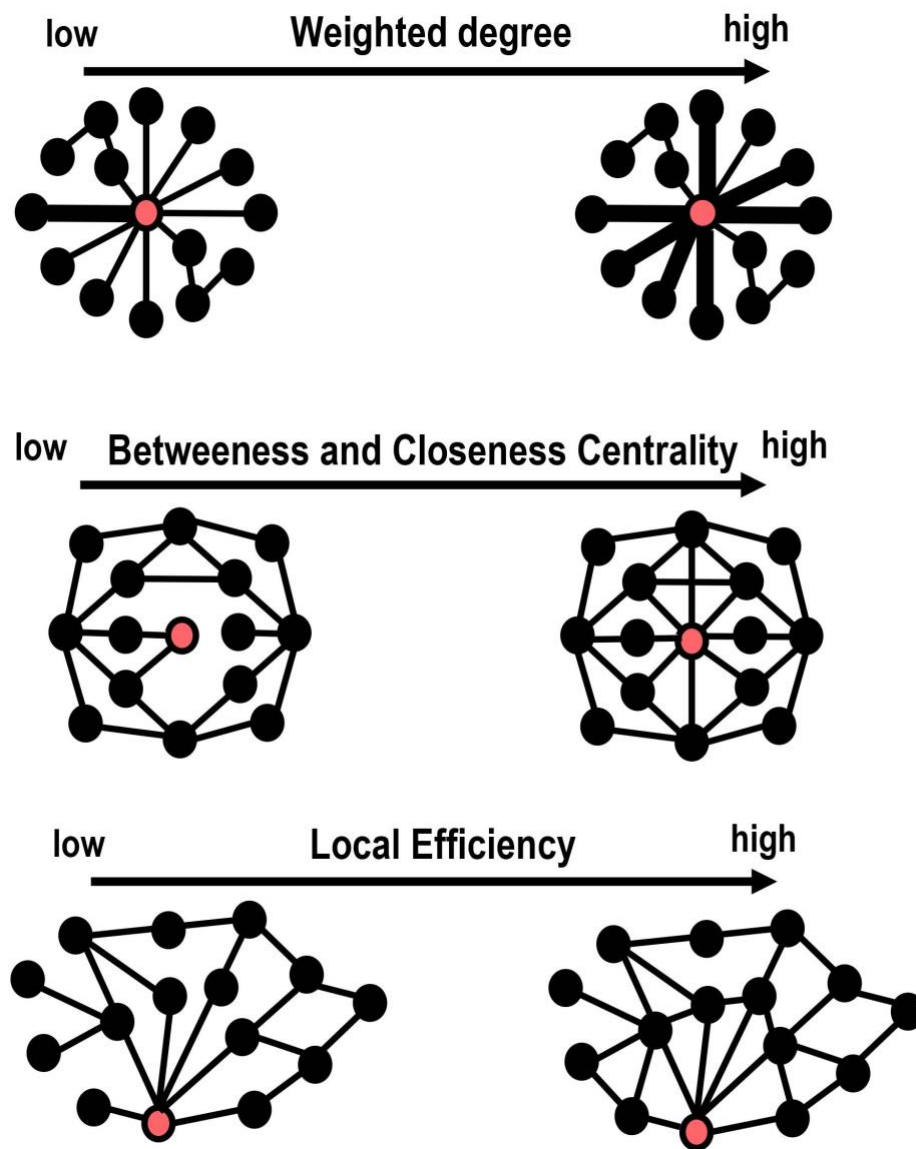


Figure 11: Pictorial representation of graph-analysis connectivity metrics.

Top row. The thicker lines indicate the existence of higher strength in the 'communications' between the network nodes. **Middle row** and **bottom row.** A variable degree of inter-connectedness between the nodes is shown. The node in red is the reference node in the examples of high or low levels of connectivity.

4.2. Main hypotheses

This study tested two hypotheses:

- 1) Brain regions that are more densely interconnected accrue more tau pathology.
- 2) In Alzheimer's disease, where tau accumulation is predominantly cortical, the functional consequence is that affected nodes become more weakly connected and local efficiency of information transfer is reduced.

To test these hypotheses, we assessed, in patients with AD pathology (clinically probable AD patients and MCI amyloid positive patients, MCI+), relative to controls, the role of *in vivo* tau burden, as assessed by the PET ligand [¹⁸F] AV-1451, in mediating graph measures of rsfMRI data.

4.3. Participants

Fifteen patients with AD pathology, including patients with clinical diagnosis of probable AD according to consensus criteria (n=9) (McKhann *et al.* 2011b), and MCI with positive amyloid PET scan (n=6) (MCI+) were included (Okello *et al.* 2009d). We also recruited 12 age- and gender-matched healthy controls.

Both groups overlapped with the participants described in the previous chapter with the exception of one control participant who was excluded in the present study due to poor quality of his rsfMRI data (excessive head movement, i.e., >3mm).

4.4. rsfMRI data acquisition and pre-processing

rsfMRI multi-echo data were obtained for 10 minutes. Pre-processing employed the ME-ICA pipeline (Kundu *et al.* 2012a, 2013b), which uses independent component analysis to classify BOLD and non-BOLD signals based on the identification of echo time (TE) dependent components. This

provides an optimal approach to correct for movement-related and non-neuronal signals, and is therefore particularly well suited to this study, in which systematic differences in head movement might have reasonably been expected in the AD/MCI+ group.

The Harvard-Oxford atlas was sub-parcellated into 598 regions of equal volume. rsfMRI images were co-registered to a T1-weighted image from the same session and then warped to the template space by the flow fields generated from a study-specific anatomical template created using DARTEL (Ashburner 2007). The whole-brain was parcellated into nodes of equal size (separately for patients and controls), therefore the graph metrics calculated at each node represented the connectivity at that node independently of the volume.

The BOLD time series for each node was extracted using the CONN functional connectivity toolbox (Whitfield-Gabrieli & Nieto-Castanon 2012). Between-node association matrices were generated, and then z-transformed for further analysis.

4.5. rsfMRI connectivity analyses

Graph theoretical analysis was used to investigate the global and local characteristics of brain networks. These metrics were calculated in python using the Maybrain software (github.com/ritman/maybrain) and networkx (version 1.11). Here we examined network thresholds from $1 < x < 10\%$, representing a range of graphs from sparse to dense (Alexander-Bloch *et al.* 2010). Very sparse graphs contain less information and can miss important relationships. Conversely, very dense graphs are more subject to noise and, when binarized, begin to provide less meaningful information. Therefore, in what follows, we present the primary statistical analyses at an intermediate density of 6%, with statistical detail given for this density.

Weighted degree was analysed in its raw form, and all other metrics were dissociated from variation in degree by binarisation after thresholding and normalisation against 1,000 random graphs with the same number of connections at each node.

4.6. Statistical analyses

All statistical analyses were performed in Matlab 2015b. The primary between-subject analysis was undertaken across the whole-brain. For each individual, we first calculated a measure of disease-related tau burden. For patients with AD, in whom tau deposition increases in both magnitude and distribution as disease progresses (Braak & Braak 1995), tau pathology was calculated as average [^{18}F] AV-1451 binding across the whole-brain,. This measure of subject-specific tau burden was then correlated with whole-brain averaged graph metrics to assess the relationship between the metric in question and disease burden in each group separately.

The region-specific tau burden per subject was correlated with the graph metric values at each node and next the gradient of the best fit linear regression within each group was the outcome measure. The data in the superior cerebellar region were not included (as this was the reference region for PET imaging), while the remaining regional maps were collapsed into a vector. This was correlated with a matching vector of local tau burden at each node, calculated as the group-averaged increase in [^{18}F] AV-1451 binding potential (the group average refers to the average within each group, i.e., AD/MCI+ and controls, separately).

4.7. Results

4.7.1. More Tau pathology in densely connected nodes

As we parcellated the brain into nodes of equal size, the weighted degree is a measure of the volume of cortex to which a node is connected, and the strength of these connections. In other words, the calculation of the weighted degree took into account the volumetric differences between patients and controls at each node.

In AD/MCI+ patients, the more strongly connected nodes had higher ^{18}F -AV-1451 binding (Pearson's $r = 0.48$, $P < 0.0001$, Spearman's $\rho = 0.48$, $P < 0.0001$) (**Figure 12 left**). This was also true when examining the data for the clinically probable AD and MCI+ patients, separately (AD, Pearson's $r = 0.34$, $P < 0.001$, MCI+ Spearman's $\rho = 0.28$, $P < 0.01$). This relationship was also observed within patients, although their early disease stage did not enable further analyses of the impact of the Braak's stage on the main findings.

In contrast, controls did not show a relationship between the weighted degree and ^{18}F -AV-1451 binding (Pearson's $r = 0.03$, Spearman's $\rho = 0.11$) (**Figure 12 right**). Finally, all these findings were confirmed at all examined network density thresholds.

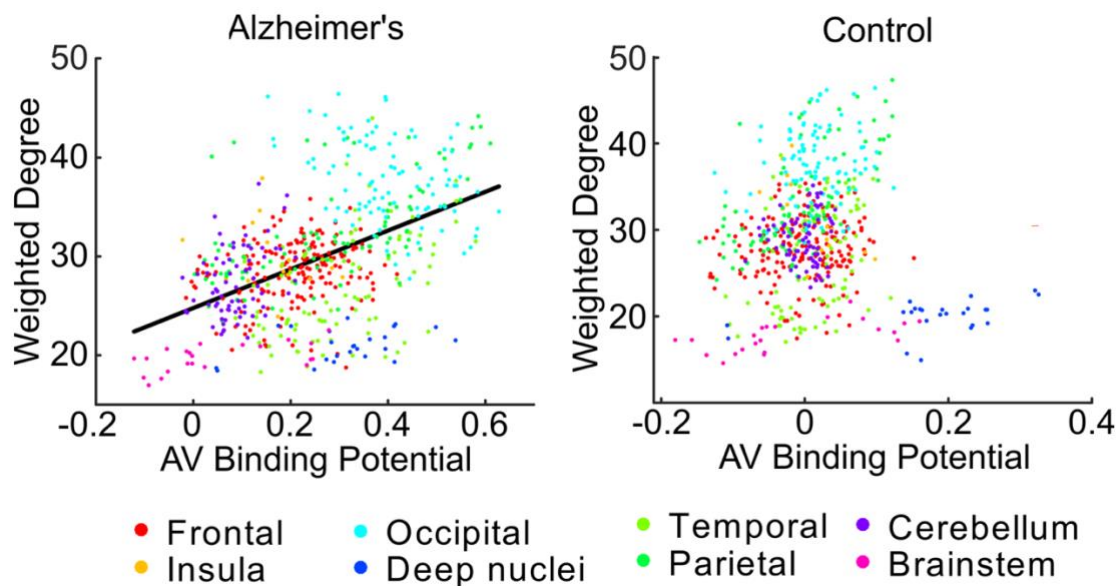


Figure 12: Relationship between tau pathology and weighted degree.

Connection strength (weighted degree) at each node plotted against ^{18}F -AV-1451 binding potential at that node. A statistically significant linear relationship is only found in Alzheimer's disease but not controls.

4.7.2. Reduced cortical connectivity strength in AD

To assess the impact of the presence of tau on connection strength, we first averaged weighted degree across the whole brain, resulting in a single measure for each individual. As the overall number of connections in each individual graph was thresholded at an identical network density, this measure represented the average strength of the strongest X% of connections.

To assess global disease burden in AD, we averaged [^{18}F] AV-1451 binding values across the whole-brain. In AD patients, a negative correlation between average connection strength and global tau burden was found ($r=-0.58$, $p=0.015$). We hypothesised that this effect would be greatest in those regions that display the strongest functional connectivity in the healthy brain, and which we have demonstrated to accrue most tau in AD. We assessed this by repeating the correlation of global disease burden against weighted degree at every individual node. The gradient of this node-wise relationship reflects a measure of local change in weighted degree with disease burden (**Figure 13**).

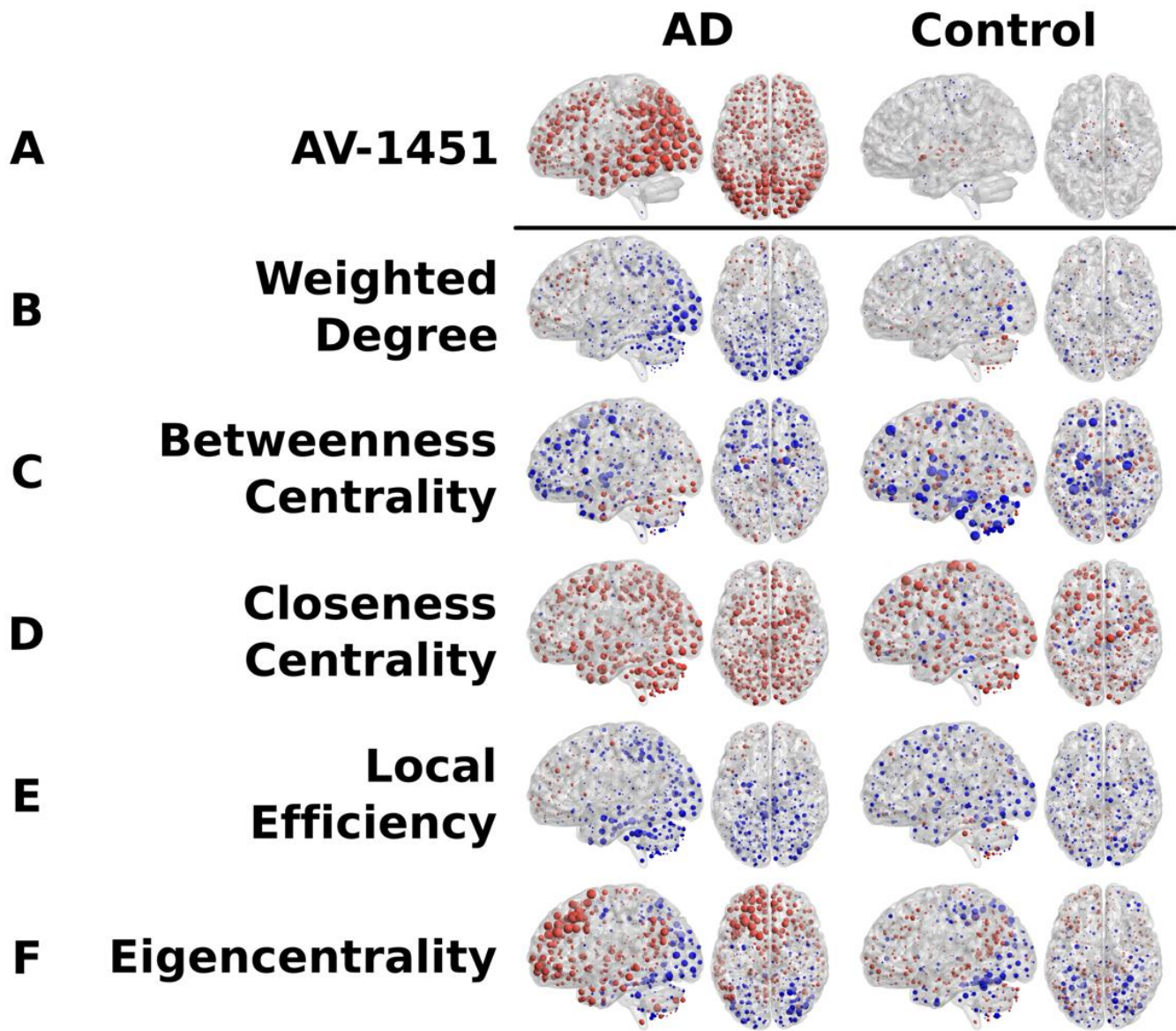


Figure 13: Relationship between tau pathology and local connectomic indices.

(A) Average ^{18}F -AV-1451 binding potential at each node in Alzheimer's disease (AD) patients and controls. (B-F) The local tau burden-related change in terms of connectomic metrics is plotted for each group at each node. *Red* spheres represent local *increases* as a result of greater overall tau burden; *blue* spheres represent local *decreases*.

Firstly, we examined whether the whole-brain average relationship could be replicated in these individual gradients, by performing sign tests. For AD, a negative relationship was confirmed ($Z=-13.0$, $P<0.0001$); while for controls no relationship was demonstrated using either whole brain ($Z=-1.1$, $P=0.27$) or deep brain ($Z=1.1$, $P=0.27$) tau burden.

Next, we assessed whether the functional connectivity change at each node related to local tau burden, by correlating the gradient of the disease-related change with the disease-associated increase in [^{18}F] AV-1451 binding potential at each node (**Figure 13**). A negative correlation between these measures was demonstrated in AD ($r=-0.30$, $P<0.0001$) but not controls ($r=-0.01$, $P=0.75$). Finally, we assessed whether the functional connectivity change at each node related to the strength of its connections in the healthy control brain. As would be expected from the propensity of highly connected nodes to accrue tau, a negative relationship was demonstrated in AD ($r=-0.23$, $P<0.0001$). Importantly, however, this relationship explained less variance than AV binding, with which we have demonstrated it to be correlated.

In summary, nodes that are constitutionally more strongly connected, such as those in parietal and occipital lobes, are more likely to accrue tau pathology in AD patients. Once present, the tau pathology causes local functional connectivity strength to fall.

4.7.3. Local connectivity reorganization relates to local tau pathology in AD

As illustrated in **Figure 14**, the reorganisation of graph metrics followed two distinct patterns.

Closeness centrality displayed a global effect, with most nodes increasing in AD. This was not related to local [^{18}F] AV-1451 binding potential in AD ($r=0.05$, $P=0.25$).

By contrast, eigen-centrality was more strongly related to local [^{18}F] AV-1451 binding in AD ($r=-0.28$, $P<0.0001$). Strikingly, the positive relationship we demonstrated across the whole brain masked opposing regional effects. As global tau burden increased, the functional influence of frontal regions on all other regions increased, while that of occipital regions decreased.

Both local efficiency and betweenness centrality displayed an intermediate degree of regional specificity in AD, being moderately correlated with change in [^{18}F] AV-1451 binding in AD (local efficiency $r=-0.16$, $P<0.0001$, betweenness centrality $r=-0.19$, $P<0.0001$).

Weighted Degree

Betweenness Centrality

Closeness Centrality

Local Efficiency

Eigencentrality

- Frontal
- Insula
- Temporal
- Parietal
- Occipital
- Deep nuclei
- Cerebellum
- Brainstem

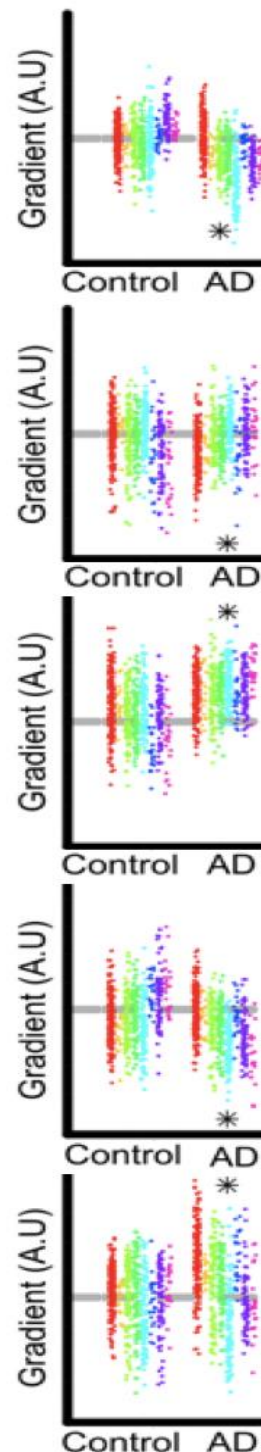


Figure 14: The magnitude of disease-related change at each node. The magnitude of disease-related change at each node is plotted as a single point, grouped by lobe. Stars represent statistically significant excesses of positive or negative gradients in each group. AD, Alzheimer's disease group.

4.8. Discussion

We have demonstrated that in Alzheimer's disease a relationship exists between the propensity of a node to display elevated 18F-AV-1451 binding and the volume of cortex to which it is connected.

Furthermore, we have explored the consequences of tau accumulation with cross-sectional analyses at a variety of spatial scales. In Alzheimer's disease, we have demonstrated that with greater levels of tau pathology the strongest internodal connections are weakened. This reorganization of the brain network leads to more direct long-range connections passing through fewer nodes, at the cost of lower local efficiency.

It has been proposed that the pathological mechanisms underlying AD begin in a single, vulnerable location and spread from cell to cell, rather than occurring independently in a large number of vulnerable cell populations (Guo and Lee, 2014; Goedert, 2015). The primary direct evidence for such propagation of tau comes from rodent studies. For example, the injection of brain extract from transgenic mice expressing mutant tau into mice expressing wild-type human tau caused wild-type tau to form filaments and spread to neighbouring brain regions (Clavaguera *et al.*, 2009).

Furthermore, pathological tau from human brains causes disease in wild-type mice, in which the pathological human tau species becomes self-propagating (Clavaguera *et al.*, 2013). This tau propagation is mediated by the presence and strength of synaptic connectivity rather than spatial proximity (Liu *et al.*, 2012; Iba *et al.*, 2013; Ahmed *et al.*, 2014). Associative studies of the healthy brain have demonstrated that large-scale, functionally connected neural networks strongly resemble the known patterns of atrophy in distinct neurodegenerative syndromes (Zhou *et al.*, 2012).

Here, we go beyond these studies to measure tau burden and functional connectivity in the same individuals at both the whole-brain and regional

level. We observe that those brain areas that are more functionally connected show more tau pathology in Alzheimer's disease. We demonstrate that the presence of tau is not, in itself, inducing stronger regional connectivity by our cross-sectional analysis of the Alzheimer's disease group, in which we demonstrate that higher cortical tau relates to overall lower functional connectivity.

Crucially, we demonstrate that ^{18}F -AV-1451 binding potential at each node is better than the connectivity of that node in the healthy brain at accounting for regional variance in connectivity change, arguing against the presence of tau being a secondary marker of neurodegeneration in vulnerable hubs. In other words, it is not coincidence that Alzheimer's disease tends to impact large networks; it is a predictable consequence of trans-neuronal spread of a disease-causing protein. Graph theoretic models of transmissible disease epidemics are in agreement that the likelihood of an individual becoming infected (and the dose of the infectious agent received) is directly proportional to its number of infected neighbours and their infectivity (Durrett, 2010).

As our nodes represent brain regions of equal volume, the binary portion of degree represents a surrogate measure of the number of neurons to which a brain region is connected, and the weighted portion of degree is a measure of the strength of these connections. By the time Alzheimer's disease is sufficiently advanced to cause symptoms, tau is generally already present to some degree throughout the neocortex (Markesbery, 2010), and therefore reaching a disease stage at which the number of neighbours more closely approximates the number of infected neighbours, and the connection strength between infected neighbours (here the weighted portion of degree) becomes a strong driver of infectivity.

Conversely, our analyses do not provide support for models of hub vulnerability in Alzheimer's disease. It is important to acknowledge that this does not mean that these mechanisms are unimportant, but rather that

they may be a downstream event of tau accumulation. In other words, while we demonstrate that the propensity of a node to accrue tau is not related to trophic support, these factors might still contribute to determining the vulnerability of brain regions to the presence of a given amount of tau. This hypothesis could be addressed in future studies by relating the information content of tau ligand binding to other measures of neurodegeneration such as longitudinal changes in grey matter volume.

There are a series of limitations of our study. First, our analysis was cross-sectional, and we used 18F-AV-1451 binding as a surrogate marker of tau burden. By making observations about the relationship between tau burden and functional connectivity in this way, we assume a uniformity of effect within our disease groups. Longitudinal assessment of tau burden and functional connectivity in the same individuals will be an important and powerful validation of our results. Evidence of the causal relationship between tau and connectivity will also require interventional studies targeting tau pathology.

Second, it should also be noted that 18F-AV-1451 binding identifies predominantly aggregated tau in tangles, and does not directly measure oligomeric tau, nor extracellular forms of tau that may mediate spread of pathology and which may be more toxic to the cell and synaptic plasticity.

Third, our analysis is focused towards cortico-cortical functional connectivity. In particular, multi-echo MRI might have a poor signal-to-noise ratio in deep brain structures, although the main advantage of using this sequence is that it enables robust de-noising of movement-related artefacts pipeline (Kundu et al., 2012, 2013). This is critical in clinical populations, in which functional MRI data may differentially suffer from quality degradation due to head movements.

Fourth, by examining proportionately thresholded graphs with 1–10% density, our analysis focusses on the strongest interregional functional

connections. However, it is possible that we are missing additional effects of neurodegeneration on weak or medium-strength connections. Tract-tracing studies indicate that there are weak anatomical connections, equivalent to a few axons, between some cortical areas (Ypma and Bullmore, 2016). Such weak links may have functional importance in complex networks (Granovetter, 1983). However, weak connections are difficult to evaluate with functional MRI, as it is not possible to disentangle them from correlation arising from signal noise. Future evaluation of these weaker connections with in vivo tractography, neuropathology or novel methods might reveal additional effects not evident in our dataset.

In the interim, the thresholding procedure retains several advantages; by retaining only the most strongly correlated edges one is less likely to include false positive correlations and topologically random edges. It also allows the computationally intense process of normalization of metrics against random graphs of equal density. The consistency between the results using thresholded nodal weighted degree and unthresholded nodal connectivity strength provides reassurance in the choice of thresholding of connections.

To conclude, this study reveals the relationship between tau burden and functional connectivity in AD. Our results have wide-ranging implications, from the corroboration of models of tau trafficking in humans to validating computational models of hub compensation in Alzheimer's disease. These insights into the relationship between tau burden and brain connectivity changes will inform translational models and clinical trials of disease-modifying therapies.

Chapter 5 | [¹¹C]PK11195 PET to assess microglia activation in Alzheimer's disease

5.1. Introduction

In this Chapter, I present part of the findings of my recently published study, in which I assess *in vivo* neuroinflammation in AD via PET imaging (Passamonti *et al.* 2018).

Neuro-inflammation is a common feature in the pathogenesis of AD and other neurodegenerative disorders. Animal and human studies have indeed provided converging evidence that microglia, the brain's principal innate immune system, show increased activation in AD, Parkinson's disease (PD), Huntington's disease (HD), and other neurodegenerative disorders (Fernandez-Botran *et al.* 2011b; Edison *et al.* 2013b; Schuitmaker *et al.* 2013b; Fan *et al.* 2015b; Stefaniak & O'Brien 2016b).

For example, the release of cytokines like interleukin-1 β and TNF- β , mediated by the microglia, can accelerate neurodegeneration and synaptic loss in AD (Fernandez-Botran *et al.* 2011b), while microglia can also promote phagocytosis and clearance of amyloid plaques (Wisniewski *et al.* 1991).

In addition, genetic associations studies in different neurodegenerative disorders reveal variations in genes that contribute to immune signalling and response (Villegas-Llerena *et al.* 2016). For example, variations in genes such as *SORL1* (sortilin-related receptor) and *TREM2* (triggering receptor expressed on myeloid cells 2) that have been involved in inflammation and immune responses have been suggested as risk factors of late onset AD on the basis of a genome-wide association studies (GWAS) (Villegas-Llerena *et al.* 2016).

This raises the possibility of immune-therapeutic strategies for prevention and disease modification.

However, key issues remain to be addressed before such strategies could be employed, including the confirmation of clinico-pathological correlations of inflammation and the potential utility of imaging biomarkers for measuring and tracking inflammation in the central nervous system. Despite the importance of neuro-inflammation in AD, there is still insufficient information regarding the extent and regional distribution of microglia-activation in patients with AD, and the clinical correlates of inflammatory biomarkers.

Inflammation in the central nervous system can be measured indirectly, using positron emission tomography (PET) in conjunction with radio-ligands like [¹¹C]PK11195 which bind to the mitochondrial translocator protein (TSPO) in activated microglia. Ligands such as [¹¹C]PK11195 are well established biomarkers of neuro-inflammation, although one must bear in mind that microglial activation represents only part of the complex cascade of events in neuro-inflammation (Agostinho *et al.* 2010). Relative to controls, [¹¹C]PK11195 PET has been shown to be abnormal in AD, PD, Huntington's disease (Cagnin *et al.* 2001a; Gerhard *et al.* 2006a, 2006b; Anderson *et al.* 2007; Edison *et al.* 2013a); although results across studies were mixed (Kropholler *et al.* 2007; Wiley *et al.* 2009).

Differences in the magnitude and regional distribution of microglial activation also need to be related to the cognitive deficit. In this study, I used the [¹¹C]PK11195 tracer, a well-established PET marker of *in vivo* microglial activation (Agostinho *et al.* 2010) to assess the magnitude and patterns of [¹¹C]PK11195 binding in patients with AD and MCI (with positive amyloid PET PiB scan) in comparison to age- and education-matched healthy controls. I also assessed whether the [¹¹C]PK11195 binding in different brain regions related to cognitive deficit in AD.

5.2. Main aim and hypotheses

The main aim of the study described in this chapter were to test the following hypotheses:

1) that patients with AD and MCI+ show increased microglia activation in cortical and sub-cortical areas typically associated with AD pathology, including the medial temporal lobe as well as parietal and lateral temporal cortices (Serrano-Pozo *et al.* 2011).

2) that higher microglia activation in brain regions which are characteristic of AD-related pathology (e.g., medial temporal lobe) is correlated with cognitive deficit.

5.3. Participants

The same group of AD and MCI+ patients previously described in chapter 3 and chapter 4 was included in this study.

However, a different group of thirteen age-, education-, and sex-matched healthy controls with no history of major psychiatric or neurological illnesses, head injury or any other significant medical co-morbidity (in particular, systemic inflammatory or auto-immune disorders disorders) was included here to allow group-wise comparisons with the AD cohort.

The control participants included in this study were different from those described in chapter 3 and 4 due to ethical reasons that limited the amount of PET-related radiation in healthy participants.

Details of participant demographics and cognitive features are provided in **Table 5**. **Table 6** also shows that there are no demographic or clinical differences between the group of clinically probable AD patients and the MCI+ patients.

Demographic & Clinical data	AD / MCI+ (n=15)	Controls (n=13)	Group difference
Sex (males/females)	9/6	5/8	N/S
Age (years) (SD, range)	71.6 (\pm 8.7, 54-85)	68.0 (\pm 5.3, 59-81)	NS
Education (years) (SD, range)	13.8 (\pm 3.1, 10-19)	14.1 (\pm 2.7, 10-19)	NS
MMSE (SD, range)	25.5 (\pm 2.8, 18-28)	28.7 (\pm 1.0, 27-30)	F=7.60, P=0.002
ACE-R (SD, range)	75.9 (\pm 11.0, 51-89)	91.3 (\pm 5.3, 79-99)	F=7.58, P=0.002
RAVLT (SD, range)	1.3 (\pm 1.4, 0-4)	9.7 (\pm 3.2, 3-15)	F=8.93, P<0.0001

Table 5: Participants' demographic and clinical details (microglia PET study).

Participant details (mean, with standard deviation (SD) and range in parentheses) and group differences by chi-squared test or one-way analysis of variance. AD/MCI+: Alzheimer's disease/mild cognitive impairment (amyloid positive on Pittsburgh Compound-B positron emission tomography scan); MMSE: Mini Mental State Examination; ACE-R: Addenbrooke's Cognitive Examination Revised, RAVLT: Rey Auditory-Verbal Learning Test (delayed recall, 30 minutes). NS, not significant at $P<0.05$ (uncorrected).

Demographic & Clinical data	AD (n=9)	MCI+ (n=6)	Controls (n=13)	Group difference
Sex (males/females)	2/7	4/2	5/8	N/S
Age (years) (SD, range)	69.4 (\pm 10, 54-85)	72.2 (\pm 9.7, 58-83)	68.0 (\pm 5.3, 59-81)	NS
Education (years) (SD, range)	15.1 (\pm 3.2, 10-19)	13.0 (\pm 2.9, 10-18)	14.1 (\pm 2.7, 10-19)	NS
MMSE (SD, range)	25.1 (\pm 3.4, 18-28)	26.2 (\pm 1.1, 25-28)	28.7 (\pm 1.0, 27-30)	F=6.43, P=0.04
ACE-R (SD, range)	72.9 (\pm 11.7, 51-89)	80.3 (\pm 8.0, 66-87)	91.3 (\pm 5.3, 79-99)	F=4.9, P=0.02
RAVLT (SD, range)	0.9 (\pm 1.3, 0-4)	1.2 (\pm 1.2, 0-3)	9.7 (\pm 3.2, 3-15)	F=11.3, P<0.0001

Table 6: Clinical details in AD, MCI+, and controls (microglia PET study).

Participant details (mean, with standard deviation (SD) and range in parentheses) and group differences by chi-squared test or one-way analysis of variance. AD/MCI+: Alzheimer's disease/mild cognitive impairment (amyloid positive on Pittsburgh Compound-B positron emission tomography scan); MMSE: Mini Mental State Examination; ACE-R: Addenbrooke's Cognitive Examination Revised, RAVLT: Rey Auditory-Verbal Learning Test (delayed recall, 30 minutes). NS, not significant at $P<0.05$ (uncorrected).

5.4. PET protocol

[¹¹C]PK11195 was produced with high radiochemical purity (>95%). [¹¹C]PK11195 specific activity was around 85 GBq/μmol at end of synthesis. The emission protocol was 75 minutes of dynamic imaging (55 frames) starting concurrently with a 500 MBq [¹¹C]PK11195 injection.

Each emission frame was reconstructed using the PROMIS 3-dimensional filtered back projection algorithm into a 128x128 matrix 30cm trans-axial field of view, with a trans-axial Hann filter cut-off at the Nyquist frequency (Kinahan & Rogers 1989b). Corrections were applied for randoms, dead time, normalization, scatter, attenuation, and sensitivity. Each emission image series was aligned using SPM8 to reduce the effect of patient motion during data acquisition.

The mean aligned PET image (and hence the corresponding aligned PET image series) was rigidly registered to the T1-weighted MR image. For [¹¹C]PK11195, supervised cluster analysis was used to determine the reference tissue time-activity curve (Turkheimer *et al.* 2007). All ROI data were corrected for CSF contamination through division with the mean ROI probability (normalized to 1) of grey + white matter, using SPM8 probability maps smoothed to PET resolution. To test whether correction for CSF affected the main results, I repeated all the [¹¹C]PK11195 ROI PET analyses using data not corrected for CSF contamination.

To compare [¹¹C]PK11195 binding across groups (AD/MCI+ and controls), individual ROI binding values for [¹¹C]PK11195 were used in a repeated-measures general linear model (GLM) to test for the main effect of ROI, main effect of group, and group × ROI interaction. Age and sex were included as covariates of no interest. For the AD/MCI+ group, we also tested Pearson's correlations between regional [¹¹C]PK11195 BP_{ND} and cognitive impairment using the RAVLT scores. All analyses were repeated using [¹¹C]PK11195 BP_{ND} values that were not corrected for CSF partial volume effects.

5.5. PET findings

The mean [^{11}C]PK11195 BP_{ND} voxel-wise maps (**Figure 15**) and ROI analyses (**Figure 16**), indicated that in both groups (including controls), the highest binding of [^{11}C]PK11195 was localized to the thalamus, basal ganglia, and brainstem.

In the repeated-measures GLM of regional binding, we found a significant main effect of ROI ($F_{2,36}=3.8$, $P<0.001$), main effect of group ($F_{2,36}=5.7$, $P<0.006$), and a group \times ROI interaction ($F_{2,70}=2.6$, $P<0.001$). The group and interaction effects were driven by higher [^{11}C]PK11195 binding in the AD/MCI+ relative to the control group, in the occipital, parietal, and temporal cortices, as well as in the hippocampus, amygdala, and other medial temporal lobe ROIs (post-hoc t-tests, T 's >2.0 , P 's <0.05).

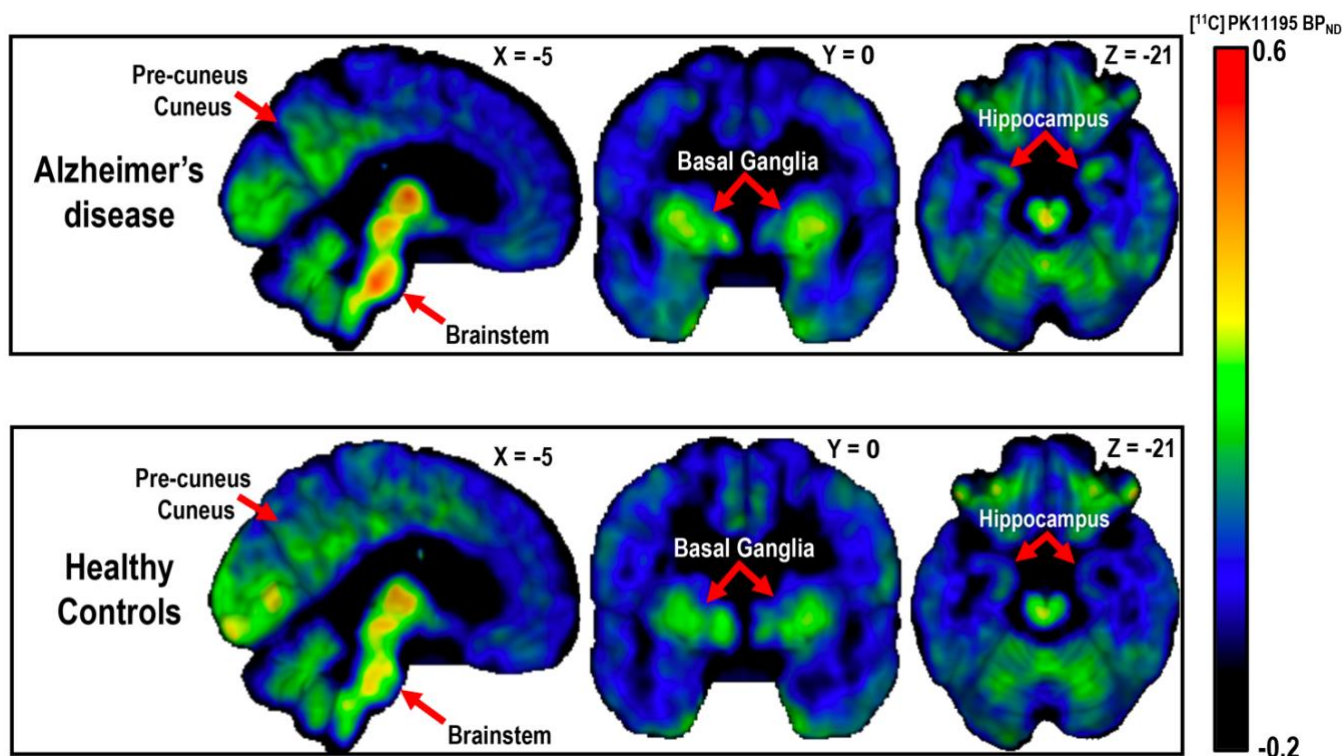


Figure 15: [^{11}C]PK11195 findings in AD/MCI+ and controls (voxel-wise data).

Mean [^{11}C]PK11195 PET map in each group. Patients with AD pathology (including clinically probable AD and MCI+ patients) showed increased [^{11}C]PK11195 binding in medial temporal lobe regions and other cortical areas, relative to controls.

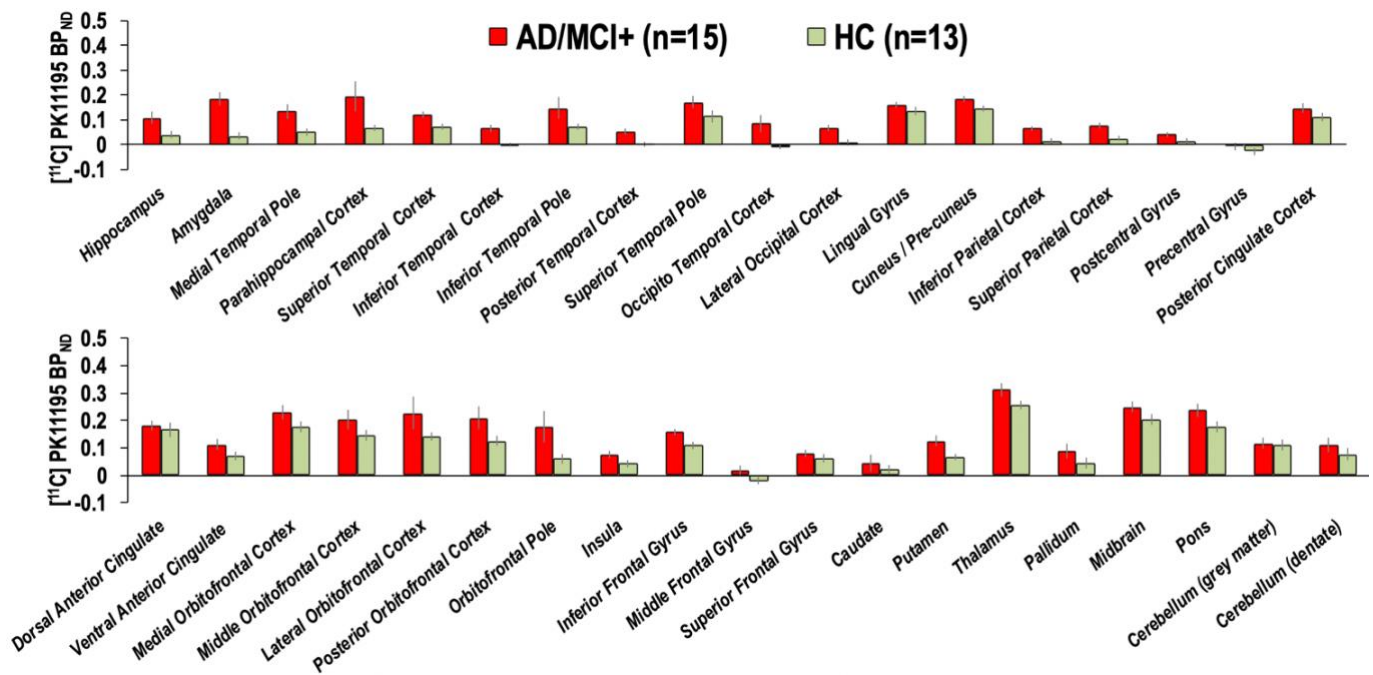


Figure 16: $[^{11}\text{C}]$ PK11195 findings in AD/MCI+ and controls (ROI analyses).

Mean (\pm standard error) $[^{11}\text{C}]$ PK11195 non-displaceable binding potential (BP_{ND}) in each region of interest for the participant groups: Alzheimer's disease (AD) and amyloid positive mild cognitive impairment (MCI+); healthy controls (HC). The $[^{11}\text{C}]$ PK11195 BP_{ND} data reported here are corrected for cerebro-spinal fluid (CSF) contamination.

Next, I examined the $[^{11}\text{C}]$ PK11195 ROI binding in AD and MCI+ groups separately, relative to controls, with the caveat of the small sample size in each group of patients (AD=9, MCI+=6). Nevertheless, there were still group and interaction effects that were driven by higher $[^{11}\text{C}]$ PK11195 binding in the patients' groups relative to controls ($F=3.8$, $P<0.01$), although the difference between AD and MCI+ patients were overall not significant (post-hoc t-tests, T 's <1.7 , P 's >0.09) (**Figure 17**).

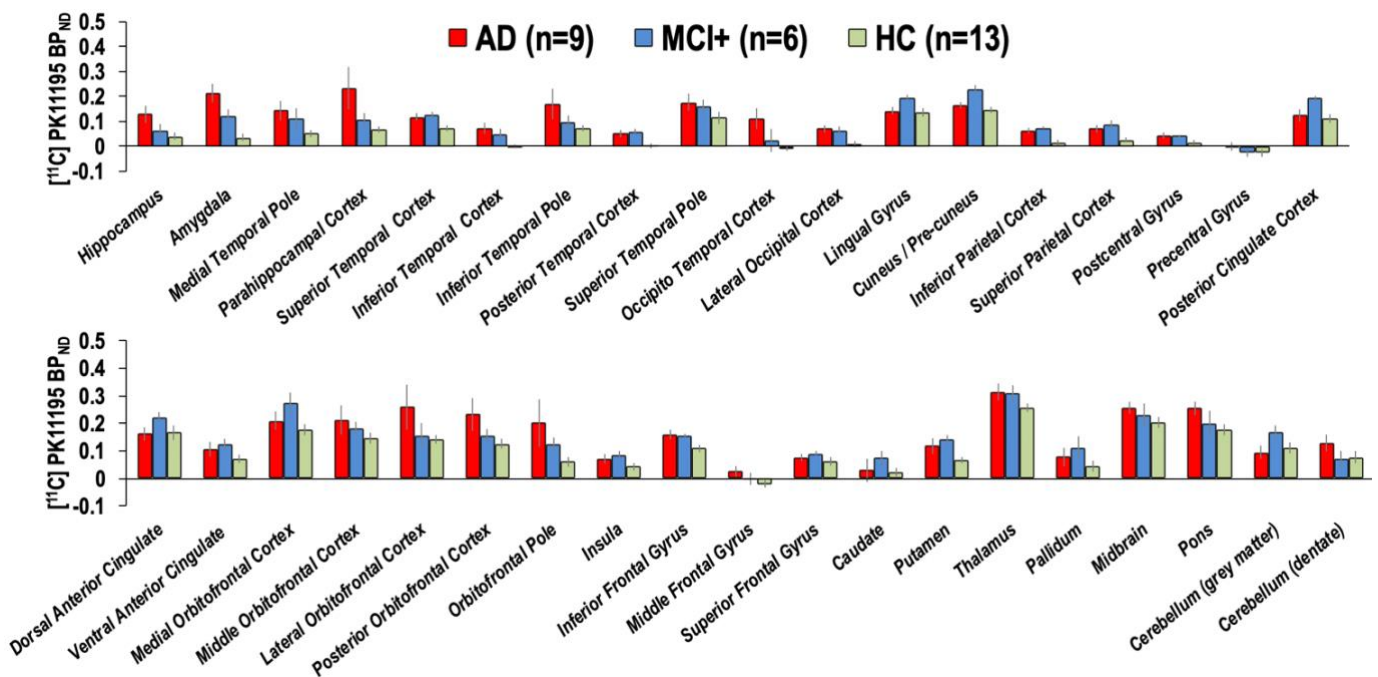


Figure 17: $[^{11}\text{C}]$ PK11195 findings in AD, MCI+, and controls (ROI analyses).

Mean (\pm standard error) $[^{11}\text{C}]$ PK11195 non-displaceable binding potential (BP_{ND}) in each region of interest for the participant groups: clinically probable Alzheimer's disease (AD), amyloid positive mild cognitive impairment (MCI+) (red bars); healthy controls (HC) (green bars). The $[^{11}\text{C}]$ PK11195 BP_{ND} data reported here are corrected for cerebro-spinal fluid (CSF) contamination.

Repeating these analyses using the ROI $[^{11}\text{C}]$ PK11195 binding values that were not corrected for CSF partial volume effects yielded similar results ($F=2.2$, $P<0.0001$, for the main effect of ROIs; $F=6.1$, $P<0.006$ for the main effect of group; and $F=2.0$, $P<0.0001$ for the group \times ROI interaction). This additional analysis demonstrate that our main findings were robust against between-groups effects that might have been driven by differences in grey-matter atrophy between patients and controls.

We then tested whether regional $[^{11}\text{C}]$ PK11195 binding related to memory deficits in patients with AD/MCI+. In this group, there was a significant *negative* correlation between the RAVLT scores (delayed recall at 30 minutes) and $[^{11}\text{C}]$ PK11195 binding in the cuneus / pre-cuneus ($r=0.50$, $P<0.05$). Repeating the correlation analyses when using the ROI $[^{11}\text{C}]$ PK11195 binding values that were not corrected for CSF volume made the result in the AD/MCI+ group not-significant ($R=0.31$, $P=0.2$).

5.6. Discussion

This study demonstrates that AD, in the form of clinically probable AD and MCI with biomarker evidence of AD pathology is associated with significantly increased *in vivo* microglia activation, as indexed by the [¹¹C]PK11195 ligand.

The brain regions with the most marked abnormalities of [¹¹C]PK11195 binding in AD/MCI+ were those predicted from the established distribution of neurodegeneration in AD. Specifically, patients showed increased inflammation in the medial temporal lobe as well as parietal and lateral temporal cortices relative to controls (Braak & Braak 1995; Braak *et al.* 2006a; Ossenkoppele *et al.* 2016b; Scholl *et al.* 2016b; Schwarz *et al.* 2016c).

Together, these data demonstrate that the density and distribution of activated microglia in living patients with AD mirror the typical pathological changes characteristic of this disorder. This could result from a causal link between neuroinflammation and neurodegeneration, although the association might also derive from the process of neurodegeneration *itself*.

A cross-sectional and non-interventional study such as this one cannot alone provide the direction of causality. Nevertheless, the disease-specific anatomical distributions of activated microglia in AD suggest a regional association rather than a side effect of a global increased [¹¹C]PK11195 binding in response to a systemic inflammatory insult.

Our PET data are also in keeping with *post mortem* findings, which demonstrated that microglia burden (as assessed via LN3-immunostaining) and cytokine expression (i.e., IL-1 β and TGF- β expression) show a disease-specific topological relationship with the pathological hallmarks of AD (McGeer & McGeer 2001).

More specifically, AD patients have significantly higher microglia density and IL-1 β expression in the parietal and other posterior cortices when compared to controls. The expression of TGF- β is also increased in the same cortices in AD patients, relative to controls. Overall, this suggests that microglia activation and cytokine expression co-exist with the pathogenic processes underlying AD and could contribute to the on-going neurodegeneration. If this is the case, this would warrant the further investigation of immune-therapeutic strategies to modulate neuro-inflammation in AD, although evidence from earlier anti-inflammatory trials in AD remains controversial (Adapt Research Group *et al.* 2007, 2008).

My data also confirmed the hypothesis that [^{11}C]PK11195 binding correlates with episodic memory impairment as assessed via the RAVLT in patients with AD/MCI+, although these findings were only evident when the data were corrected for partial volume (which may reflect an effect of local grey-matter atrophy). Nevertheless, as for the main effect of group, this effect was not a global correlation, but adhered to the functional anatomy of typical cognitive symptoms in the amnesic form of AD and MCI with amyloid pathology.

Technical aspects of the PET methods need consideration. In particular, the supervised cluster method for estimating [^{11}C]PK11195 BP_{ND} could have introduced an under-estimation bias, as the reference tissue may have still included specific binding of the radio-ligand. If present, this would be likely to have reduced the effect sizes (increased type II error) rather than increasing type I error.

I also highlight that my data are specific to [^{11}C]PK11195 and do not inevitably generalize to second-generation ligands (e.g., PBR28) or alternative tracers of neuroinflammation over and above those that bind to the mitochondrial translocator protein (TSPO) (e.g., COX-1, MPO, macrophage infiltration) (Suridjan *et al.* 2015; Hamelin *et al.* 2016; Yokokura *et al.* 2016).

Further studies could assess the utility of such novel markers for *in vivo* imaging of neuroinflammation, bearing in mind that the binding of second-generation TSPO tracers such as PBR28 may be affected by genetic variations (i.e., the rs6971 polymorphism in the TSPO gene)(Owen *et al.* 2012).

In conclusion, my data provided evidence that [^{11}C]PK11195 is a sensitive PET ligand for *in vivo* studies of microglia activation in AD and its prodromal stage of MCI. This supports the further use of [^{11}C]PK11195 PET to assess microglia activation in neurodegenerative disorders and in clinical trials that aim to modulate neuroinflammation in AD.

Chapter 6 | Microglia activation and network dysfunction in Alzheimer's disease

6.1. Introduction

In this chapter, I examine the impact of *in vivo* neuroinflammation (described in Chapter 5) on brain-wide network function in AD. I also study how this functionally-relevant neuroinflammation is linked to cognitive deficit in AD. I undertake a multi-modal and multivariate imaging approach to combine [^{11}C]PK11195 quantification of regional neuroinflammation with resting-state functional imaging (rsfMRI) in patients at different stages of AD. Patients with AD and MCI+ were compared to age-, sex-, and education-matched healthy controls in terms of neuroinflammatory patterns, rsfMRI connectivity, and their relationship in mediating cognitive deficit.

Neuroinflammation plays a key role in the etio-pathogenesis of Alzheimer's disease and other neurodegenerative disorders (Edison *et al.* 2008a; Fernandez-Botran *et al.* 2011b; Fan *et al.* 2015b; Stefaniak & O'Brien 2016b). Pre-clinical models (Heppner *et al.* 2015; Hoeijmakers *et al.* 2016; Villegas-Llerena *et al.* 2016; Li *et al.* 2018; Wang *et al.* 2018), and research in humans (Edison *et al.* 2008a; Fernandez-Botran *et al.* 2011b; Fan *et al.* 2015b; Stefaniak & O'Brien 2016b), demonstrate that the microglia, part of the brain's innate immune system, are activated in Alzheimer's and related diseases.

Although the mechanisms and mediators of inflammatory risk in Alzheimer's disease are not fully understood, synaptic and neuronal injury may arise from the release of cytokines and pro-inflammatory molecules such as interleukin-1 β and TGF- β (Fernandez-Botran *et al.* 2011b), or direct microglial injury to synapses (Hong *et al.* 2016; Hong & Stevens 2016).

These, in turn, impair synaptic function, network communication, and may accelerate neurodegeneration and synaptic loss (Heppner *et al.* 2015; Hoeijmakers *et al.* 2016; Villegas-Llerena *et al.* 2016; Li *et al.* 2018; Wang *et al.* 2018). In addition, genetic association studies have demonstrated a link between Alzheimer's disease and polymorphisms and mutations of genes linked to immune responses (Villegas-Llerena *et al.* 2016).

Clinical studies of neuroinflammation in dementia have exploited positron emission tomography (PET) ligands that bind to the mitochondrial translocator protein (TSPO) in activated microglia (Cagnin *et al.* 2001b; Gerhard *et al.* 2004, 2006a; Edison *et al.* 2013a, 2013a; Fan *et al.* 2015c)[1, 2, 10, 13-17]. As shown in Chapter 5, patients with Alzheimer's disease, relative to controls, have higher [11C]PK11195 binding in the hippocampus, other medial-temporal lobe regions, and posterior cortices such as the pre-cuneus, which in turn correlates with cognitive deficit (Passamonti *et al.* 2018).

A critical and unanswered question is whether regional neuroinflammation changes the functional connectivity of large-scale networks. Such large-scale neural networks represent an intermediate phenotypic expression of pathology in many diseases, that can be non-invasively quantified with resting-state functional magnetic resonance imaging. A challenge is that neither the anatomical substrates of cognition nor the targets of neurodegenerative disease are mediated by single brain regions: they are in contrast distributed across multi-variate and interactive networks. In other words, neuroinflammation in AD is distributed across multiple brain networks, and the impact of AD may be seen through changes in multiple modalities of neural and cognitive functions. This multivariate nature of neuroinflammatory and cognitive mechanisms in AD calls for a different statistical approach to that used so far.

We therefore undertook a multimodal and multi-variate statistical approach to combine [^{11}C]PK11195 quantification of distributed neuroinflammation with resting-state functional imaging in patients at different stages of Alzheimer's disease (i.e., clinically probable AD and MCI with evidence of amyloid pathology).

The set of PET, rsfMRI, and cognitive data was complex, and our sample size was relatively small. Therefore, to reduce the dimensionality (i.e., complexity) of data we used the novel "source-based inflammetry" (SBI, directly analogous to 'source-based morphometry' of brain volumes). SBI is a statistical procedure that decomposes the PET images across all individuals in a set of spatially independent sources (Xu *et al.* 2009). This way it is possible to compute a spatially distributed (i.e., voxel-wise) single measure of microglia activation in each individual. This index can be next employed as a regressor term in second level analyses including functional connectivity patterns in the whole-brain as the main outcome measure.

SBI was augmented by multiple linear regression models that associated neuroinflammation, functional network connectivity in distinct components, and cognition.

6.2. Main hypotheses

I tested two hypotheses:

- 1) that microglia activation is associated with significant changes in large-scale functional connectivity in patients with AD, relative to controls;
- 2) that the relationship between microglia activation and functional connectivity changes is linked to cognitive impairment in AD.

6.3. Participants & Methods

In the analyses reported in this Chapter, I included 14 patients meeting clinical diagnostic criteria for probable AD (McKhann *et al.* 2011b), and 14 patients with MCI and biomarker evidence of amyloid pathology (positive Pittsburgh Compound-B PET scan) (MCI+) (Okello *et al.* 2009d).

Therefore, relative to the patients described in Chapter 3 and 5, an extra n=5 AD and n=8 MCI+ patients were included in this Chapter due to an additional recruitment wave that intercurrent across the studies. One further control was also enrolled since the experiments described in Chapter 3 and 5 leading to a total of fourteen age-, sex-, and education-matched healthy controls. A new table (**Table 7**) of demographic and clinical data is thus provided for comparison with Table 4 and 6.

Demographic & Clinical data	AD/MCI+ (N=28)	Controls (N=14)	Group differences
Sex (females/males)	12/16	8/6	NS
Age (years) (SD, range)	72.7 (\pm 8.5, 53-86)	68.3 (\pm 5.4, 59-81)	NS
Education (years) (SD, range)	12.9 (\pm 3.0, 10-19)	14.1 (\pm 2.7, 10-19)	NS
MMSE (SD, range)	25.6 (\pm 2.2, 21-30)	28.8 (\pm 1.0, 27-30)	T=4.9, P<0.0001
ACE-R (SD, range)	78.9 (\pm 7.7, 62-91)	91.6 (\pm 5.3, 79-99)	T=5.5, P<0.0001
RAVLT (SD, range)	1.5 (\pm 1.6, 0-6)	9.6 (\pm 3.2, 3-15)	T=10.8, P<0.0001

Table 7: Demographic and clinical data.

Participant details (mean, with standard deviation (SD) and range in parentheses) and group differences by chi-squared test, one-way analysis of variance or independent samples t-test. AD/MCI+: Alzheimer's disease/mild cognitive impairment (amyloid positive on Pittsburgh Compound-B positron emission tomography scan); MMSE: Mini Mental State Examination; ACE-R: Addenbrooke's Cognitive Examination Revised, RAVLT: Rey Auditory-Verbal Learning Test (delayed recall). NS, not significant with $p>0.05$ (uncorrected).

6.3.1. Clinical and cognitive assessment

Clinical indices of cognitive decline included Mini Mental State Examination (MMSE), Addenbrooke's Cognitive Examination-Revised (ACE-R), and Rey auditory verbal learning test (RAVLT).

For a single summary measure across the three cognitive scales, I conducted a Principal Component Analysis (PCA) on the ACE-R, MMSE, and RAVLT scores to reduce the dimensionality into one latent variable (cognitive deficit) which summarizes the largest portion of shared variance as the first principal component (COG-PC1).

6.3.2. rsfMRI pipeline

The location of the key cortical regions in each network was identified by spatial independent component analysis (ICA) using the Group ICA of fMRI Toolbox (GIFT)(Calhoun *et al.* 2001b) in an independent dataset of 298 age-matched healthy individuals from a large population-based cohort in the Cambridge Centre for Ageing and Neuroscience (Shafto *et al.* 2014b). Further details about pre-processing and node definition can be found in Tsvetanov and colleagues (Tsvetanov *et al.* 2016b).

Four networks were identified by spatially matching to pre-existing templates (Shirer *et al.* 2012b). First, the default mode network (DMN), which contained six nodes: the ventral anterior cingulate cortex (vACC), the middle posterior cingulate cortex (PCC), and the dorsal PCC (dPCC) which further divided in the left dPCC and right dPCC), and right and left inferior parietal lobes (rIPL and lIPL). Second, the frontoparietal network (FPN) which was defined using the left and right superior frontal gyrus (rSFG and lSFG) and left and right angular gyrus (rAG and lAG). Third, the cognitive network which included the right and left middle frontal gyrus (rMFG, lMFG). Fourth, the subcortical network that included the bilateral putamen (rPut and lPut) and hippocampus (rHipp and lHipp). The node time-series were defined as the first principal component resulting from the singular value

decomposition of voxels in a 8mm radius sphere, which was centred on the peak voxel for each node (Tsvetanov *et al.* 2016b). After extracting nodal time-series we sought to reduce the effects of noise confounds on functional connectivity effects of node time-series using a general linear model, GLM. This model included linear trends, expansions of realignment parameters, as well as average signal in the white-matter (WM) and cerebrospinal (CSF), including their derivative and quadratic regressors from the time-courses of each node. The WM and CSF signals were created by using the average across all voxels with corresponding tissue probability larger than 0.7 in associated tissue probability maps available in SPM12 (<http://www.fil.ion.ucl.ac.uk/spm/software/spm12/>).

A band-pass filter (0.0078-0.1 Hz) was implemented by including a discrete cosine transform set in the GLM, ensuring that nuisance regression and filtering were performed simultaneously. The GLM excluded the initial five volumes to allow for T1 equilibration. The total head motion for each participant, which was used in subsequent between-subject analysis as a covariate of no interest, was quantified using the approach reported in Jenkinson and colleagues (Jenkinson *et al.* 2002b), i.e. the root mean square of volume-to-volume displacement. As for the analyses reported in Chapter 4, we also used independent component analyses that separate the changes in the fMRI signal linked to the BOLD response from that associated with non-BOLD components (Kundu *et al.* 2012b, 2013a). This procedure has been shown to be particularly robust in de-noising fMRI data from several sources of noise including head movement (Kundu *et al.* 2012b, 2013a). Finally, the functional connectivity between each pair of nodes was computed using Pearson's correlation on post-processed time-series.

6.3.3. PET acquisition and analysis pipeline

All participants underwent [11C]PK11195 PET imaging to assess the extent and distribution of neuroinflammation while patients with MCI also underwent [11C]PiB (Pittsburgh compound-B PET) scanning to evaluate the degree of β -amyloid accumulation. [11C]PK11195 and [11C]PiB PET were

produced with high radiochemical purity (>95%), with [^{11}C]PiB PET having a specific activity >150 GBq/ μmol at the end of synthesis, whereas [^{11}C]PK11195 specific activity was ~85 GBq/ μmol at the end of synthesis. PET scanning used a GE Advance PET scanner (GE Healthcare) and a GE Discovery 690 PET/CT, with attenuation correction provided by a 15 min $^{68}\text{Ge}/^{68}\text{Ga}$ transmission scan and a low dose computed tomography scan, respectively. The emission protocols were 550 MBq [^{11}C]PiB injection followed by imaging from 40 to 70 min postinjection, and 75 min of dynamic imaging (55 frames) starting concurrently with a 500 MBq [^{11}C]PK11195 injection. Each emission frame was reconstructed using the PROMIS 3-dimensional filtered back projection algorithm into a 128×128 matrix 30 cm trans-axial field-of-view, with a trans-axial Hann filter cutoff at the Nyquist frequency (Kinahan and Rogers, 1989). Corrections were applied for randoms, dead time, normalization, scatter, attenuation, and sensitivity.

The [^{11}C]PK11195 maps were co-registered and warped to the Montreal Neurological Institute (MNI) space using the flow fields. To minimise the noise effects from non-GM regions, the normalised PK maps were masked with a group-based GM mask based on voxels having grey-matter tissue probability larger than 0.3 in GM-segmented images across all individuals. The normalised images were smoothed using a 6mm Gaussian kernel. We then used independent component analysis (ICA) across participants to derive spatial patterns of PK maps across voxels expressed by the group in a small number of independent components.

All PK maps were spatially concatenated and submitted to source-based 'inflammometry' (SBI) to decompose images across all individuals in a set of spatially independent sources without providing any information about the group, using the GIFT toolbox.

Specifically, the n -by- m matrix of participants-by-voxels was decomposed into:

- 1) a source matrix that maps Independent Components (ICs) to voxels (here referred to as PK_{IC} maps),

2) a mixing matrix that maps PKICs to participants.

The mixing matrix consists of loading values (1 per participant) indicating the degree to which a participant expresses a defined PKIC. The independent component loading values for the PKIC were taken forward to between-participant analysis of functional connectivity (**Figure 18**), if they were:

(1) differentially expressed by controls vs. patients with AD pathology;

(2) were associated with atrophy (see Results and **Figure 19**).

Only one dependent variable (IC3) met these criteria.

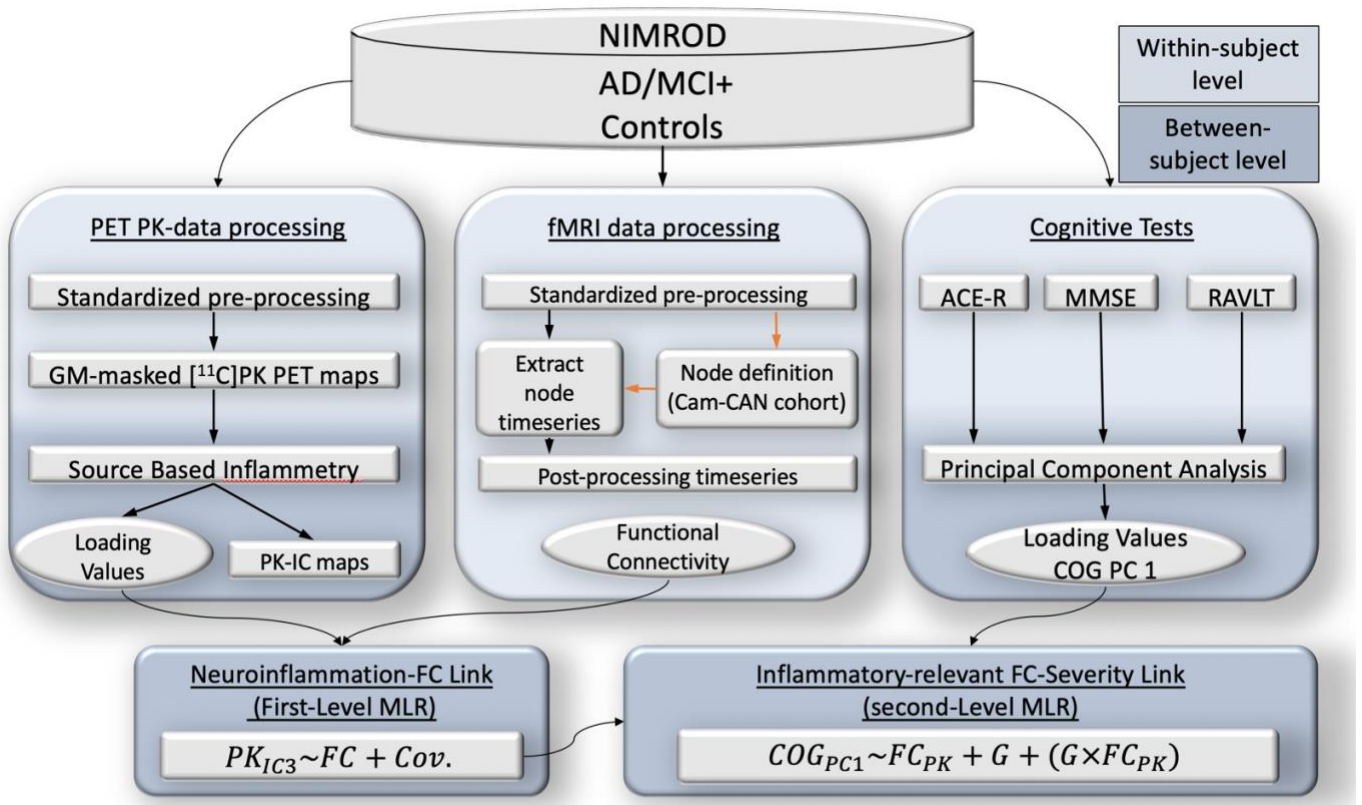


Figure 18: Pipeline analyses for the combined PET (microglia) and rsfMRI study.

Schematic representation of various modality datasets in the study, their processing pipelines on a within-subject level (light blue), as well as data-reduction techniques and statistical strategy on between-subject level (dark blue) to test for associations between the datasets. Abbreviations: PK_{IC} (Independent component [¹¹C]PK11195 maps); FC (functional connectivity); Cov. (covariates); COG PC1 (latent variable (cognitive deficit) which summarizes the largest portion of shared variance as the first principal component); MMSE (Mini Mental State Examination), ACE-R (Addenbrooke's Cognitive Examination-Revised); RAVLT (Rey auditory verbal learning test); GM (grey-matter); PiB (Pittsburgh Compound-B positron emission tomography); Cam-CAN (Cambridge Centre for Ageing and Neuroscience); AD/MCI+ (Alzheimer's disease and MCI PiB positive mild cognitive impairment patients); MLR (multiple linear regression analyses); NIMROD (Neuroimaging of Inflammation in MemoRy and Other Disorders study)

6.3.4. Statistical analyses

I adopted a two-level procedure, where at the first-level I sought to identify functional connectivity differences associated with differences in [^{11}C]PK11195 (PK) binding. In a second-level analysis we tested whether individual variability in PK-relevant functional connectivity (from first-level analysis) is specifically associated with variability in cognitive decline in the AD/MCI+ group.

For the first-level analysis, we used multiple linear regression (MLR) with well-conditioned shrinkage regularization to identify correlated structured sources of variance between functional connectivity and neuroinflammation measures. In particular, this analysis describes the linear relationship between functional connectivity and SBM-PK maps on a between-subject level, in terms of structure coefficients, by providing *subject scores* (i.e. a latent variable) of the functional connectivity measures that are optimised to be highly correlated with the between-subject variability in the expression of the PK maps. Namely, connectivity strength between pairs of network nodes for each individual defined the independent variables, and PK_{IC} subject-specific loading values for group differentiating components were employed as dependent variable. Covariates of no interest included age, years of education, gender, and head motion. This first-level MLR was integrated with a 5-Fold Cross-Validation.

To further minimize the non-negligible variance of traditional k-Fold cross-validation procedure, we repeated each k-Fold 1,000 times with random partitioning of the folds to produce an R-value distribution, for which we report the median values. Next, we tested the hypothesis that the effect of neuroinflammation on functional connectivity is related to cognitive deficits, in AD patients relative to controls. To this end, we performed a second-level MLR analysis.

Independent variables included subjects' brain scores from first level MLR, group information, and their interaction term (brain scores x group). The dependent variable was subjects' loading values of the first PCA across the three cognitive tests. Covariates of no interest included age, gender, head movement, and global GM volume.

6.4. Results

6.4.1. Source-Based 'Inflammation' (SBI)

The optimal number of components ($n=5$) was detected with minimum-distance length (MDL) criteria. One component showed significant differences between the AD and control groups in terms of their loading values (PK_{IC3} , t -value = -2.1, p -value = 0.046) (**Figure 19, right panel**).

The spatial extent of this PK_{IC3} included voxels with high values in cortical and subcortical regions, including the inferior temporal cortex and hippocampus, indicating that individuals with higher loading values, in this case the AD/MCI+ group, had high [^{11}C]PK11195 binding in these regions (**Figure 19, left panel**).

The other components did not differentiate patients from controls (**Figure 20, first row**). Interestingly, the PK_{IC3} component, which differed between AD patients and controls, was also the only SBI component that negatively correlated with total grey-matter values in AD patients but not controls (**Figure 20, 2nd and 3rd row**).

In other words, the AD patients expressing higher [^{11}C]PK11195 binding in the inferior temporal cortex and hippocampus showed also higher levels of cortical atrophy (**Figure 20, 2nd and 3rd row**). This implies that the PK_{IC3} component reflects AD-specific patterns of neuroinflammation and neurodegeneration. These patterns were next tested in terms of their relevance for changes in large-scale network function and their interactive effect in predicting cognitive deficit in AD.

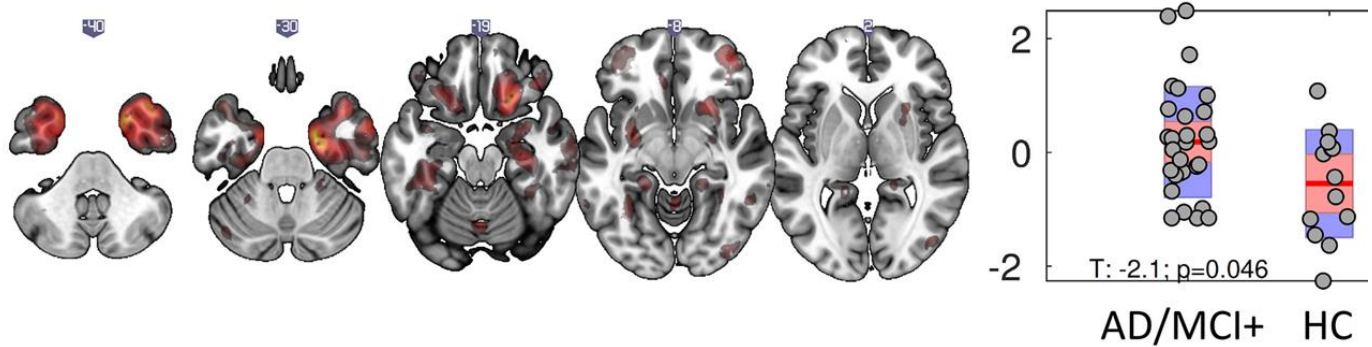


Figure 19: Source-based-'inflammation' (SBI) from $[^{11}\text{C}]\text{PK11195}$ PET imaging.

Source-Based Inflammation for the component differentially expressed between groups: (left) independent component (IC) spatial map reflecting increase in $[^{11}\text{C}]\text{PK11195}$ binding values in cortical and subcortical areas including inferior temporal cortex and hippocampus, regionally specific increase over and above global PK differences between groups (regions in red), (right) bar plot of subject loading values for AD/MCI+ and control group (each circle represents an individual) indicating higher loading values for AD/MCI+ than control group as informed by two-sample unpaired permutation test. AD/MCI+ (Alzheimer's disease and MCI PiB positive mild cognitive impairment patients).

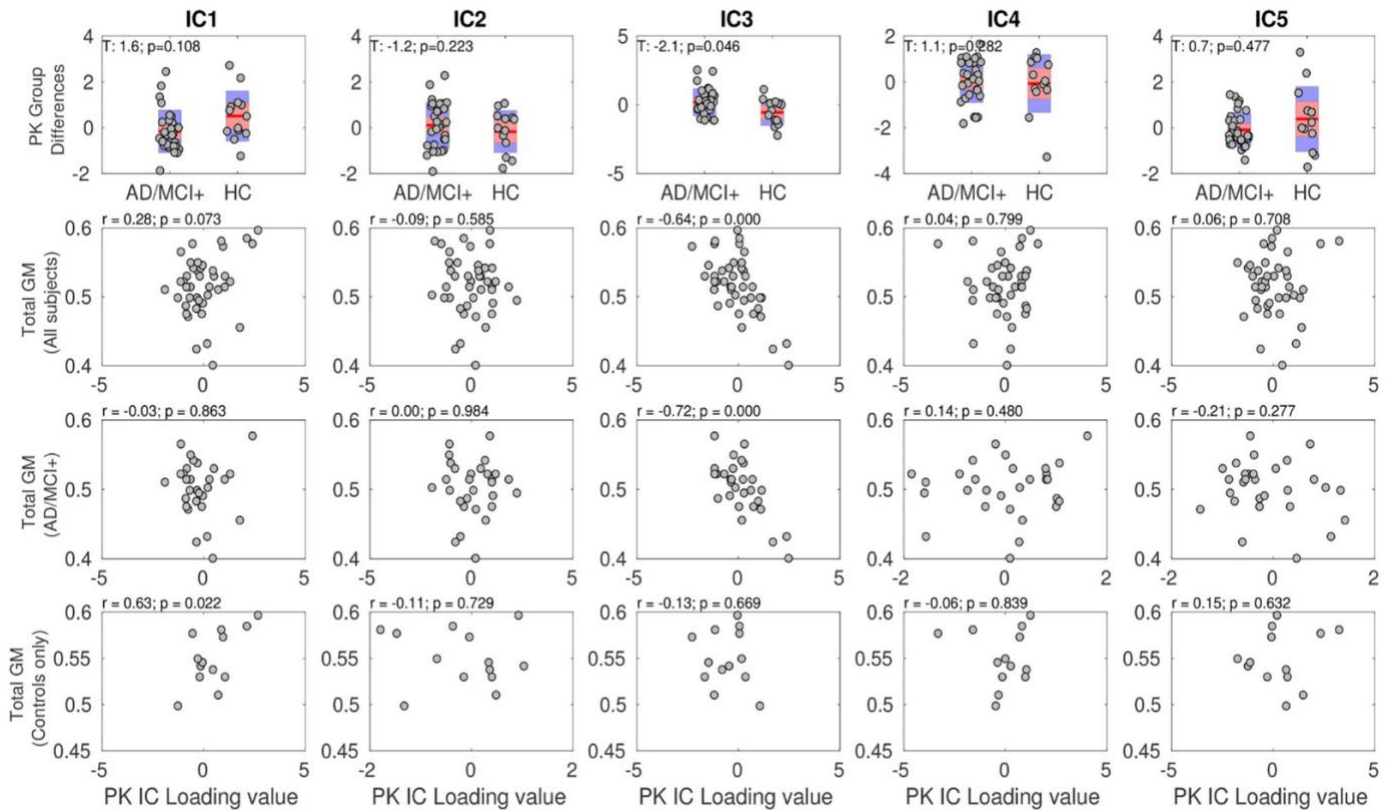


Figure 20: Source-based-'inflammation' (SBI) derived independent components .

The Source-Based Inflammation (SBI) identified five independent components (IC) which reflected [^{11}C]PK11195 (PK) binding values in cortical and subcortical areas. The PKIC3 component was the only component which differed between AD/MCI+ patients and controls (first row, third column). The PKIC3 component was also the only SBI component that negatively correlated with grey-matter volumes across the whole-brain in all individuals as well as in AD patients alone (but not controls) (second, third, and fourth rows). In other words, the AD patients expressing higher [^{11}C]PK11195 binding PKIC3 component (reflecting higher binding in the inferior temporal cortex and hippocampus as shown in Figure 2) also displayed higher levels of brain-wide atrophy.

6.4.2. Functional connectivity

There was a strong positive functional connectivity between all nodes within the four networks previously identified by spatially matching to pre-existing templates (**Figure 21, left panel**). In terms of group differences, the functional connectivity within the DMN and between the DMN and hippocampus was weaker in patients with AD/MCI+ relative to controls (**Figure 21, right panel**).

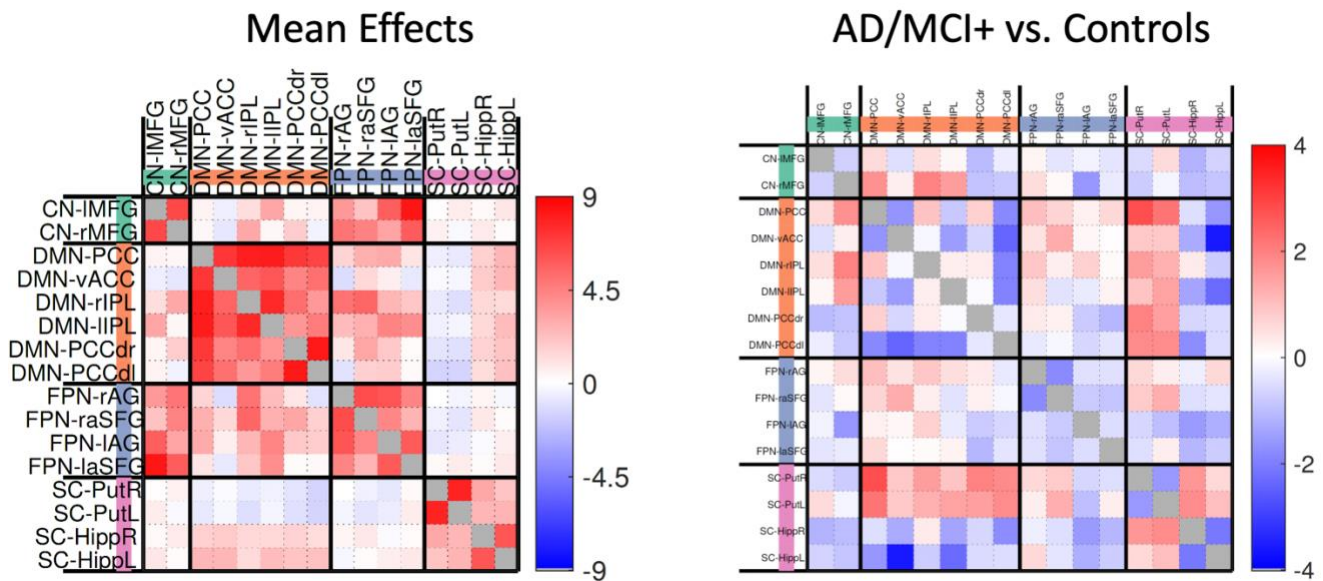


Figure 21: Mean effects of functional connectivity data from rsfMRI.

Mean effects (left) and group difference effects (AD/MCI+>Controls, right) between default mode network (DMN) and subcortical regions using univariate approach. CN- cognitive network, SC, sub-cortical network. ACC – anterior cingulate cortex; PCC – posterior cingulate cortex; IPL – intraparietal lobule; FPN – fronto-parietal network; Put – Putamen; Hipp – Hippocampus, AG – angular gyrus; SFG – superior frontal gyrus; R, right; L, left.

6.4.3. Functional connectivity and neuroinflammation

The first-level multiple linear regression (MLR) model assessing the relationship between PK_{IC3} maps and rs-fMRI connectivity data was significant ($r=0.52$, $p<0.001$).

The standard coefficients indicated a positive association between the PK_{IC3} loading values and variability in functional connectivity (**Figure 22, left panel**). In other words, individuals with higher [¹¹C]PK11195 binding values in the inferior temporal cortex and medial temporal lobe regions (as reflect by higher PK_{IC3} values) showed: 1) increased connectivity between the DMN and the hippocampus and other subcortical regions (putamen), and 2) weaker connectivity for nodes within DMN.

6.4.4. Linking neuroinflammation and connectivity to cognitive deficit

The first cognitive component explained the 80% of the variance across cognitive tests (coefficients: .61, .61 and .52 for ACE-R, MMSE, and RAVLT, respectively).

To investigate whether the effects of neuroinflammation on functional connectivity measures were specific to the AD/MCI+ group, especially in relation to cognitive deficits, we tested whether the interaction between group and *brain scores* from first level MLR was associated with COG_{PC1} using second-level MLR (see methods).

The interaction term was significant ($t=-3.4$, $p=0.004$). A *post-hoc* test within each group separately indicated opposite association between COG_{PC1} and functional connectivity/PK indices (i.e., the residuals) in the AD/MCI+ group ($r= -0.51$, $p=0.005$) and controls ($r=0.46$, $p=0.096$) (**Figure 22, right panel**).

The negative association in the AD/MCI+ group indicated that patients who expressed more strongly the pattern of functional connectivity associated with higher [^{11}C]PK11195 binding in cortical (i.e., inferior temporal cortex) and subcortical (i.e., hippocampus) regions performed worse on a summary measure of cognitive deficit.

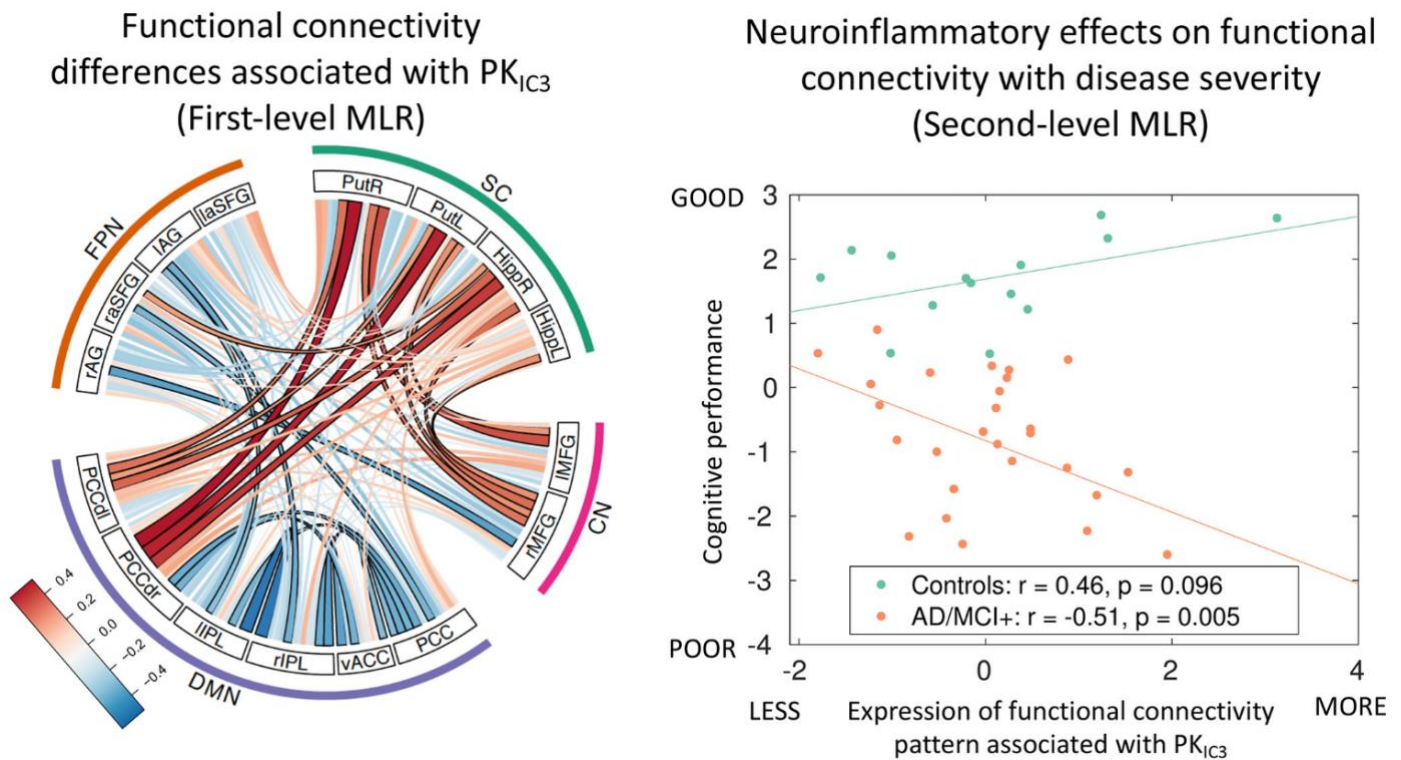


Figure 22: Microglia activation, functional connectivity, and cognition in AD.

(Left) First-level multiple linear regression (MLR) indicating that functional connectivity differences (deviating from groups effects in Figure 3) are associated positively with [^{11}C]PK11195-related independent component measures (PK_{IC3}).

(Right) Second level MLR testing the association between PK_{IC3} pattern of functional connectivity and cognitive performance for AD/MCI+ (orange) and control (green) groups. ACC – anterior cingulate cortex; PCC – posterior cingulate cortex; IPL – intraparietal lobule; FPN – fronto-parietal network; SC– subcortical, DMN – default mode network, DMNd – dorsal DMN, Put– Putamen; Hipp – Hippocampus, AG – angular gyrus; SFG – superior frontal gyrus; R, right; L, left.

6.5. Discussion

This study shows that that stronger microglial activation in AD is associated with the disruption of large-scale functional connectivity underlying cognitive performance. Specifically, the degree to which a patient expressed the pattern of abnormal connectivity associated with neuroinflammation correlated with the amount of cognitive deficit, across the spectrum of patients with AD and MCI+. This is consistent with the hypothesis that microglia activation relates to brain-wide connectivity in AD and mediates clinically relevant cognitive deficit. Proof of this direction of causality in the associations will require anti-inflammatory interventions in AD/MCI+, but we suggest that the novel SBI method would be a suitable tool for experimental medicine studies.

There are different mechanisms by which microglia activation might alter neuronal firing as well as network function and large-scale connectivity patterns. For instance, microglia are important contributors in the process of synaptic pruning and in monitoring synaptic activity (Hong *et al.* 2016; Hong & Stevens 2016). These functions are mediated by microglia's highly mobile and ramified branches that can reach and surround the synaptic terminals to promote phagocytosis and synaptic demise (Hong *et al.* 2016; Hong & Stevens 2016). Microglia-induced complement activation might also contribute to synaptic dysfunction and loss, especially in the context of amyloid deposition and neuritic plaque formation (Hong *et al.* 2016; Hong & Stevens 2016).

The anatomical distribution of microglia activation in AD and its distinct effects on network function within the default mode network (DMN) and between the DMN and medial temporal lobe supports the notion that neuroinflammation may be an early event in the etio-pathogenesis of AD. The DMN and medial temporal lobe are key circuits in the episodic memory system and have been consistently implicated in the pathophysiology of early stages of AD.

In terms of limitations, I recognize that the multi-variate method of statistical associations used here does not *in itself* demonstrate causality between microglia activation, network dysfunction, and cognition. Recent longitudinal studies in AD have shown that changes in [^{11}C]PK11195 binding may be linked with disease progression (Fan *et al.* 2015a; Kreisl *et al.* 2016), although this does still not prove causality for which pre-clinical experiments are necessary. Further research is also needed to assess whether longitudinal changes in [^{11}C]PK11195 binding relate to changes in network function.

Even more importantly, it remains to be ascertained whether the putative effects of anti-inflammatory therapies have an impact in reducing the deleterious effect of neuroinflammation on brain functioning and consequently cognitive performance.

There are other limitations to consider. These include the necessity to replicate our findings in independent and larger clinical cohorts, although the difficulty in terms of costs and recruitment should not be dismissed.

To mitigate the notoriously challenging issues related to head motion artefacts in fMRI studies, I have adopted two main strategies that included:

- 1) a robust pre-processing pipeline using Multi-Echo Independent Components Analysis (ME-ICA), to classify blood oxygenation dependant (BOLD) and non-BOLD signals;
- 2) the inclusion, as covariates of no interest, of movement-related parameters in the second-level statistical analyses.

At the clinical and phenotypic level, it remains to be determined whether the deleterious impact of microglia activation on network function can be revealed in pre-symptomatic carriers of genetic mutations linked to familiar forms of AD. Answering this question has important consequences for

understanding the timing of neuroinflammation in AD and its relationship to neuronal dysfunction, cell loss, and cognitive decline.

In conclusion, this study suggests that microglia activation plays an important role in mediating functionally relevant changes in brain connectivity in AD. Heterogeneity in cognitive performance is associated with variability in neuroinflammation-related brain dysfunction.

Alongside the data presented in chapter 4, these findings emphasize the importance of using multi-modal neuroimaging to study how different aspects of the molecular pathology in AD affect network function and cognitive impairment.

Chapter 7 | General Discussion

7.1. Summary

The main aim of my thesis was to improve our understanding of *in vivo* tau pathology and neuroinflammation in relation to network dysfunction and cognitive deficit in AD. To this end, I used multi-modal imaging that combined specific PET ligands and state-of-art rsfMRI graph and multivariate analyses.

I studied a cohort of patients with clinically probable AD and MCI with PET biomarker evidence of amyloid pathology. This phenotypically variable group of patients was also defined in terms of individual differences in neuropsychological profiles and was compared to groups of age-, sex-, and education-matched healthy controls. The cognitive profile in patients with AD/MCI+ was fully consistent with previous findings in larger populations.

However, I acknowledge that the phenotypic spectrum and variability in clinical severity in the patients' group included in my thesis was limited by the inclusion of participants with early stages of the disease. This, alongside the small sample sizes in each of the clinical groups, did not offer sufficient power to decompose the effects of Braak's staging on the main imaging findings.

Furthermore, my thesis did not examine the relationship between tau pathology and neuroinflammation in AD, neither how the interplay of these molecular pathologies affected brain function and cognition. These are certainly interesting and important aspects to study in future research, but they were beyond the more focused scope of my PhD (although see preliminary data reported in **Figure 23**).

My thesis tested two main hypotheses:

- 1) that the extent and localization of *in vivo* tau pathology and neuroinflammation in patients with AD/MCI+ mirrored the disease-specific patterns of degeneration, especially in brain areas that are affected early in the disease (e.g., medial temporal lobe regions);
- 2) that *in vivo* tau pathology and neuroinflammation mediated network dysfunction and severity of cognitive deficit.

Overall, my studies support the idea that tau burden and microglia activation are key pathophysiological mechanisms underlying Alzheimer's disease and its associated clinical heterogeneity. Despite previous progresses in understanding the molecular pathologies leading to AD, the clinical and intermediate phenotypic correlates (i.e., network function) of tau pathology and neuroinflammation have remained unclear and poorly studied.

The main contribution of my findings is that they provide a 'bridge' between basic and clinical research and facilitate future developments of translation work that will improve the clinical management and disease-modifying treatment of AD.

The findings of my studies have also other implications.

The data presented in chapters 3 and 4 provide evidence , in humans, that the tau burden in AD shows specific neuroanatomical patterns and is associated with the degree of functional connectivity rather than depending on the proximity of brain regions (Goedert 2015). This trans-neuronal hypothesis of tau abnormal diffusion was initially proposed on the basis of rodent studies which showed that the injection of brain extract from tau transgenic mice into mice expressing wild-type human tau causes this wild-type tau to develop abnormal tau filaments that spread across the brain

(Clavaguera *et al.* 2009). Similarly, pathological tau extract from brains of AD patients produce AD-like disease in wild-type mice, in whom pathological human tau becomes self-propagating (Clavaguera *et al.* 2013). This spreading of abnormal tau is mediated by the strength of synaptic connectivity rather than by the spatial proximity of the brain regions or neurons (Liu *et al.* 2012; Iba *et al.* 2013; Ahmed *et al.* 2014).

In my studies, we were able to measure *in vivo* tau burden, via [¹⁸F]AV-1451 PET, and directly link this measure with indices of resting-state functional connectivity in living patients with AD. Our data showed that the brain areas that were more strongly connected accrued more tau pathology, consistently with the hypothesis of trans-neuronal propagation of the tau protein. We also found that the presence of tau pathology *itself* was not linked with higher regional connectivity but in contrast increased tau accumulation was associated with weaker functional connectivity in AD. The fact that in healthy people the [¹⁸F]AV-1451 binding at each node explained more regional variance in connectivity changes rather than connectivity of that node also suggest that tau is not a secondary marker of neurodegeneration in vulnerable hubs.

The data presented in chapters 5 and 6 provide support to the notion that microglia activation and neuroinflammation are not merely epiphenomena of neurodegeneration, but are important etio-pathogenetic mediators of AD symptomatology (Villegas-Llerena *et al.* 2016). Recent genome-wide association studies have challenged the previous assumption that neuroinflammation is a by-product of neurodegeneration and have in contrast sustained a primary role of microglia activation in the aetiology of AD (Guerreiro *et al.* 2013a; Jonsson *et al.* 2013b). For instance, mutations in TREM2, an immune cells receptor expressed on microglia, have been shown to represent an important risk factor for sporadic and late-onset cases of AD (Guerreiro *et al.* 2013a; Jonsson *et al.* 2013b). Together with the results presented in chapter 5 and 6, this lends further support to the proposal that targeting neuroinflammation might reduce the progression of

AD. In more general terms, my findings reinforce the value of using biomarkers based on PET imaging and network function as indices of relevant intermediate phenotypes, between pathology and clinic. My data also support the idea that functional dys-connectivity can be considered an important intermediate phenotypic expression of tau and inflammatory pathology in AD. This is relevant to new strategies for stratifying patients and quantifying outcome measures in future clinical trials that aim to target abnormal tau accumulation and neuroinflammation.

This is a key issue, especially when considering the striking contrast between the positive findings from basic research on the role of tau pathology and microglia activation in AD (Heppner *et al.* 2015), and the negative findings from human studies which have provided so far little support for immune-therapeutic strategies in AD (Adapt Research Group *et al.* 2007, 2008), despite initial epidemiological evidence (Breitner & Zandi 2001; in t' Veld *et al.* 2001).

These apparently conflicting results may be reconciled by investigating how tau propagation and neuroinflammation influence the intermediate phenotypes of large-scale network functional connectivity in AD. Clinical trials may fail to demonstrate a role for immune-therapeutic strategies targeting tau pathology and microglia activation in AD due to elevated heterogeneity in patients' data. The data presented in chapter 6 confirm the marked heterogeneity in the relationship between resting-state functional connectivity and neuroinflammation in AD patients. This variance was also significantly related to inter-individual differences in cognitive performance.

Overall, my studies are in keeping with the literature emphasizing the molecular and clinical complexity of AD and the necessity to target different aspects of this disorder to provide more realistic and efficient treatments as well as to empower and de-risk clinical trials. The observation of the high heterogeneity in terms of tau burden, microglia activation, and network

dysfunction across the spectrum of AD syndromes has important implications for the planning of future studies and clinical trials.

For example, clinical and non-clinical research attempting to assess the molecular and phenotypic complexity of AD may benefit from stratifying patients based on the presence and severity of tau burden and neuroinflammation, rather than on diagnostic categories alone. The choice of the most appropriate and sensitive outcome measures is critical for more efficient clinical trials; hence, *in vivo* and pathological-specific assessment tools are desperately warranted in AD research.

Clarifying the link between tau pathology, microglia activation, and cognitive decline in AD is thus critical for developing novel therapies. Together or even in isolation, tau burden and neuroinflammation may represent important biomarkers of AD which might help identifying and stratifying patients with the most severe or rapidly progressive forms of the disease.

For example, if tau propagation and/or neuroinflammation occur early in AD, they can represent markers of initial disease changes, or “pre-diagnostic” tools to track the risk of cognitive deterioration and development of dementia. However, it remains to be clarified when tau pathology and neuroinflammation become fully apparent and which is their causal relationship. Studies on pre-symptomatic carriers of genetic mutations known to cause AD may be able to show brain changes in terms of tau burden and neuroinflammation 5-10 years prior to the onset of full-blown dementia (Rohrer *et al.* 2015).

These pre-symptomatic individuals may exhibit molecular and neuronal changes that occur years before the functional decline that triggers a clinical diagnosis of AD. Whether increased tau burden and/or neuroinflammation is evident in these genetically predisposed people warrants further investigation in large cohorts of individuals and using the appropriate

assessment tools which include PET and functional imaging; in essence the multi-imaging approach that I have employed in my thesis.

Another open issue is the impact of tau pathology and neuroinflammation on 'cognitive reserve'. This theoretical concept suggests that specific factors, such as sex, education, pre-morbid intelligence, and even bilingualism, can influence the subject-specific capacity of the brain to sustain neurodegenerative insult which in turn can modulate the disease onset and clinical manifestation of AD (Garibotto *et al.* 2012; Perani & Abutalebi 2015; Malpetti *et al.* 2017; Perani *et al.* 2017; Borsa *et al.* 2018).

The individuals with greater cognitive reserve are therefore hypothesized to have increased brain networks' flexibility, which increases their ability to sustain greater levels of pathology before presenting clinical symptoms. My hypothesis is that individuals with higher cognitive reserve may be able to tolerate higher levels of tau pathology and neuroinflammation.

Future studies aiming to disentangle the complexity of tau pathology and neuroinflammation in AD, as well as their intermediate brain phenotypes at the structural and functional connectivity level should be developed to classify patients based on the presence and severity of tau pathology and microglia activation. Furthermore, the future choice of assessment and therapeutic tools should be tailored on single patients' needs which might depend on individual levels of tau burden, neuroinflammation, and network function.

Better translational tools are required for this. The *in vivo* assessment of tau pathology and microglia activation might provide good face validity and may offer a better platform for translation between pre-clinical and human studies. Carefully designed clinical trials targeting the relevant patients and using the appropriate outcome measures will clarify whether effective intervention directed at tau propagation and neuroinflammation, simultaneously or independently, is disease modifying.

7.2. Limitations

7.2.1. Demographic and clinical limitations

I only included patients with the typical clinical forms of AD and MCI (i.e., amnesic type of AD and MCI+). Although the inclusion of cognitively milder forms of AD (i.e., MCI+) extended the variability of the clinical spectrum to power the analyses looking at individual differences in terms of *in vivo* brain pathologies and network function, my inclusion and exclusion criteria have inevitably limited the relevance of my findings to the broader phenotypic spectrum of AD.

The clinical phenotype of AD is wide and includes typical and atypical forms of AD such as the posterior cortical atrophy (PCA), the corticobasal syndrome (CBS), and the logopenic variant of primary progressive aphasia (lvPPA). The fact that I did not include in my thesis these distinct, although clinically and pathologically overlapping groups, reduced the generalizability of my findings in terms of answering important mechanistic questions about the relationship between tau pathology, neuroinflammation, brain function, and clinical severity in the broader spectrum of AD disorders.

A recruitment bias may occur towards or away from those patients with early disease stages. This is a common issue in complex studies like NIMROD in which the intense clinical, behavioural, and multi-modal imaging assessment typically biases the recruitment to those individuals who are sufficiently 'robust' to complete a challenging study protocol. In other words, patients with severe forms of AD that significantly limited patients' functioning in daily activities were less likely to be recruited in our studies. The presence of a reliable carer was also another aspect that may have biased the recruitment to those patients with stronger family support. On the other hand, people with early stage symptomatic disease may not be diagnosed or engaged in research until several years have passed.

Overall, these demographic and enrolment criteria, as well as the fact that some of the patients were recruited from highly specialized tertiary clinics

for memory disorders in Cambridge, can have led to the inclusion of a less representative sample of patients with AD than those present in the general population. This is also in part due to the lack of the inclusion of those patients with co-morbidities, mixed dementia, or severe disease stages.

7.2.2. Technical limitations

Two different PET scanners were used during the NIMROD study. This depended on hardware changes and installations of new PET-MR scanner at the Wolfson Brain Imaging Centre (WBIC), following the study start with PET-CT. Fortunately, this technological issue was only present in $n=6$ participants and the number of patients and controls were equally distributed across the two scanners. Nevertheless, the use of two different scanners inevitably caused an uncontrolled source of noise and variability in the data. We also considered to include the scanner site as a covariate of no interest in the statistical models, but successively we decided against this as the inclusion of another variable could have further reduced the degrees of freedom and consequently the statistical power.

There is also variability in the dose of the radioligands administered to each participant. We tried to minimize this problem by pre-determining a minimum dose that was needed in order to proceed to the scanning of the participants. This implies that any dose difference across participants was over and above a minimum threshold that was set up to provide a sufficient signal to noise ratio for robust modelling and pre-processing of the PET data.

A final, but important, technical limitation of the AV1451 ligand regards its off-target binding. Despite its strong *in vivo* and *post mortem* binding to AD-related tau pathology, there is also evidence that AV1451 can bind to other, non tau-pathologies such as for example TDP43 pathology (Bevan-Jones *et al.* 2017a). Other studies have also suggested alternative 'off-target' binding sites including neuromelanin (Marquié *et al.* 2015) and monoamine oxidase B (Harada *et al.* 2017; Jang *et al.* 2018). Consequently,

this off-target binding has spread concerns and caution regarding the use of AV1451 as a reliable marker of tau pathology.

However, it should be noted that the 'off-target' sites of the AV1451 binding are likely to vary according to the brain region and pathological effects examined. For instance, the neuromelanin 'off-target' binding can only be expected in the substantia nigra and locus coeruleus, two brainstem regions which are rich of neuromelanin, a pigmented polymer that accumulates as a consequence of the presence of cytosol catecholamines like dopamine and noradrenaline. This is not the case in the basal ganglia nor in cortical regions which do not contain or accumulate neuromelanin (Hansen *et al.* 2016). In other words, the neuromelanin hypothesis of the 'off-target' binding of AV1451 cannot explain in itself the high unspecific binding that we and others observed *in vivo* in the basal ganglia (see **Figure 9**).

Our *post mortem* data published in Passamonti *et al.*, 2017 (Brain), also clearly showed that off-target binding to neuromelanin cannot be the cause for [¹⁸F]AV1451 uptake in the basal ganglia or the cortex. In particular, we found significant *in vivo* [¹⁸F]AV1451 uptake in the basal ganglia (in all groups including healthy controls) (**Figure 9 and 10**) in the absence of *post mortem* neuromelanin-containing cells in these sub-cortical regions (Passamonti *et al.* 2017b). This shows that neuromelanin is not the main target of off-target binding for [¹⁸F]AV1451, at least in the basal ganglia and the cortex which do not display accumulation or deposit of neuromelanin (Passamonti *et al.* 2017b).

In the basal ganglia, however, the MAO-A enzyme is significantly expressed and this has been offered as an alternative explanation for the 'off-target' binding of tau PET compounds like THK5351 (Ng *et al.* 2017). Other work has also proposed the MAO-A enzyme as another off-target binding site of AV1451 (Vermeiren *et al.* 2018), although a definitive displacement study has not been conducted yet.

Another important aspect regards the fact that the MAO enzyme (albeit of type B not A) has been found to be expressed in activated microglia, which raises the critical issue of whether the AV1451 binding relates not only to tau pathology in AD, but also to activated microglia, the typical binding site of the TSPO PK11195 ligand. However, this hypothesis is not confirmed by our recent data in a pre-symptomatic carrier of a MAPT genetic mutation which showed that PK11195 binding is possible in the absence of AV1451 uptake (Bevan-Jones *et al.* 2019). Nevertheless, we could not be sure of presence of tau pathology in this single case as *post mortem* data were not available so further studies need to be conducted to reveal the exact nature of the 'off-target' binding of the AV1451 tracer. Additional studies are also necessary to study the relationship between AV1451 binding in non-AD and non tau-related degenerative diseases such as TDP43 disorders (e.g., semantic dementia) (Bevan-Jones *et al.* 2017b, 2018).

7.2.3. Methodological limitations

My studies have also limitations in terms of the analytical methods employed to analyse the PET and rsfMRI data.

7.2.3.1 PET methodological limitations

First, I acknowledge the arbitrary selection of the reference region that is used to modelling the PET tissue specific binding. This arises for the [18F]-AV1451 imaging pre-processing procedures for which arterial sampling reference data from the literature were not available at the time of the data acquisition (due to the novelty of this PET compound). It was also beyond the scope of the NIMROD study to acquire normative data for unspecific binding of the AV1451 tracer which would have required a separate ethical approval and funding structure.

As reference region for the PET AV1451 tracer unspecific binding, we decided to use the white-matter in the superior cerebellum as this area was unlikely to be affected by AD pathology, especially at relatively early stages

of the disease. This idea was corroborated by our *post mortem* findings published in the supplementary material of Passamonti et al, 2017 (Brain) in which we showed the absence of tau pathology in the white-matter of the superior cerebellum in AD.

For the PK11195 PET imaging, the reference region was determined with a fully automated and data driven approach that employed supervised cluster analysis and avoided the use of arbitrarily chosen brain reference areas. This was possible because arterial reference data for unspecific binding were available from a large literature of previous studies using the PK11195 compound.

Second, our regional PET analyses used partial volume correction for cerebrospinal fluid (CSF), which controlled for differences in CSF signal contamination within each region and across the different diagnostic groups (i.e., AD/MCI+ and healthy control groups). This approach is important to reduce the potential influence of brain volume loss (i.e., atrophy) that is typically observed in AD, although it can artificially introduce errors due to the imperfect co-registration of PET and MRI data. I note, however, that this potential issue was significantly mitigated by the fact that the main results were replicated when using uncorrected PET data (see Results section of Chapter 3 and 5).

7.2.3.2 rsfMRI methodological limitations

Two main limitations of the rsfMRI analytical pipelines are discussed:

First, I acknowledge that associative methods do not *in themselves* demonstrate causality between tau pathology neuroinflammation, network dysfunction, and cognition. To address the causal chain leading to cognitive dysfunctions in AD, from their molecular and brain antecedents to the clinical symptoms, longitudinal and interventional studies are needed alongside mediation analyses. This clearly spans not only rsfMRI data alone,

but any type of data included in my thesis such as PET as well as clinical and behavioural data.

Second, the confounding effect of head motion on functional imaging has been fully recognized as both a challenging and critical factor for interpretation of functional imaging studies, especially in clinical populations which can present with an increased rate of head movement during fMRI scanning. To minimize this potentially important confound, we adopted two procedures.

1) We used independent component analyses that had been previously validated to neatly separate the changes in the fMRI signal that are related to the BOLD and non-BOLD components (Kundu *et al.* 2012b, 2013a). This procedure has been shown to be particularly robust in de-noising fMRI data from several sources of noise including head movement (Kundu *et al.* 2012b, 2013a).

2) we included movement-related parameters as covariates of no interest in second-level analyses, as well as motion and physiological signals in first-level analyses. This co-variance approach was employed to mitigate the residual effects of movements on brain functional components estimated in the statistical models used to assess network connectivity.

7.3. Final discussion and future directions

Despite the above described limitations in the 'off-target' binding of the [^{18}F]AV1451, the confidence regarding this PET compound as a biomarker of tau pathology in AD remain high. The new longitudinal findings showing that [^{18}F]AV1451 PET is able to track the disease progression and clinical severity, alongside the complexity of the phenotypic spectrum in AD is encouraging and supports the view that this tracer is a reliable and valid marker for assessing and tracking *in vivo* tau pathology in AD (Harrison *et al.* 2019; Pontecorvo *et al.* 2019).

The disease specific pattern of binding of the [^{18}F]AV1451 PET ligand also remains a useful intermediate phenotype of tau pathology in AD to characterize the tau-related network dys-connectivity that is typically observed in AD (Cope et al., 2018, Brain). These properties can have further applications in terms of development of more sensitive and specific biomarkers for the diagnosis of AD and for additional studies assessing the pathophysiological mechanisms that relate to cognitive dysfunction and disease severity in AD. Future longitudinal studies will be also determinant in assessing the effect of the newly developed anti-tau disease-modifying therapies on intermediate phenotypes of brain pathology and function, before the clinical endpoints (Ossenkoppele *et al.* 2018).

In terms of the potential utility of [^{18}F]AV1451 PET to discriminate between AD- and non-AD tauopathies or other neurodegenerative disorders this has not been fully evaluated yet, although initial findings from our group are promising (Passamonti et al., 2017, Brain).

Another aspect that is central in my thesis is the key etio-pathogenetic role of neuroinflammation in AD, and especially its contribution in mediating anomalies in functional connectivity, and cognitive impairment. This is in keeping with the mechanistic evidence showing increased microglial activation and neuroinflammation as the disease progresses. Nevertheless, despite the epidemiological (McGeer *et al.* 1996; in 't Veld *et al.* 2001), genetic (Malik *et al.* 2015; Zhang *et al.* 2015) and PET (Edison *et al.* 2008b; Esposito *et al.* 2008; Carter *et al.* 2012) evidence providing strong support for neuroinflammation in AD, its *causal* role in the pathogenesis of AD remains to be confirmed.

Several, and not necessarily mutually exclusive, possibilities exist to explain the involvement of microglia activation and neuroinflammation in AD: (i) these molecular processes can be independent causes of AD, over and above tau and amyloid pathologies; (ii) they may be secondary effects of tau protein aggregation or amyloid deposition or even secondary event to the generation of protein oligomers, before pathological protein aggregation

and diffusion; (iii) they might be reactive consequences of neuronal death and synaptic loss (which is an unlikely hypothesis but still does not to be completely ruled out). Only interventional and longitudinal studies using causal statistical modelling (e.g., mediation analyses, Bayesian inference) can resolve these critical issues and answer these open questions.

Past epidemiological evidence using retrospective data have suggested a partially protective effect of anti-inflammatories in the progression or even development of AD. However, these studies were correlational in nature and did not employ randomised placebo-controlled interventional designs that can overcome the classic shortcomings of some epidemiological research.

Nevertheless, our finding of an association between microglia activation and cognitive impairment, as well as between neuroinflammation, network dysfunction and individual differences in cognitive deficit represent a promising set of data that further motivate studying and assessment of the role of neuroinflammation in AD.

I also would like to reiterate that my thesis did not examine the relationship between tau pathology and neuroinflammation in AD, neither how the interplay of these molecular pathologies affected brain function and cognition.

It is however worth noting that my colleagues in the NIMROD team have already began to investigate the intriguing association between *in vivo* neuroinflammation and tau pathology in AD. For example, we have initial (i.e., submitted but not published yet) data showing that tau pathology (as assessed via AV PET) positively relate to microglia activation (as assessed via PK PET) in AD.

These preliminary findings are shown in **Figure 23**, in which strong positive associations between [^{18}F]AV1451 and [^{11}C]PK11195 binding can be observed across several brain ROIs in AD.

Alzheimer's disease

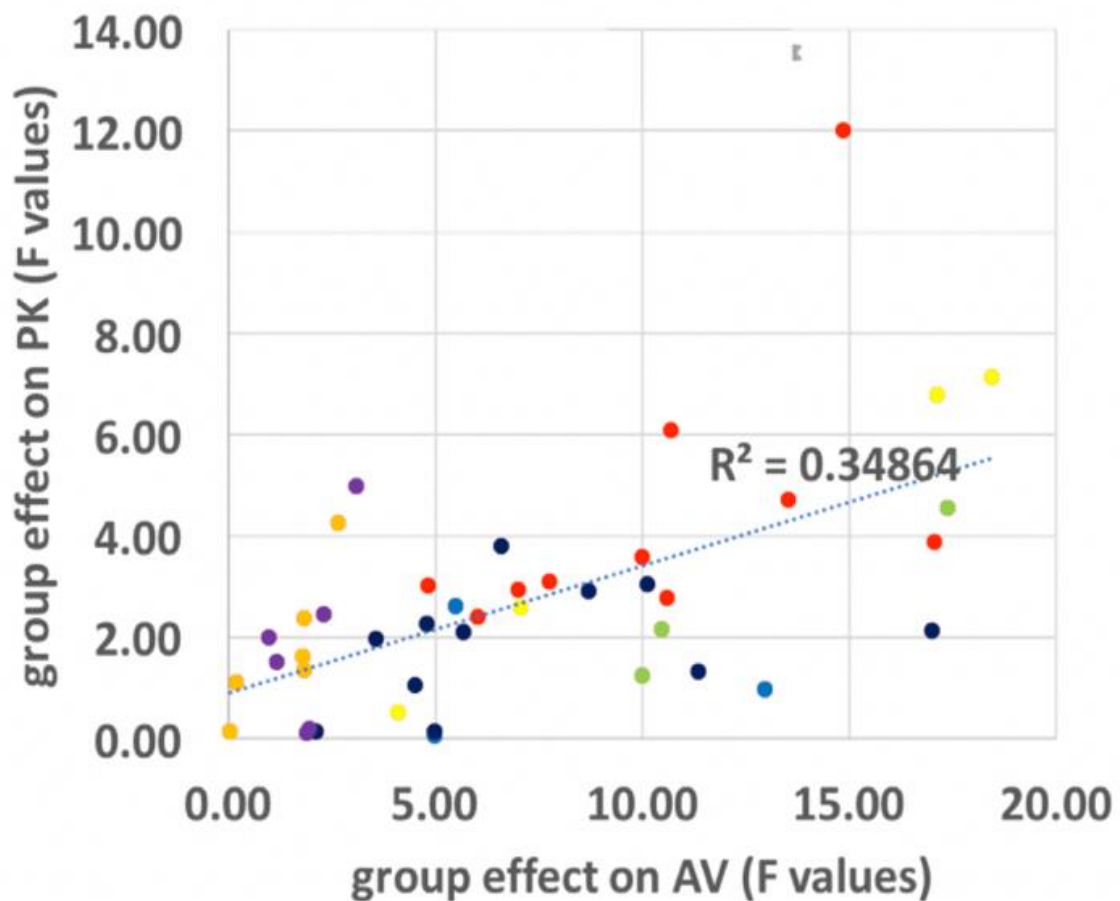


Figure 23: Relation between tau burden and neuroinflammation in AD.

There is a positive relationship between [^{18}F]AV-1451 and [^{11}C]PK-11195 PET binding across different brain regions (coded with different colours) in AD.

Another key aspect that forthcoming studies need to tackle regards the use of larger sample sizes to improve the generalizability of the findings to the broad phenotypic spectrum of AD and to better assess the high clinical variability in the different cognitive features that characterize AD patients. Such studies will have enhanced statistical power to detect significant associations between markers of brain pathology, measures of network function, and heterogeneity in behavioural and cognitive symptoms. If sufficiently large, these studies can also have the power to assess the effect of genetic risk factors on brain intermediate phenotypes of pathologies as well as on brain structure and function.

Thus far the study by Ossenkoppele and colleagues has been seminal in this direction as it clearly demonstrated that different types of AD including the amnestic-AD, PCA-AD and logopenic variant of AD were robustly associated with specific patterns of tau pathology but not amyloid deposition (Ossenkoppele *et al.* 2016c).

I also envisage the obvious necessity to develop second generation tracers with increased sensitivity and specificity for AD-related tau pathology and, paraps even more importantly, with the ability to discriminate between the 3R and 4R isoforms of tau that will enhance the differential diagnosis between AD- and non-AD tauopathies. Currently, PBB3 seems to show promises in that direction, although additional data are needed (Talakad Lohith, Idriss Bennacef, Zhizhen Zeng, Marie Holahan, Michel Koole, Koen Van Laere, Cyrille Sur, Arie Struyk 2016; Betthausen *et al.* 2018; Pascoal *et al.* 2018).

The final direction of future research regards the important application of tau-PET and microglia-PET to inform etio-pathological models of AD, especially via the use of multimodal neuroimaging that can offer complementary information about different, but synergistic, mechanisms of disease. Two chapters in this thesis (Chapter 4 and Chapter 6) present encouraging findings showing that tau-PET and inflammatory-PET can be

individually combined with another imaging modality (rsfMRI) to test the 'transmission hypothesis' of tau spreading in humans (in which tau diffusion follows specific connectivity patterns rather than proximity rules) and the role of neuroinflammatory dependent dysconnectivity in mediating clinical severity in AD. Over and above our studies, in the last few years, there has been a growing interest in assessing different pathophysiological aspects of AD via the complimentary use of different neuroimaging techniques (Brundin *et al.* 2010; Lee *et al.* 2010; Jucker & Walker 2011).

Although this approach poses some conceptual, technical, and methodological challenges that I have discussed throughout this thesis (e.g., reduction of data dimensionality), multimodal neuroimaging can play an important role in disentangling the complex nature of the pathologies underlying AD. This and other neurodegenerative disorders are caused by a multifaceted number of factors that are likely to interact at many different levels in the brain. Our cross-modal multivariate analyses and findings emphasize the value of multi-modal neuroimaging to study how different aspects of the molecular pathologies of AD mediate brain function and cognition. Improved stratification procedures may facilitate more efficient therapeutic trials in AD, based not only on tau pathology, neuroinflammation, brain atrophy or functional connectivity, but on their compound interplay that leads to individual differences in cognitive impairment.

7.4. Conclusion

My research shows the advantages of multi-modal imaging approaches to assess a pathologically and clinically complex neurodegenerative disorder such as AD.

The causal interactions between tau burden, neuroinflammation, network function in AD remain to be elucidated and linked to cognitive decline before new disease-modifying treatments can be developed and implemented in the clinical practice. Novel, pathologically-specific, and translational

therapies should consider the individual degree of tau burden and/or microglia activation in single patients with AD, moving away from including patients in clinical trials only on the basis of a clinical diagnosis that does not incorporate the 'added' informative value of biomarkers probing different phenotypic levels.

The heterogeneity across patients with AD pathologies in terms of tau burden, microglia activation, and network function should be considered to empower and de-risk future clinical trials and to improve outcome measures based non only on clinical endpoints but also on brain-derived and mechanistically-focussed measures.

The complex nature of the molecular pathways leading to AD suggests the need for combinational or 'cocktail' disease-modifying therapy, for example, targeting tau pathology and neuroinflammation simultaneously.

Reference list

- Adapt Research Group, Lyketsos CG, Breitner JC, Green RC, Martin BK, Meinert C, Piantadosi S, Sabbagh M** (2007). Naproxen and celecoxib do not prevent AD in early results from a randomized controlled trial. *Neurology* **68**, 1800–8.
- Adapt Research Group, Martin BK, Szekely C, Brandt J, Piantadosi S, Breitner JC, Craft S, Evans D, Green R, Mullan M** (2008). Cognitive function over time in the Alzheimer's Disease Anti-inflammatory Prevention Trial (ADAPT): results of a randomized, controlled trial of naproxen and celecoxib. *Arch Neurol* **65**, 896–905.
- Agostinho P, Cunha RA, Oliveira C** (2010). Neuroinflammation, oxidative stress and the pathogenesis of Alzheimer's disease. *Curr Pharm Des* **16**, 2766–78.
- Ahmed Z, Cooper J, Murray TK, Garn K, McNaughton E, Clarke H, Parhizkar S, Ward MA, Cavallini A, Jackson S, Bose S, Clavaguera F, Tolnay M, Lavenir I, Goedert M, Hutton ML, O'Neill MJ** (2014). A novel in vivo model of tau propagation with rapid and progressive neurofibrillary tangle pathology: the pattern of spread is determined by connectivity, not proximity. *Acta Neuropathol* **127**, 667–83.
- Albert MS, DeKosky ST, Dickson D, Dubois B, Feldman HH, Fox NC, Gamst A, Holtzman DM, Jagust WJ, Petersen RC, Snyder PJ, Carrillo MC, Thies B, Phelps CH** (2011a). The diagnosis of mild cognitive impairment due to Alzheimer's disease: Recommendations from the National Institute on Aging-Alzheimer's Association workgroups on diagnostic guidelines for Alzheimer's disease. *Alzheimer's & Dementia*
- Albert MS, DeKosky ST, Dickson D, Dubois B, Feldman HH, Fox NC, Gamst A, Holtzman DM, Jagust WJ, Petersen RC, Snyder PJ, Carrillo MC, Thies B, Phelps CH** (2011b). The diagnosis of mild cognitive impairment due to Alzheimer's disease: recommendations from the National Institute on Aging-Alzheimer's Association workgroups on diagnostic guidelines for Alzheimer's disease. *Alzheimer's & Dementia: The Journal of the Alzheimer's Association* **7**, 270–279.
- Alexander-Bloch AF, Gogtay N, Meunier D, Birn R, Clasen L, Lalonde F, Lenroot R, Giedd J, Bullmore ET** (2010). Disrupted modularity and local connectivity of brain functional networks in childhood-onset schizophrenia. *Frontiers in Systems Neuroscience* **4**, 147.
- American Psychiatric A** (2013). *Diagnostic and statistical manual of mental disorders, (DSM-5®)*. American Psychiatric Pub.

Anderson AN, Pavese N, Edison P, Tai YF, Hammers A, Gerhard A, Brooks DJ, Turkheimer FE (2007). A systematic comparison of kinetic modelling methods generating parametric maps for [(11)C]-(R)-PK11195. *Neuroimage* **36**, 28–37.

Andreadis A (2005). *Tau gene alternative splicing: Expression patterns, regulation and modulation of function in normal brain and neurodegenerative diseases*. *Biochimica et Biophysica Acta - Molecular Basis of Disease*

Arriagada P V., Growdon JH, Hedley-Whyte ET, Hyman BT (1992a). Neurofibrillary tangles but not senile plaques parallel duration and severity of Alzheimer's disease. *Neurology*

Arriagada P V., Growdon JH, Hedley-Whyte ET, Hyman BT (1992b). Neurofibrillary tangles but not senile plaques parallel duration and severity of Alzheimer's disease. *Neurology*

Ashburner J (2007). A fast diffeomorphic image registration algorithm. *Neuroimage* **38**, 95–113.

Avila J, Lucas JJ, Perez M, Hernandez F (2004). Role of tau protein in both physiological and pathological conditions. *Physiological reviews*

Badhwar A, Tam A, Dansereau C, Orban P, Hoffstaedter F, Bellec P (2017). Resting-state network dysfunction in Alzheimer's disease: A systematic review and meta-analysis. *Alzheimer's & Dementia : Diagnosis, Assessment & Disease Monitoring* **8**, 73–85.

Ballatore C, Lee VM-Y, Trojanowski JQ (2007). Tau-mediated neurodegeneration in Alzheimer's disease and related disorders. *Nature reviews. Neuroscience* **8**, 663–72.

Banati RB, Newcombe J, Gunn RN, Cagnin A, Turkheimer F, Heppner F, Price G, Wegner F, Giovannoni G, Miller DH, Perkin GD, Smith T, Hewson AK, Bydder G, Kreutzberg GW, Jones T, Cuzner ML, Myers R (2000). The peripheral benzodiazepine binding site in the brain in multiple sclerosis. Quantitative in vivo imaging of microglia as a measure of disease activity. *Brain*

Beharry C, Cohen LS, Di J, Ibrahim K, Briffa-Mirabella S, Alonso ADC (2014). *Tau-induced neurodegeneration: Mechanisms and targets*. *Neuroscience Bulletin*

Berg D, Steinberger JD, Warren Olanow C, Naidich TP, Yousry TA (2011). *Milestones in magnetic resonance imaging and transcranial sonography of movement disorders*. *Movement Disorders* **26**, 979–992.

Betthausen TJ, Cody KA, Zammit MD, Murali D, Converse AK, Barnhart TE, Stone CK, Rowley HA, Johnson SC, Christian BT (2018). In vivo characterization and quantification of neurofibrillary tau PET radioligand [¹⁸F]MK-6240 in humans from Alzheimer's disease dementia to young controls. *Journal of Nuclear Medicine*

Bevan-Jones RW, Cope TE, Jones SP, Passamonti L, Hong YT, Fryer T, Arnold R, Coles JP, Aigbirhio FA, Patterson K, O'Brien JT, Rowe JB (2018). [18F]AV-1451 binding is increased in frontotemporal dementia due to C9orf72 expansion. *Annals of Clinical and Translational Neurology*

Bevan-Jones WR, Cope TE, Jones PS, Passamonti L, Hong YT, Fryer T, Arnold R, Coles JP, Aigbirhio FI, O'Brien JT, Rowe JB (2019). In vivo evidence for pre-symptomatic neuroinflammation in a MAPT mutation carrier. *Annals of Clinical and Translational Neurology* **6**, 373–378.

Bevan-Jones WR, Cope TE, Jones PS, Passamonti L, Hong YT, Fryer TD, Arnold R, Allinson KSJ, Coles JP, Aigbirhio FI, Patterson K, O'Brien JT, Rowe JB (2017a). AV-1451 binding in vivo mirrors the expected distribution of TDP-43 pathology in the semantic variant of primary progressive aphasia. *Journal of Neurology, Neurosurgery and Psychiatry*

Bevan-Jones WR, Cope TE, Jones PS, Passamonti L, Hong YT, Fryer TD, Arnold R, Allinson KSJ, Coles JP, Aigbirhio FI, Patterson K, O'Brien JT, Rowe JB (2017b). AV-1451 binding in vivo mirrors the expected distribution of TDP-43 pathology in the semantic variant of primary progressive aphasia. *Journal of Neurology, Neurosurgery and Psychiatry*

Beyreuther K, Masters CL (1991). Amyloid Precursor Protein (APP) and B2A4 Amyloid in the Etiology of Alzheimer's Disease: Precursor-Product Relationships in the Derangement of Neuronal Function. *Brain Pathology*

Bloom GS (2014). Amyloid- β and tau: the trigger and bullet in Alzheimer disease pathogenesis. *JAMA neurology* **71**, 505–8.

Borsa VM, Perani D, Della Rosa PA, Videsott G, Guidi L, Weekes BS, Franceschini R, Abutalebi J (2018). Bilingualism and healthy aging: Aging effects and neural maintenance. *Neuropsychologia* **111**, 51–61.

Braak H, Alafuzoff I, Arzberger T, Kretschmar H, Del Tredici K (2006a). Staging of Alzheimer disease-associated neurofibrillary pathology using paraffin sections and immunocytochemistry. *Acta Neuropathol* **112**, 389–404.

Braak H, Alafuzoff I, Arzberger T, Kretschmar H, Tredici K (2006b). Staging of Alzheimer disease-associated neurofibrillary pathology using paraffin sections and immunocytochemistry. *Acta Neuropathologica* **112**, 389–404.

- Braak H, Braak E** (1991a). Neuropathological staging of Alzheimer-related changes. *Acta Neuropathologica* **82**, 239–259.
- Braak H, Braak E** (1991b). Neuropathological staging of Alzheimer-related changes. *Acta Neuropathologica*
- Braak H, Braak E** (1995). Staging of Alzheimer's disease-related neurofibrillary changes. *Neurobiol Aging* **16**, 271–8; discussion 278–84.
- Breitner JC, Zandi PP** (2001). Do nonsteroidal antiinflammatory drugs reduce the risk of Alzheimer's disease? *N Engl J Med* **345**, 1567–8.
- Brundin P, Melki R, Kopito R** (2010). Prion-like transmission of protein aggregates in neurodegenerative diseases. *Nature Reviews Molecular Cell Biology*
- Buchhave P, Minthon L, Zetterberg H, Wallin ÅK, Blennow K, Hansson O** (2012). Cerebrospinal fluid levels of Aβ-amyloid 1-42, but not of tau, are fully changed already 5 to 10 years before the onset of Alzheimer dementia. *Archives of General Psychiatry*
- Buée L, Bussière T, Buée-Scherrer V, Delacourte A, Hof PR** (2000). Tau protein isoforms, phosphorylation and role in neurodegenerative disorders. *Brain Research Reviews* **33**, 95–130.
- Cagnin A, Brooks DJ, Kennedy AM, Gunn RN, Myers R, Turkheimer FE, Jones T, Banati RB** (2001a). In-vivo measurement of activated microglia in dementia. *Lancet* **358**, 461–467.
- Cagnin A, Brooks DJ, Kennedy AM, Gunn RN, Myers R, Turkheimer FE, Jones T, Banati RB** (2001b). In-vivo measurement of activated microglia in dementia. *Lancet* **358**, 461–7.
- Cagnin A, Kassiou M, Meikle SR, Banati RB** (2006). In vivo evidence for microglial activation in neurodegenerative dementia. *Acta Neurologica Scandinavica*
- Calhoun V, Adali T, Pearlson G, Pekar J** (2001a). A method for making group inferences from functional MRI data using independent component analysis. *Human Brain Mapping* **14**, 140–151.
- Calhoun VD, Adali T, Pearlson GD, Pekar JJ** (2001b). A method for making group inferences from functional MRI data using independent component analysis. *Human brain mapping* **14**, 140–151.
- De Calignon A, Polydoro M, Suárez-Calvet M, Williams C, Adamowicz DH, Kopeikina KJ, Pitstick R, Sahara N, Ashe KH, Carlson GA, Spire-Jones TL, Hyman BT** (2012). Propagation of Tau Pathology in a Model of Early Alzheimer's Disease. *Neuron* **73**, 685–697.

Calvini P, Chincarini A, Gemme G, Penco MA, Squarcia S, Nobili F, Rodriguez G, Bellotti R, Catanzariti E, Cerello P, De Mitri I, Fantacci ME (2009). Automatic analysis of medial temporal lobe atrophy from structural MRIs for the early assessment of Alzheimer disease. *Medical Physics*

Campion D, Dumanchin C, Hannequin D, Dubois B, Belliard S, Puel M, Thomas-Anterion C, Michon A, Martin C, Charbonnier F, Raux G, Camuzat A, Penet C, Mesnage V, Martinez M, Clerget-Darpoux F, Brice A, Frebourg T (1999). Early-onset autosomal dominant Alzheimer disease: prevalence, genetic heterogeneity, and mutation spectrum. *American journal of human genetics*

Carter SF, Scholl M, Almkvist O, Wall A, Engler H, Langstrom B, Nordberg A (2012). Evidence for Astrocytosis in Prodromal Alzheimer Disease Provided by 11C-Deuterium-L-Deprenyl: A Multitracer PET Paradigm Combining 11C-Pittsburgh Compound B and 18F-FDG. *Journal of Nuclear Medicine*

Carusi DA, Disease A (1994). The Neuropsychiatric Inventory :

Chien DT, Bahri S, Szardenings AK, Walsh JC, Mu F, Su MY, Shankle WR, Elizarov A, Kolb HC (2013). Early Clinical PET Imaging Results with the Novel PHF-Tau Radioligand [F-18]-T807. *Journal of Alzheimer's Disease* **34**, 457–468.

Chien DT, Szardenings AK, Bahri S, Walsh JC, Mu F, Xia C, Shankle WR, Lerner AJ, Su MY, Elizarov A, Kolb HC (2014). Early clinical PET imaging results with the novel PHF-tau radioligand [F18]-T808. *Journal of Alzheimer's Disease*

Chou YY, Laporé N, Avedissian C, Madsen SK, Parikshak N, Hua X, Shaw LM, Trojanowski JQ, Weiner MW, Toga AW, Thompson PM (2009). Mapping correlations between ventricular expansion and CSF amyloid and tau biomarkers in 240 subjects with Alzheimer's disease, mild cognitive impairment and elderly controls. *NeuroImage*

Clavaguera F, Akatsu H, Fraser G, Crowther RA, Frank S, Hench J, Probst A, Winkler DT, Reichwald J, Staufenbiel M, Ghetti B, Goedert M, Tolnay M (2013). Brain homogenates from human tauopathies induce tau inclusions in mouse brain. *Proceedings of the National Academy of Sciences of the United States of America* **110**, 9535–9540.

Clavaguera F, Bolmont T, Crowther RA, Abramowski D, Frank S, Probst A, Fraser G, Stalder AK, Beibel M, Staufenbiel M, Jucker M, Goedert M, Tolnay M (2009). Transmission and spreading of tauopathy in transgenic mouse brain. *Nature cell biology* **11**, 909–913.

Cope TE, Rittman T, Borchert RJ, Jones PS, Vatansever D, Allinson K, Passamonti L, Vazquez Rodriguez P, Bevan-Jones WR, O'Brien JT, Rowe JB (2018). Tau burden and the functional connectome in Alzheimer's disease and progressive supranuclear palsy. *Brain* **141**, 550–567.

Corbetta M (2012). Functional connectivity and neurological recovery. *Developmental Psychobiology*

Deelen J, Beekman M, Uh HW, Helmer Q, Kuningas M, Christiansen L, Kremer D, van der Breggen R, Suchiman HED, Lakenberg N, van den Akker EB, Passtoors WM, Tiemeier H, van Heemst D, de Craen AJ, Rivadeneira F, de Geus EJ, Perola M, van der Ouderaa FJ, Gunn DA, Boomsma DI, Uitterlinden AG, Christensen K, van Duijn CM, Heijmans BT, Houwing-Duistermaat JJ, Westendorp RGJ, Slagboom PE (2011). Genome-wide association study identifies a single major locus contributing to survival into old age; the APOE locus revisited. *Aging Cell*

Desikan RS, McEvoy LK, Thompson WK, Holland D, Brewer JB, Aisen PS, Sperling RA, Dale AM, Alzheimer's Disease Neuroimaging Initiative for the (2012). Amyloid- β -Associated Clinical Decline Occurs Only in the Presence of Elevated P-tau. *Archives of Neurology*

D'Souza I, Schellenberg GD (2005). *Regulation of tau isoform expression and dementia. Biochimica et Biophysica Acta - Molecular Basis of Disease* **1739**, 104–115.

Dubois B, Burn D, Goetz C, Aarsland D, Brown RG, Broe GA, Dickson D, Duyckaerts C, Cummings J, Gauthier S, Korczyn A, Lees A, Levy R, Litvan I, Mizuno Y, McKeith IG, Olanow CW, Poewe W, Sampaio C, Tolosa E, Emre M (2007a). Diagnostic procedures for Parkinson's disease dementia: recommendations from the movement disorder society task force. *Movement Disorders: Official Journal of the Movement Disorder Society* **22**, 2314–2324.

Dubois B, Feldman HH, Jacova C, Dekosky ST, Barberger-Gateau P, Cummings J, Delacourte A, Galasko D, Gauthier S, Jicha G, Meguro K, O'Brien J, Pasquier F, Robert P, Rossor M, Salloway S, Stern Y, Visser PJ, Scheltens P (2007b). Research criteria for the diagnosis of Alzheimer's disease: revising the NINCDS-ADRDA criteria. *The Lancet. Neurology* **6**, 734–746.

van Duijn CM, de Knijff P, Cruts M, Wehnert A, Havekes LM, Hofman A, Van Broeckhoven C (1994). Apolipoprotein E4 allele in a population-based study of early-onset Alzheimer's disease. *Nature genetics*

Early Detection and Differential Diagnosis of Alzheimer ' s Disease and Depression with (2001)., 265–280.

Edison P, Ahmed I, Fan Z, Hinz R, Gelosa G, Ray Chaudhuri K, Walker Z, Turkheimer FE, Brooks DJ (2013a). Microglia, amyloid, and glucose metabolism in Parkinson's disease with and without dementia. *Neuropsychopharmacology* **38**, 938–49.

Edison P, Ahmed I, Fan Z, Hinz R, Gelosa G, Ray Chaudhuri K, Walker Z, Turkheimer FE, Brooks DJ (2013b). Microglia, amyloid, and glucose metabolism in Parkinson's disease with and without dementia. *Neuropsychopharmacology* **38**, 938–49.

Edison P, Archer HA, Gerhard A, Hinz R, Pavese N, Turkheimer FE, Hammers A, Tai YF, Fox N, Kennedy A, Rossor M, Brooks DJ (2008a). Microglia, amyloid, and cognition in Alzheimer's disease: An [11C](R)PK11195-PET and [11C]PIB-PET study. *Neurobiol Dis* **32**, 412–9.

Edison P, Archer HA, Gerhard A, Hinz R, Pavese N, Turkheimer FE, Hammers A, Tai YF, Fox N, Kennedy A, Rossor M, Brooks DJ (2008b). Microglia, amyloid, and cognition in Alzheimer's disease: An [11C](R)PK11195-PET and [11C]PIB-PET study. *Neurobiology of Disease*

Engler H, Forsberg A, Almkvist O, Blomquist G, Larsson E, Savitcheva I, Wall A, Ringheim A, Långström B, Nordberg A (2006). Two-year follow-up of amyloid deposition in patients with Alzheimer's disease. *Brain: A Journal of Neurology* **129**, 2856–2866.

Esposito G, Giovacchini G, Liow J-S, Bhattacharjee AK, Greenstein D, Schapiro M, Hallett M, Herscovitch P, Eckelman WC, Carson RE, Rapoport SI (2008). Imaging Neuroinflammation in Alzheimer's Disease with Radiolabeled Arachidonic Acid and PET. *Journal of Nuclear Medicine*

Evans MC, Barnes J, Nielsen C, Kim LG, Clegg SL, Blair M, Leung KK, Douiri A, Boyes RG, Ourselin S, Fox NC (2010). Volume changes in Alzheimer's disease and mild cognitive impairment: Cognitive associations. *European Radiology*

Fan Z, Aman Y, Ahmed I, Chetelat G, Landeau B, Ray Chaudhuri K, Brooks DJ, Edison P (2015a). Influence of microglial activation on neuronal function in Alzheimer's and Parkinson's disease dementia. *Alzheimers Dement* **11**, 608–21 e7.

Fan Z, Aman Y, Ahmed I, Chetelat G, Landeau B, Ray Chaudhuri K, Brooks DJ, Edison P (2015b). Influence of microglial activation on neuronal function in Alzheimer's and Parkinson's disease dementia. *Alzheimers Dement* **11**, 608–21 e7.

Fan Z, Okello AA, Brooks DJ, Edison P (2015c). Longitudinal influence of microglial activation and amyloid on neuronal function in Alzheimer's disease. *Brain* **138**, 3685–98.

Fernandez-Botran R, Ahmed Z, Crespo FA, Gatenbee C, Gonzalez J, Dickson DW, Litvan I (2011a). Cytokine expression and microglial activation in progressive supranuclear palsy. *Parkinsonism Relat Disord* **17**, 683–8.

Fernández-Botrán R, Ahmed Z, Crespo FA, Gatenbee C, Gonzalez J, Dickson DW, Litvan I (2011). Cytokine expression and microglial activation in progressive supranuclear palsy. *Parkinsonism & related disorders* **17**, 683–8.

Fernandez-Botran R, Ahmed Z, Crespo FA, Gatenbee C, Gonzalez J, Dickson DW, Litvan I (2011b). Cytokine expression and microglial activation in progressive supranuclear palsy. *Parkinsonism Relat Disord* **17**, 683–8.

Flicker C, Ferris SH, Reisberg B (1991). Mild cognitive impairment in the elderly: predictors of dementia. *Neurology* **41**, 1006–1009.

Flicker C, Ferris SH, Reisberg B (1993). A Two-Year Longitudinal Study of Cognitive Function in Normal Aging and Alzheimer's Disease. *Journal of Geriatric Psychiatry and Neurology*

Fodero-Tavoletti MT, Okamura N, Furumoto S, Mulligan RS, Connor AR, McLean CA, Cao D, Rigopoulos A, Cartwright GA, O'Keefe G, Gong S, Adlard PA, Barnham KJ, Rowe CC, Masters CL, Kudo Y, Cappai R, Yanai K, Villemagne VL (2011). 18F-THK523: A novel in vivo tau imaging ligand for Alzheimer's disease. *Brain*

Forsberg A, Engler H, Almkvist O, Blomquist G, Hagman G, Wall A, Ringheim A, Långström B, Nordberg A (2008). PET imaging of amyloid deposition in patients with mild cognitive impairment. *Neurobiology of Aging* **29**, 1456–1465.

Frackowiak J, Wisniewski HM, Wegiel J, Merz GS, Iqbal K, Wang KC (1992). Ultrastructure of the microglia that phagocytose amyloid and the microglia that produce beta-amyloid fibrils. *Acta Neuropathol* **84**, 225–33.

Ganguli M, Snitz BE, Saxton JA, Chang C-CH, Lee C-W, Vander Bilt J, Hughes TF, Loewenstein DA, Unverzagt FW, Petersen RC (2011). Outcomes of mild cognitive impairment by definition: a population study. *Archives of Neurology* **68**, 761–767.

Garibotto V, Borroni B, Sorbi S, Cappa SF, Padovani A, Perani D (2012). Education and occupation provide reserve in both ApoE ε4 carrier and noncarrier patients with probable Alzheimer's disease. *Neurological Sciences: Official Journal of the Italian Neurological Society and of the Italian Society of Clinical Neurophysiology* **33**, 1037–1042.

Gauthier S, Reisberg B, Zaudig M, Petersen RC, Ritchie K, Broich K, Belleville S, Brodaty H, Bennett D, Chertkow H, Cummings JL, de Leon M, Feldman H, Ganguli M, Hampel H, Scheltens P, Tierney MC, Whitehouse P, Winblad B (2006). Mild cognitive impairment. *Lancet*

Geerligs L, Tsvetanov KA, Cam-Can, Henson RN (2017). Challenges in measuring individual differences in functional connectivity using fMRI: The case of healthy aging. *Human Brain Mapping*

Gerhard A, Pavese N, Hotton G, Turkheimer F, Es M, Hammers A, Eggert K, Oertel W, Banati RB, Brooks DJ (2006a). In vivo imaging of microglial activation with [¹¹C](R)-PK11195 PET in idiopathic Parkinson's disease. *Neurobiology of Disease*

Gerhard A, Trender-Gerhard I, Turkheimer F, Quinn NP, Bhatia KP, Brooks DJ (2006b). In vivo imaging of microglial activation with [¹¹C](R)-PK11195 PET in progressive supranuclear palsy. *Mov Disord* **21**, 89–93.

Gerhard A, Watts J, Trender-Gerhard I, Turkheimer F, Banati RB, Bhatia K, Brooks DJ (2004). In vivo imaging of microglial activation with [¹¹C](R)-PK11195 PET in corticobasal degeneration. *Movement Disorders*

Goedert M (2015). NEURODEGENERATION. Alzheimer's and Parkinson's diseases: The prion concept in relation to assembled Abeta, tau, and alpha-synuclein. *Science* **349**, 1255555.

Goedert M, Jakes R (2005). *Mutations causing neurodegenerative tauopathies. Biochimica et Biophysica Acta - Molecular Basis of Disease* **1739**, 240–250.

Goedert M, Wischik C, Crowther R, Walker J, Klug A (1988). Cloning and sequencing of the cDNA encoding a core protein of the paired helical filament of Alzheimer disease: identification as the microtubule-associated protein tau. *Proceedings of the National Academy of Sciences of the United States of America* **85**, 4051–4055.

Goetz CG, Tilley BC, Shaftman SR, Stebbins GT, Fahn S, Martinez-martin P, Poewe W, Sampaio C, Stern MB, Dodel R, Dubois B, Holloway R, Jankovic J, Kulisevsky J, Lang AE, Lees A, Leurgans S, Lewitt PA, Nyenhuis D, Olanow CW, Rascol O, Schrag A, Teresi JA, Hilten JJ Van, Lapelle N (2008). Movement Disorder Society-Sponsored Revision of the Unified Parkinson's Disease Rating Scale (MDS-UPDRS): Scale Presentation and Clinimetric Testing Results. **23**, 2129–2170.

Golbe LI, Ohman-Strickland PA (2007). A clinical rating scale for progressive supranuclear palsy. *Brain* **130**, 1552–1565.

Gómez-Isla T, Hollister R, West H, Mui S, Growdon JH, Petersen RC, Parisi JE, Hyman BT (1997). Neuronal loss correlates with but exceeds neurofibrillary tangles in Alzheimer's disease. *Annals of Neurology*

Gorno-Tempini ML, Hillis AE, Weintraub S, Kertesz A, Mendez M, Cappa SF, Ogar JM, Rohrer JD, Black S, Boeve BF, Manes F, Dronkers NF, Vandenberghe R, Rascovsky K, Patterson K, Miller BL, Knopman DS, Hodges JR, Mesulam MM, Grossman M (2011). Classification of primary progressive aphasia and its variants. *Neurology* **76**, 1006–1014.

Guerreiro R, Wojtas A, Bras J, Carrasquillo M, Rogaeva E, Majounie E, Cruchaga C, Sassi C, Kauwe JS, Younkin S, Hazrati L, Collinge J, Pocock J, Lashley T, Williams J, Lambert JC, Amouyel P, Goate A, Rademakers R, Morgan K, Powell J, St George-Hyslop P, Singleton A, Hardy J, Alzheimer Genetic Analysis G (2013a). TREM2 variants in Alzheimer's disease. *N Engl J Med* **368**, 117–27.

Guerreiro R, Wojtas A, Bras J, Carrasquillo M, Rogaeva E, Majounie E, Cruchaga C, Sassi C, Kauwe JSK, Younkin S, Hazrati L, Collinge J, Pocock J, Lashley T, Williams J, Lambert J-C, Amouyel P, Goate A, Rademakers R, Morgan K, Powell J, St. George-Hyslop P, Singleton A, Hardy J (2013b). TREM2 Variants in Alzheimer's Disease. *New England Journal of Medicine*

Gulyás B, Pavlova E, Kása P, Gulya K, Bakota L, Várszegi S, Keller É, Horváth MC, Nag S, Hermecz I, Magyar K, Halldin C (2011). Activated MAO-B in the brain of alzheimer patients, demonstrated by [11C]-l-deprenyl using whole hemisphere autoradiography. *Neurochemistry International*

Gunn RN, Lammertsma AA, Hume SP, Cunningham VJ (1997). Parametric imaging of ligand-receptor binding in PET using a simplified reference region model. *Neuroimage* **6**, 279–287.

Hallquist MN, Hwang K, Luna B (2013). The nuisance of nuisance regression: spectral misspecification in a common approach to resting-state fMRI preprocessing reintroduces noise and obscures functional connectivity. *Neuroimage* **82**, 208–225.

Hamelin L, Lagarde J, Dorothee G, Leroy C, Labit M, Comley RA, de Souza LC, Corne H, Dauphinot L, Bertoux M, Dubois B, Gervais P, Colliot O, Potier MC, Bottlaender M, Sarazin M, Clinical Imab team (2016). Early and protective microglial activation in Alzheimer's disease: a prospective study using 18F-DPA-714 PET imaging. *Brain* **139**, 1252–64.

Hammers A, Allom R, Koepp MJ, Free SL, Myers R, Lemieux L, Mitchell TN, Brooks DJ, Duncan JS (2003). Three-dimensional maximum probability atlas of the human brain, with particular reference to the temporal lobe. *Human Brain Mapping* **19**, 224–247.

Hansen AK, Knudsen K, Lillethorup TP, Landau AM, Parbo P, Fedorova T, Audrain H, Bender D, Østergaard K, Brooks DJ, Borghammer P (2016). In vivo imaging of neuromelanin in Parkinson's disease using 18F-AV-1451 PET. *Brain*

Harada R, Ishiki A, Kai H, Sato N, Furukawa K, Furumoto S, Tago T, Tomita N, Watanuki S, Hiraoka K, Ishikawa Y, Funaki Y, Nakamura T, Yoshikawa T, Iwata R, Tashiro M, Sasano H, Kitamoto T, Yanai K, Arai H, Kudo Y, Okamura N (2017). Correlations of ¹⁸F-THK5351 PET with post-mortem burden of tau and astrogliosis in Alzheimer's disease. *Journal of Nuclear Medicine*

Hardy J, Allsop D (1991). Amyloid deposition as the central event in the aetiology of Alzheimer's disease. *Trends in Pharmacological Sciences*

Harrison TM, La Joie R, Maass A, Baker SL, Swinnerton K, Fenton L, Mellinger TJ, Edwards L, Pham J, Miller BL, Rabinovici GD, Jagust WJ (2019). Longitudinal tau accumulation and atrophy in aging and alzheimer disease. *Annals of Neurology* **85**, 229–240.

Hashimoto H, Kawamura K, Igarashi N, Takei M, Fujishiro T, Aihara Y, Shiomi S, Muto M, Ito T, Furutsuka K, Yamasaki T, Yui J, Xie L, Ono M, Hatori A, Nemoto K, Suhara T, Higuchi M, Zhang M-R (2014). Radiosynthesis, Photoisomerization, Biodistribution, and Metabolite Analysis of ¹¹C-PBB3 as a Clinically Useful PET Probe for Imaging of Tau Pathology. *Journal of Nuclear Medicine*

Hatashita S, Yamasaki H (2013). Diagnosed Mild Cognitive Impairment Due to Alzheimer's Disease with PET Biomarkers of Beta Amyloid and Neuronal Dysfunction. *PLoS ONE* **8**

Heppner FL, Ransohoff RM, Becher B (2015). Immune attack: the role of inflammation in Alzheimer disease. *Nat Rev Neurosci* **16**, 358–72.

Hippius H, Neundörfer G (2003). The discovery of Alzheimer's disease. *Dialogues in Clinical Neuroscience* **5**, 101–108.

Hirvonen J, Kailajärvi M, Haltia T, Koskimies S, Ngren K, Virsu P, Oikonen V, Sipilä H, Ruokoniemi P, Virtanen K, Scheinin M, Rinne JO (2009). Assessment of MAO-B occupancy in the brain with PET and ¹¹C-L-deprenyl-D 2: A dose-finding study with a novel MAO-B inhibitor, EVT 301. *Clinical Pharmacology and Therapeutics*

Ho AJ, Hua X, Lee S, Leow AD, Yanovsky I, Gutman B, Dinov ID, Leporé N, Stein JL, Toga AW, Jack CR, Bernstein MA, Reiman EM, Harvey DJ, Kornak J, Schuff N, Alexander GE, Weiner MW, Thompson PM (2010). Comparing 3 T and 1.5 T MRI for tracking Alzheimer's disease progression with tensor-based morphometry. *Human Brain Mapping*

Hoeijmakers L, Heinen Y, van Dam AM, Lucassen PJ, Korosi A (2016). Microglial Priming and Alzheimer's Disease: A Possible Role for (Early) Immune Challenges and Epigenetics? *Front Hum Neurosci* **10**, 398.

Hong S, Beja-Glasser VF, Nfonoyim BM, Frouin A, Li S, Ramakrishnan S, Merry KM, Shi Q, Rosenthal A, Barres BA, Lemere CA, Selkoe DJ, Stevens B (2016). Complement and microglia mediate early synapse loss in Alzheimer mouse models. *Science* **352**, 712–716.

Hong S, Stevens B (2016). Microglia: Phagocytosing to Clear, Sculpt, and Eliminate. *Dev Cell* **38**, 126–8.

<http://www.cambridgecognition.com/tests/simple-reaction-time-srt> (n.d.).

Hughes CP, Berg L, Danziger WL, Coben L, Martin RL (1982). A New Clinical Scale for the Staging of Dementia

Iba M, Guo JL, McBride JD, Zhang B, Trojanowski JQ, Lee VM-Y (2013). Synthetic tau fibrils mediate transmission of neurofibrillary tangles in a transgenic mouse model of Alzheimer's-like tauopathy. *The Journal of Neuroscience: The Official Journal of the Society for Neuroscience* **33**, 1024–1037.

Iwata M (2005). [MRI diagnosis of neurodegenerative disorders]. *Rinshō shinkeigaku = Clinical neurology* **45**, 947–951.

Jack CR, Albert MS, Knopman DS, McKhann GM, Sperling RA, Carrillo MC, Thies B, Phelps CH (2011). Introduction to the recommendations from the National Institute on Aging-Alzheimer's Association workgroups on diagnostic guidelines for Alzheimer's disease. *Alzheimer's & Dementia: The Journal of the Alzheimer's Association* **7**, 257–262.

Jack CR, Holtzman DM (2013). Biomarker modeling of alzheimer's disease. *Neuron*

Jack CR, Lowe VJ, Senjem ML, Weigand SD, Kemp BJ, Shiung MM, Knopman DS, Boeve BF, Klunk WE, Mathis CA, Petersen RC (2008). 11C PiB and structural MRI provide complementary information in imaging of Alzheimer's disease and amnesic mild cognitive impairment. *Brain: A Journal of Neurology* **131**, 665–680.

Jack CR, Wiste HJ, Schwarz CG, Lowe VJ, Senjem ML, Vemuri P, Weigand SD, Therneau TM, Knopman DS, Gunter JL, Jones DT, Graff-Radford J, Kantarci K, Roberts RO, Mielke MM, MacHulda MM, Petersen RC (2018). Longitudinal tau PET in ageing and Alzheimer's disease. *Brain*

Jang YK, Lyoo CH, Park S, Oh SJ, Cho H, Oh M, Ryu YH, Choi JY, Rabinovici GD, Kim HJ, Moon SH, Jang H, Lee JS, Jagust WJ, Na DL, Kim JS, Seo SW (2018). Head to head comparison of [18F] AV-1451 and [18F] THK5351 for tau imaging in Alzheimer's disease and frontotemporal dementia. *European Journal of Nuclear Medicine and Molecular Imaging*

Jarmolowicz AI, Chen H-Y, Panegyres PK (2015). The Patterns of Inheritance in Early-Onset Dementia: Alzheimer's Disease and Frontotemporal Dementia. *American Journal of Alzheimer's Disease and Other Dementias*

Jenkinson M, Bannister P, Brady M, Smith S (2002a). Improved optimization for the robust and accurate linear registration and motion correction of brain images. *Neuroimage* **17**, 825–841.

Jenkinson M, Bannister P, Brady M, Smith S (2002b). Improved optimization for the robust and accurate linear registration and motion correction of brain images. *Neuroimage* **17**, 825–841.

Jicha GA, Parisi JE, Dickson DW, Johnson K, Cha R, Ivnik RJ, Tangalos EG, Boeve BF, Knopman DS, Braak H, Petersen RC (2006). Neuropathologic outcome of mild cognitive impairment following progression to clinical dementia. *Archives of Neurology* **63**, 674–681.

Johnson KA, Fox NC, Sperling RA, Klunk WE (2012). Brain imaging in Alzheimer disease. *Cold Spring Harbor Perspectives in Medicine* **2**, a006213.

Johnson KA, Schultz A, Betensky RA, Becker JA, Sepulcre J, Rentz D, Mormino E, Chhatwal J, Amariglio R, Papp K, Marshall G, Albers M, Mauro S, Pepin L, Alverio J, Judge K, Philiossaint M, Shoup T, Yokell D, Dickerson B, Gomez-Isla T, Hyman B, Vasdev N, Sperling R (2016). Tau positron emission tomographic imaging in aging and early Alzheimer disease. *Ann Neurol* **79**, 110–9.

Jonsson T, Stefansson H, Steinberg S, Jonsdottir I, Jonsson P V, Snaedal J, Bjornsson S, Huttenlocher J, Levey AI, Lah JJ, Rujescu D, Hampel H, Giegling I, Andreassen OA, Engedal K, Ulstein I, Djurovic S, Ibrahim-Verbaas C, Hofman A, Ikram MA, van Duijn CM, Thorsteinsdottir U, Kong A, Stefansson K (2013a). Variant of {TREM}2 associated with the risk of {Alzheimer}'s disease. *N. Engl. J. Med.*

Jonsson T, Stefansson H, Steinberg S, Jonsdottir I, Jonsson PV, Snaedal J, Bjornsson S, Huttenlocher J, Levey AI, Lah JJ, Rujescu D, Hampel H, Giegling I, Andreassen OA, Engedal K, Ulstein I, Djurovic S, Ibrahim-Verbaas C, Hofman A, Ikram MA, van Duijn CM, Thorsteinsdottir U, Kong A, Stefansson K (2013b). Variant of TREM2 associated with the risk of Alzheimer's disease. *N Engl J Med* **368**, 107–16.

Jonsson T, Stefansson H, Steinberg S, Jonsdottir I, Palmi V. Jonsson, M.D., Jon Snaedal, M.D., Sigurbjorn Bjornsson, M.D., Johanna Huttenlocher, B.S., Allan I. Levey, M.D., Ph.D., James J. Lah, M.D., Ph. PhD, From (2013c). Variant of TREM2 associated with the risk of AD. *New England Journal of Medicine*

- Jucker M, Walker LC** (2011). Pathogenic protein seeding in Alzheimer disease and other neurodegenerative disorders. *Annals of Neurology*
- Kaat LD, Boon AJW, Azmani A, Kamphorst W, Breteler MMB, Anar B, Heutink P, Van Swieten JC** (2009). Familial aggregation of parkinsonism in progressive supranuclear palsy. *Neurology* **73**, 98–105.
- Kinahan PE, Rogers JG** (1989a). Analytic 3D image reconstruction using all detected events. *IEEE Transactions on Nuclear Science* **36**, 964–968.
- Kinahan PE, Rogers JG** (1989b). Analytic 3D image reconstruction using all detected events. *IEEE Transactions on Nuclear Science* **36**, 964–968.
- Kitzbichler MG, Henson RNA, Smith ML, Nathan PJ, Bullmore ET** (2011). Cognitive Effort Drives Workspace Configuration of Human Brain Functional Networks. *Journal of Neuroscience*
- Klunk WE, Engler H, Nordberg A, Wang Y, Blomqvist G, Holt DP, Bergström M, Savitcheva I, Huang G, Estrada S, Ausén B, Debnath ML, Barletta J, Price JC, Sandell J, Lopresti BJ, Wall A, Koivisto P, Antoni G, Mathis CA, Långström B** (2004). Imaging brain amyloid in Alzheimer's disease with Pittsburgh Compound-B. *Annals of Neurology* **55**, 306–319.
- Kreisl WC, Lyoo CH, Liow JS, Wei M, Snow J, Page E, Jenko KJ, Morse CL, Zoghbi SS, Pike VW, Turner RS, Innis RB** (2016). (11)C-PBR28 binding to translocator protein increases with progression of Alzheimer's disease. *Neurobiol Aging* **44**, 53–61.
- Kropholler MA, Boellaard R, van Berckel BN, Schuitemaker A, Kloet RW, Lubberink MJ, Jonker C, Scheltens P, Lammertsma AA** (2007). Evaluation of reference regions for (R)-[(11)C]PK11195 studies in Alzheimer's disease and mild cognitive impairment. *J Cereb Blood Flow Metab* **27**, 1965–74.
- Kumar A, Muzik O, Shandal V, Chugani D, Chakraborty P, Chugani HT** (2012). Evaluation of age-related changes in translocator protein (TSPO) in human brain using 11C-[R]-PK11195 PET. *Journal of Neuroinflammation*
- Kundu P, Brenowitz ND, Voon V, Worbe Y, Vértes PE, Inati SJ, Saad ZS, Bandettini PA, Bullmore ET** (2013a). Integrated strategy for improving functional connectivity mapping using multiecho fMRI. *Proceedings of the National Academy of Sciences* **110**, 16187–16192.
- Kundu P, Brenowitz ND, Voon V, Worbe Y, Vértes PE, Inati SJ, Saad ZS, Bandettini PA, Bullmore ET** (2013b). Integrated strategy for improving functional connectivity mapping using multiecho fMRI. *Proceedings of the National Academy of Sciences* **110**, 16187–16192.

Kundu P, Inati SJ, Evans JW, Luh W-M, Bandettini PA (2012a). Differentiating BOLD and non-BOLD signals in fMRI time series using multi-echo EPI. *NeuroImage* **60**, 1759–1770.

Kundu P, Inati SJ, Evans JW, Luh W-M, Bandettini PA (2012b). Differentiating BOLD and non-BOLD signals in fMRI time series using multi-echo EPI. *NeuroImage* **60**, 1759–1770.

Lee S, Desplats P, Sigurdson C (2010). Cell-to-cell transmission of non-prion protein aggregates. *Nature reviews. Neurology*

Li JW, Zong Y, Cao XP, Tan L, Tan L (2018). Microglial priming in Alzheimer's disease. *Ann Transl Med* **6**, 176.

Lindquist M, Geuter S, Wager T, Caffo B (2018). Modular preprocessing pipelines can reintroduce artifacts into fMRI data. . Cold Spring Harbor Laboratory *bioRxiv*, 407676.

Litvan I, Agid Y, Calne D, Campbell G, Dubois B, Duvoisin RC, Goetz CG, Golbe LI, Grafman J, Growdon JH, Hallett M, Jankovic J, Quinn NP, Tolosa E, Zee DS (1996). Clinical research criteria for the diagnosis of progressive supranuclear palsy (Steele-Richardson-Olszewski syndrome): report of the NINDS-SPSP international workshop. *Neurology* **47**, 1–9.

Liu L, Drouet V, Wu JW, Witter MP, Small SA, Clelland C, Duff K (2012). Trans-synaptic spread of tau pathology in vivo. *PLoS One* **7**, e31302.

Liu WK, Le T V., Adamson J, Baker M, Cookson N, Hardy J, Hutton M, Yen SH, Dickson DW (2001). Relationship of the extended tau haplotype to tau biochemistry and neuropathology in progressive supranuclear palsy. *Annals of Neurology*

Loewenstein DA, Acevedo A, Small BJ, Agron J, Crocco E, Duara R (2009). Stability of Different Subtypes of Mild Cognitive Impairment among the Elderly over a 2- to 3-Year Follow-Up Period. *Dementia and Geriatric Cognitive Disorders* **27**, 418–423.

Lowe VJ, Wiste HJ, Senjem ML, Weigand SD, Therneau TM, Boeve BF, Josephs KA, Fang P, Pandey MK, Murray ME, Kantarci K, Jones DT, Vemuri P, Graff-Radford J, Schwarz CG, Machulda MM, Mielke MM, Roberts RO, Knopman DS, Petersen RC, Jack CR (2018). Widespread brain tau and its association with ageing, Braak stage and Alzheimer's dementia. *Brain*

- Mak E, Bethlehem RAI, Romero-Garcia R, Cervenka S, Rittman T, Gabel S, Surendranathan A, Bevan-Jones RW, Passamonti L, Vázquez Rodríguez P, Su L, Arnold R, Williams GB, Hong YT, Fryer TD, Aigbirhio FI, Rowe JB, O'Brien JT** (2018). In vivo coupling of tau pathology and cortical thinning in Alzheimer's disease. *Alzheimer's & Dementia: Diagnosis, Assessment & Disease Monitoring*
- Malik M, Parikh I, Vasquez JB, Smith C, Tai L, Bu G, Ladu MJ, Fardo DW, Rebeck GW, Estus S** (2015). Genetics ignite focus on microglial inflammation in Alzheimer's disease. *Molecular Neurodegeneration*
- Malpetti M, Ballarini T, Presotto L, Garibotto V, Tettamanti M, Perani D, Alzheimer's Disease Neuroimaging Initiative (ADNI) database;, Network for Efficiency and Standardization of Dementia Diagnosis (NEST-DD) database** (2017). Gender differences in healthy aging and Alzheimer's Dementia: A 18 F-FDG-PET study of brain and cognitive reserve. *Human Brain Mapping* **38**, 4212–4227.
- Marquié M, Normandin MD, Vanderburg CR, Costantino IM, Bien EA, Rycyna LG, Klunk WE, Mathis CA, Ikonomic MD, Debnath ML, Vasdev N, Dickerson BC, Gomperts SN, Growdon JH, Johnson KA, Frosch MP, Hyman BT, Gómez-Isla T** (2015). Validating novel tau positron emission tomography tracer [F-18]-AV-1451 (T807) on postmortem brain tissue. *Annals of Neurology* **78**, 787–800.
- Marquie M, Normandin MD, Vanderburg CR, Costantino IM, Bien EA, Rycyna LG, Klunk WE, Mathis CA, Ikonomic MD, Debnath ML, Vasdev N, Dickerson BC, Gomperts SN, Growdon JH, Johnson KA, Frosch MP, Hyman BT, Gomez-Isla T** (2015). Validating novel tau positron emission tomography tracer [F-18]-AV-1451 (T807) on postmortem brain tissue. *Ann Neurol* **78**, 787–800.
- Martin L, Latypova X, Terro F** (2011). Post-translational modifications of tau protein: Implications for Alzheimer's disease. *Neurochemistry International* **58**, 458–471.
- Martinez G, Vernooij RW, Fuentes Padilla P, Zamora J, Bonfill Cosp X, Flicker L** (2017). 18F PET with florbetapir for the early diagnosis of Alzheimer's disease dementia and other dementias in people with mild cognitive impairment (MCI). *The Cochrane database of systematic reviews*
- Maruyama M, Shimada H, Suhara T, Shinotoh H, Ji B, Maeda J, Zhang MR, Trojanowski J, Lee VY, Ono M, Masamoto K, Takano H, Sahara N, Iwata N, Okamura N, Furumoto S, Kudo Y, Chang Q, Saido T, Takashima A, Lewis J, Jang MK, Aoki I, Ito H, Higuchi M** (2013a). Imaging of tau pathology in a tauopathy mouse model and in alzheimer patients compared to normal controls. *Neuron* **79**, 1094–1108.

Maruyama M, Shimada H, Suhara T, Shinotoh H, Ji B, Maeda J, Zhang MR, Trojanowski JQ, Lee VMY, Ono M, Masamoto K, Takano H, Sahara N, Iwata N, Okamura N, Furumoto S, Kudo Y, Chang Q, Saido TC, Takashima A, Lewis J, Jang MK, Aoki I, Ito H, Higuchi M (2013b). Imaging of tau pathology in a tauopathy mouse model and in alzheimer patients compared to normal controls. *Neuron*

Mathis CA, Bacskai BJ, Kajdasz ST, McLellan ME, Frosch MP, Hyman BT, Holt DP, Wang Y, Huang G-F, Debnath ML, Klunk WE (2002). A lipophilic thioflavin-T derivative for positron emission tomography (PET) imaging of amyloid in brain. *Bioorganic & Medicinal Chemistry Letters*

McEvoy LK, Fennema-Notestine C, Roddey JC, Hagler DJ, Holland D, Karow DS, Pung CJ, Brewer JB, Dale AM (2009). Alzheimer Disease: Quantitative Structural Neuroimaging for Detection and Prediction of Clinical and Structural Changes in Mild Cognitive Impairment. *Radiology*

McGeer PL, McGeer EG (2001). Inflammation, autotoxicity and Alzheimer disease. *Neurobiol Aging* **22**, 799–809.

McGeer PL, Schulzer M, McGeer EG (1996). Arthritis and anti-inflammatory agents as possible protective factors for Alzheimer's disease: A review of 17 epidemiologic studies. *Neurology*

McKeith IG, Dickson DW, Lowe J, Emre M, O'Brien JT, Feldman H, Cummings J, Duda JE, Lippa C, Perry EK, Aarsland D, Arai H, Ballard CG, Boeve B, Burn DJ, Costa D, Del Ser T, Dubois B, Galasko D, Gauthier S, Goetz CG, Gomez-Tortosa E, Halliday G, Hansen LA, Hardy J, Iwatsubo T, Kalaria RN, Kaufer D, Kenny RA, Korczyn A, Kosaka K, Lee VMY, Lees A, Litvan I, Londos E, Lopez OL, Minoshima S, Mizuno Y, Molina JA, Mukaetova-Ladinska EB, Pasquier F, Perry RH, Schulz JB, Trojanowski JQ, Yamada M, Consortium on DLB (2005). Diagnosis and management of dementia with Lewy bodies: third report of the DLB Consortium. *Neurology* **65**, 1863–1872.

McKhann GM, Knopman DS, Chertkow H, Hyman BT, Jack CR, Kawas CH, Klunk WE, Koroshetz WJ, Manly JJ, Mayeux R, Mohs RC, Morris JC, Rossor MN, Scheltens P, Carrillo MC, Thies B, Weintraub S, Phelps CH (2011a). The diagnosis of dementia due to Alzheimer's disease: Recommendations from the National Institute on Aging-Alzheimer's Association workgroups on diagnostic guidelines for Alzheimer's disease. *Alzheimer's & dementia : the journal of the Alzheimer's Association* **7**, 263–269.

McKhann GM, Knopman DS, Chertkow H, Hyman BT, Jack CR, Kawas CH, Klunk WE, Koroshetz WJ, Manly JJ, Mayeux R, Mohs RC, Morris JC, Rossor MN, Scheltens P, Carrillo MC, Thies B, Weintraub S, Phelps CH (2011b). The diagnosis of dementia due to Alzheimer's disease: recommendations from the National Institute on Aging-Alzheimer's Association workgroups on diagnostic guidelines for Alzheimer's disease. *Alzheimers Dement* **7**, 263–9.

Mioshi E, Dawson K, Mitchell J, Arnold R, Hodges JR (2006). The Addenbrooke 's Cognitive Examination Revised (ACE-R): a brief cognitive test battery for dementia screening, 1078–1085.

Misra C, Fan Y, Davatzikos C (2009). Baseline and longitudinal patterns of brain atrophy in MCI patients, and their use in prediction of short-term conversion to AD: Results from ADNI. *NeuroImage*

Montgomery A (1979). Scale Designed to be Sensitive to Change

Morra JH, Tu Z, Apostolova LG, Green AE, Avedissian C, Madsen SK, Parikshak N, Hua X, Toga AW, Jack CR, Schuff N, Weiner MW, Thompson PM (2009). Automated 3D mapping of hippocampal atrophy and its clinical correlates in 400 subjects with Alzheimer's disease, mild cognitive impairment, and elderly controls. *Human Brain Mapping*

Murray ME, Kouri N, Lin WL, Jack CR, Dickson DW, Vemuri P (2014). *Clinicopathologic assessment and imaging of tauopathies in neurodegenerative dementias*. *Alzheimer's Research and Therapy* **6**

Nelson PT, Alafuzoff I, Bigio EH, Bouras C, Braak H, Cairns NJ, Castellani RJ, Crain BJ, Davies P, Tredici K Del, Duyckaerts C, Frosch MP, Haroutunian V, Hof PR, Hulette CM, Hyman BT, Iwatsubo T, Jellinger KA, Jicha GA, Kövari E, Kukull WA, Leverenz JB, Love S, MacKenzie IR, Mann DM, Masliah E, McKee AC, Montine TJ, Morris JC, Schneider JA, Sonnen JA, Thal DR, Trojanowski JQ, Troncoso JC, Wisniewski T, Woltjer RL, Beach TG (2012). *Correlation of alzheimer disease neuropathologic changes with cognitive status: A review of the literature*. *Journal of Neuropathology and Experimental Neurology*

Nestor SM, Rupsingh R, Borrie M, Smith M, Accomazzi V, Wells JL, Fogarty J, Bartha R (2008). Ventricular enlargement as a possible measure of Alzheimer's disease progression validated using the Alzheimer's disease neuroimaging initiative database. *Brain*

Neumann H, Daly MJ (2013). Variant *TREM2* as Risk Factor for Alzheimer's Disease. *New England Journal of Medicine*

Neve RL, Harris P, Kosik KS, Kurnit DM, Donlon TA (1986). Identification of cDNA clones for the human microtubule-associated protein tau and chromosomal localization of the genes for tau and microtubule-associated protein 2. *Molecular Brain Research*

Ng KP, Pascoal TA, Mathotaarachchi S, Therriault J, Kang MS, Shin M, Guiot M-C, Guo Q, Harada R, Comley RA, Massarweh G, Soucy J-P, Okamura N, Gauthier S, Rosa-Neto P (2017). Monoamine oxidase B inhibitor, selegiline, reduces 18F-THK5351 uptake in the human brain. *Alzheimer's Research & Therapy*

Nobili F, Morbelli S (2010). [18F] FDG-PET as a Biomarker for Early Alzheimer ' s Disease. *The Open Nuclear Medicine Journal*

Okamura N, Furumoto S, Harada R, Tago T, Yoshikawa T, Fodero-Tavoletti M, Mulligan RS, Villemagne VL, Akatsu H, Yamamoto T, Arai H, Iwata R, Yanai K, Kudo Y (2013a). Novel 18F-Labeled Arylquinoline Derivatives for Noninvasive Imaging of Tau Pathology in Alzheimer Disease. *Journal of Nuclear Medicine*

Okamura N, Furumoto S, Harada R, Tago T, Yoshikawa T, Fodero-Tavoletti M, Mulligan RS, Villemagne VL, Akatsu H, Yamamoto T, Arai H, Iwata R, Yanai K, Kudo Y (2013b). Novel 18F-Labeled Arylquinoline Derivatives for Noninvasive Imaging of Tau Pathology in Alzheimer Disease. *Journal of Nuclear Medicine* **54**, 1420–1427.

Okello A, Koivunen J, Edison P, Archer HA, Turkheimer FE, Någren K, Bullock R, Walker Z, Kennedy A, Fox NC, Rossor MN, Rinne JO, Brooks DJ (2009a). Conversion of amyloid positive and negative MCI to AD over 3 years: an 11C-PIB PET study. *Neurology* **73**, 754–760.

Okello A, Koivunen J, Edison P, Archer HA, Turkheimer FE, Någren K, Bullock R, Walker Z, Kennedy A, Fox NC, Rossor MN, Rinne JO, Brooks DJ (2009b). Conversion of amyloid positive and negative MCI to AD over 3 years: an 11C-PIB PET study. *Neurology* **73**, 754–760.

Okello A, Koivunen J, Edison P, Archer HA, Turkheimer FE, Nagren K, Bullock R, Walker Z, Kennedy A, Fox NC, Rossor MN, Rinne JO, Brooks DJ (2009c). Conversion of amyloid positive and negative MCI to AD over 3 years: an 11C-PIB PET study. *Neurology* **73**, 754–60.

Okello A, Koivunen J, Edison P, Archer HA, Turkheimer FE, Nagren K, Bullock R, Walker Z, Kennedy A, Fox NC, Rossor MN, Rinne JO, Brooks DJ (2009d). Conversion of amyloid positive and negative MCI to AD over 3 years: an 11C-PIB PET study. *Neurology* **73**, 754–60.

Ong K, Villemagne VL, Bahar-Fuchs A, Lamb F, Chételat G, Raniga P, Mulligan RS, Salvado O, Putz B, Roth K, Masters CL, Reiningner CB, Rowe CC (2013). 18F-florbetaben A β imaging in mild cognitive impairment. *Alzheimer's Research & Therapy*

Ossenkoppele R, Rabinovici GD, Smith R, Cho H, Scholl M, Strandberg O, Palmqvist S, Mattsson N, Janelidze S, Santillo A, Ohlsson T, Jogi J, Tsai R, La Joie R, Kramer J, Boxer AL, Gorno-Tempini ML, Miller BL, Choi JY, Ryu YH, Lyoo CH, Hansson O (2018). Discriminative accuracy of [¹⁸F]flortaucipir positron emission tomography for Alzheimer disease vs other neurodegenerative disorders. *JAMA - Journal of the American Medical Association*

Ossenkoppele R, Schonhaut DR, Baker SL, O'Neil JP, Janabi M, Ghosh PM, Santos M, Miller ZA, Bettcher BM, Gorno-Tempini ML, Miller BL, Jagust WJ, Rabinovici GD (2015a). Tau, amyloid, and hypometabolism in a patient with posterior cortical atrophy. *Annals of Neurology* **77**, 338–342.

Ossenkoppele R, Schonhaut DR, Baker SL, O'Neil JP, Janabi M, Ghosh PM, Santos M, Miller ZA, Bettcher BM, Gorno-Tempini ML, Miller BL, Jagust WJ, Rabinovici GD (2015b). Tau, amyloid, and hypometabolism in a patient with posterior cortical atrophy. *Annals of Neurology* **77**, 338–342.

Ossenkoppele R, Schonhaut DR, Schöll M, Lockhart SN, Ayakta N, Baker SL, O'Neil JP, Janabi M, Lazaris A, Cantwell A, Vogel J, Santos M, Miller ZA, Bettcher BM, Vessel KA, Kramer JH, Gorno-Tempini ML, Miller BL, Jagust WJ, Rabinovici GD (2016a). Tau PET patterns mirror clinical and neuroanatomical variability in Alzheimer's disease. *Brain* **139**, 1551–1567.

Ossenkoppele R, Schonhaut DR, Scholl M, Lockhart SN, Ayakta N, Baker SL, O'Neil JP, Janabi M, Lazaris A, Cantwell A, Vogel J, Santos M, Miller ZA, Bettcher BM, Vessel KA, Kramer JH, Gorno-Tempini ML, Miller BL, Jagust WJ, Rabinovici GD (2016b). Tau PET patterns mirror clinical and neuroanatomical variability in Alzheimer's disease. *Brain* **139**, 1551–67.

Ossenkoppele R, Schonhaut DR, Schöll M, Lockhart SN, Ayakta N, Baker SL, O'Neil JP, Janabi M, Lazaris A, Cantwell A, Vogel J, Santos M, Miller ZA, Bettcher BM, Vessel KA, Kramer JH, Gorno-Tempini ML, Miller BL, Jagust WJ, Rabinovici GD (2016c). Tau PET patterns mirror clinical and neuroanatomical variability in Alzheimer's disease. *Brain*

O'Sullivan MJ, Vann SD (2016). Amyloid imaging and Alzheimer's disease: the unsolved cases. *Brain* **139**, 2342–2344.

Owen DR, Yeo AJ, Gunn RN, Song K, Wadsworth G, Lewis A, Rhodes C, Pulford DJ, Bennacef I, Parker CA, StJean PL, Cardon LR, Mooser VE, Matthews PM, Rabiner EA, Rubio JP (2012). An 18-kDa translocator protein (TSPO) polymorphism explains differences in binding affinity of the PET radioligand PBR28. *J Cereb Blood Flow Metab* **32**, 1–5.

Pascoal TA, Shin M, Kang MS, Chamoun M, Chartrand D, Mathotaarachchi S, Bennacef I, Therriault J, Ng KP, Hopewell R, Bouhachi R, Hsiao HH, Benedet AL, Soucy JP, Massarweh G, Gauthier S, Rosa-Neto P (2018). In vivo quantification of neurofibrillary tangles with [¹⁸F]MK-6240. *Alzheimer's Research and Therapy*

Passamonti L, Rodríguez PV, Hong YT, Allinson KSJ, Bevan-Jones WR, Williamson D, Jones PS, Arnold R, Borchert RJ, Surendranathan A, Mak E, Su L, Fryer TD, Aigbirhio FI, O'Brien JT, Rowe JB (2018). [¹¹C]PK11195 binding in Alzheimer disease and progressive supranuclear palsy. *Neurology* **90**, e1989–e1996.

Passamonti L, Tsvetanov KA, Jones PS, Bevan-Jones WR, Arnold R, Borchert RJ, Mak E, Su L, O'Brien JT, Rowe JB (2019). Neuroinflammation and Functional Connectivity in Alzheimer's Disease: Interactive Influences on Cognitive Performance. *The Journal of Neuroscience: The Official Journal of the Society for Neuroscience* **39**, 7218–7226.

Passamonti L, Vazquez Rodriguez P, Hong YT, Allinson KS, Williamson D, Borchert RJ, Sami S, Cope TE, Bevan-Jones WR, Jones PS, Arnold R, Surendranathan A, Mak E, Su L, Fryer TD, Aigbirhio FI, O'Brien JT, Rowe JB (2017a). ¹⁸F-AV-1451 positron emission tomography in Alzheimer's disease and progressive supranuclear palsy. *Brain* **140**, 781–791.

Passamonti L, Vázquez Rodríguez P, Hong YT, Allinson KSJ, Williamson D, Borchert RJ, Sami S, Cope TE, Bevan-Jones WR, Jones PS, Arnold R, Surendranathan A, Mak E, Su L, Fryer TD, Aigbirhio FI, O'Brien JT, Rowe JB (2017b). ¹⁸F-AV-1451 positron emission tomography in Alzheimer's disease and progressive supranuclear palsy. *Brain: A Journal of Neurology* **140**, 781–791.

Pavese N, Gerhard A, Tai YF, Ho AK, Turkheimer F, Barker RA, Brooks DJ, Piccini P (2006). Microglial activation correlates with severity in Huntington disease: A clinical and PET study. *Neurology*

Perani D, Abutalebi J (2015). Bilingualism, dementia, cognitive and neural reserve. *Current Opinion in Neurology* **28**, 618–625.

Perani D, Farsad M, Ballarini T, Lubian F, Malpetti M, Fracchetti A, Magnani G, March A, Abutalebi J (2017). The impact of bilingualism on brain reserve and metabolic connectivity in Alzheimer's dementia. *Proceedings of the National Academy of Sciences of the United States of America* **114**, 1690–1695.

Pievani M, de Haan W, Wu T, Seeley WW, Frisoni GB (2011). Functional network disruption in the degenerative dementias. *The Lancet Neurology*

Pontecorvo MJ, Devous MD, Kennedy I, Navitsky M, Lu M, Galante N, Salloway S, Doraiswamy PM, Southeekal S, Arora AK, McGeehan A, Lim NC, Xiong H, Trucchio SP, Joshi AD, Shcherbinin S, Teske B, Fleisher AS, Mintun MA (2019). A multicentre longitudinal study of flortaucipir (18F) in normal ageing, mild cognitive impairment and Alzheimer's disease dementia. *Brain: A Journal of Neurology* **142**, 1723–1735.

Price CJS, Wang D, Menon DK, Guadagno J V., Cleij M, Fryer T, Aigbirhio F, Baron JC, Warburton EA (2006). Intrinsic activated microglia map to the peri-infarct zone in the subacute phase of ischemic stroke. *Stroke*

Price JL, Davis PB, Morris JC, White DL (1991). The distribution of tangles, plaques and related immunohistochemical markers in healthy aging and Alzheimer's disease. *Neurobiology of Aging*

Prince M, Jackson J (2009). World Alzheimer Report 2009. *Alzheimer's Disease International*

Rascovsky K, Hodges JR, Knopman D, Mendez MF, Kramer JH, Neuhaus J, van Swieten JC, Seelaar H, Dopper EGP, Onyike CU, Hillis AE, Josephs KA, Boeve BF, Kertesz A, Seeley WW, Rankin KP, Johnson JK, Gorno-Tempini M-L, Rosen H, Prioleau-Latham CE, Lee A, Kipps CM, Lillo P, Piguet O, Rohrer JD, Rossor MN, Warren JD, Fox NC, Galasko D, Salmon DP, Black SE, Mesulam M, Weintraub S, Dickerson BC, Diehl-Schmid J, Pasquier F, Deramecourt V, Lebert F, Pijnenburg Y, Chow TW, Manes F, Grafman J, Cappa SF, Freedman M, Grossman M, Miller BL (2011). Sensitivity of revised diagnostic criteria for the behavioural variant of frontotemporal dementia. *Brain* **134**, 2456–2477.

Reiman EM, Chen K, Liu X, Bandy D, Yu M, Lee W, Ayutyanont N, Keppler J, Reeder SA, Langbaum JBS, Alexander GE, Klunk WE, Mathis CA, Price JC, Aizenstein HJ, DeKosky ST, Caselli RJ (2009). Fibrillar amyloid-beta burden in cognitively normal people at 3 levels of genetic risk for Alzheimer's disease. *Proceedings of the National Academy of Sciences of the United States of America* **106**, 6820–6825.

Reisberg B, Ferris SH, De Leon MJ, Crook T (1982). The global deterioration scale for assessment of primary degenerative dementia. *American Journal of Psychiatry*

Risacher S, Saykin A, Wes J, Shen L, Firpi H, McDonald B (2009). Baseline MRI Predictors of Conversion from MCI to Probable AD in the ADNI Cohort. *Current Alzheimer Research*

Risacher SL, Shen L, West JD, Kim S, McDonald BC, Beckett LA, Harvey DJ, Jack CR, Weiner MW, Saykin AJ (2010). Longitudinal MRI atrophy biomarkers: Relationship to conversion in the ADNI cohort. *Neurobiology of Aging*

Robbins TW, James M, Owen AM, Sahakian BJ, Lawrence AD, Mcinnes L, Rabbitt PMA (1998). A study of performance on tests from the CANTAB battery sensitive to frontal lobe dysfunction in a large sample of normal volunteers : Implications for theories of executive functioning and cognitive aging, 474–490.

Rogaeva E, Meng Y, Lee JH, Gu Y, Kawarai T, Zou F, Katayama T, Baldwin CT, Cheng R, Hasegawa H, Chen F, Shibata N, Lunetta KL, Pardossi-Piquard R, Bohm C, Wakutani Y, Cupples LA, Cuenco KT, Green RC, Pinessi L, Rainero I, Sorbi S, Bruni A, Duara R, Friedland RP, Inzelberg R, Hampe W, Bujo H, Song YQ, Andersen OM, Willnow TE, Graff-Radford N, Petersen RC, Dickson D, Der SD, Fraser PE, Schmitt-Ulms G, Younkin S, Mayeux R, Farrer LA, St. George-Hyslop P (2007). The neuronal sortilin-related receptor SORL1 is genetically associated with Alzheimer disease. *Nature Genetics*

Rohrer JD, Nicholas JM, Cash DM, van Swieten J, Dopper E, Jiskoot L, van Minkelen R, Rombouts SA, Cardoso MJ, Clegg S, Espak M, Mead S, Thomas DL, De Vita E, Masellis M, Black SE, Freedman M, Keren R, MacIntosh BJ, Rogaeva E, Tang-Wai D, Tartaglia MC, Laforce Jr. R, Tagliavini F, Tiraboschi P, Redaelli V, Prioni S, Grisoli M, Borroni B, Padovani A, Galimberti D, Scarpini E, Arighi A, Fumagalli G, Rowe JB, Coyle-Gilchrist I, Graff C, Fallstrom M, Jelic V, Stahlbom AK, Andersson C, Thonberg H, Lilius L, Frisoni GB, Pievani M, Bocchetta M, Benussi L, Ghidoni R, Finger E, Sorbi S, Nacmias B, Lombardi G, Polito C, Warren JD, Ourselin S, Fox NC, Rossor MN (2015). Presymptomatic cognitive and neuroanatomical changes in genetic frontotemporal dementia in the Genetic Frontotemporal dementia Initiative (GENFI) study: a cross-sectional analysis. *Lancet Neurol* **14**, 253–262.

Rolstad S, Berg AI, Bjerke M, Johansson B, Zetterberg H, Wallin A (2013). Cerebrospinal fluid biomarkers mirror rate of cognitive decline. *Journal of Alzheimer's Disease*

Sahara N, Shimojo M, Ono M, Takuwa H, Febo M, Higuchi M, Suhara T (2017). *In vivo tau imaging for a diagnostic platform of tauopathy using the rTg4510 mouse line. Frontiers in Neurology*

Satterthwaite TD, Elliott MA, Gerraty RT, Ruparel K, Loughead J, Calkins ME, Eickhoff SB, Hakonarson H, Gur RC, Gur RE (2013). An improved framework for confound regression and filtering for control of motion artifact in the preprocessing of resting-state functional connectivity data. *Neuroimage* **64**, 240–256.

Scholl M, Lockhart SN, Schonhaut DR, O'Neil JP, Janabi M, Ossenkoppele R, Baker SL, Vogel JW, Faria J, Schwimmer HD, Rabinovici GD, Jagust WJ (2016a). PET Imaging of Tau Deposition in the Aging Human Brain. *Neuron* **89**, 971–82.

Schöll M, Lockhart SN, Schonhaut DR, O'Neil JP, Janabi M, Ossenkoppele R, Baker SL, Vogel JW, Faria J, Schwimmer HD, Rabinovici GD, Jagust WJ (2016). PET Imaging of Tau Deposition in the Aging Human Brain. *Neuron* **89**, 971–982.

Scholl M, Lockhart SN, Schonhaut DR, O'Neil JP, Janabi M, Ossenkoppele R, Baker SL, Vogel JW, Faria J, Schwimmer HD, Rabinovici GD, Jagust WJ (2016b). PET Imaging of Tau Deposition in the Aging Human Brain. *Neuron* **89**, 971–82.

Schöll M, Ossenkoppele R, Strandberg O, Palmqvist S, Jögi J, Ohlsson T, Smith R, Hansson O (2017). Distinct 18F-AV-1451 tau PET retention patterns in early- and late-onset Alzheimer's disease. *Brain*

Schuitemaker A, Kropholler MA, Boellaard R, van der Flier WM, Kloet RW, van der Doef TF, Knol DL, Windhorst AD, Luurtsema G, Barkhof F, Jonker C, Lammertsma AA, Scheltens P, van Berckel BN (2013a). Microglial activation in Alzheimer's disease: an (R)-[(1)(1)C]PK11195 positron emission tomography study. *Neurobiol Aging* **34**, 128–36.

Schuitemaker A, Kropholler MA, Boellaard R, van der Flier WM, Kloet RW, van der Doef TF, Knol DL, Windhorst AD, Luurtsema G, Barkhof F, Jonker C, Lammertsma AA, Scheltens P, van Berckel BN (2013b). Microglial activation in Alzheimer's disease: an (R)-[(1)(1)C]PK11195 positron emission tomography study. *Neurobiol Aging* **34**, 128–36.

Schwarz AJ, Yu P, Miller BB, Shcherbinin S, Dickson J, Navitsky M, Joshi AD, Devous MD, Mintun MS (2016a). Regional profiles of the candidate tau PET ligand 18F-AV-1451 recapitulate key features of Braak histopathological stages. *Brain* **139**, 1539–50.

Schwarz AJ, Yu P, Miller BB, Shcherbinin S, Dickson J, Navitsky M, Joshi AD, Devous MD, Mintun MS (2016b). Regional profiles of the candidate tau PET ligand 18F-AV-1451 recapitulate key features of Braak histopathological stages. *Brain* **139**, 1539–1550.

Schwarz AJ, Yu P, Miller BB, Shcherbinin S, Dickson J, Navitsky M, Joshi AD, Devous MD, Mintun MS (2016c). Regional profiles of the candidate tau PET ligand 18F-AV-1451 recapitulate key features of Braak histopathological stages. *Brain* **139**, 1539–50.

Sebastiani P, Solovieff N, DeWan AT, Walsh KM, Puca A, Hartley SW, Melista E, Andersen S, Dworkis DA, Wilk JB, Myers RH, Steinberg MH, Montano M, Baldwin CT, Hoh J, Perls TT (2012). Genetic signatures of exceptional longevity in humans. *PLoS ONE*

Seeley WW, Crawford RK, Zhou J, Miller BL, Greicius MD (2009). Neurodegenerative Diseases Target Large-Scale Human Brain Networks. *Neuron*

Serrano-Pozo A, Frosch MP, Masliah E, Hyman BT (2011). Neuropathological alterations in Alzheimer disease. *Cold Spring Harb Perspect Med* **1**, a006189.

Shafte MA, Tyler LK, Dixon M, Taylor JR, Rowe JB, Cusack R, Calder AJ, Marslen-Wilson WD, Duncan J, Dalgleish T (2014a). The Cambridge Centre for Ageing and Neuroscience (Cam-CAN) study protocol: a cross-sectional, lifespan, multidisciplinary examination of healthy cognitive ageing. *BMC neurology* **14**, 204.

Shafte MA, Tyler LK, Dixon M, Taylor JR, Rowe JB, Cusack R, Calder AJ, Marslen-Wilson WD, Duncan J, Dalgleish T (2014b). The Cambridge Centre for Ageing and Neuroscience (Cam-CAN) study protocol: a cross-sectional, lifespan, multidisciplinary examination of healthy cognitive ageing. *BMC neurology* **14**, 204.

Shimada H, Suhara T, Shinotoh H, Hirano S, Yamada M, Kimura Y, Sahara N, Zhang MR, Ito H, Kuwabara S, Higuchi M (2016). Clinical significance of tau accumulation assessed by [¹¹C]PBB3 PET in diverse tauopathies. *Molecular Imaging and Biology*

Shirer WR, Ryali S, Rykhlevskaia E, Menon V, Greicius MD (2012a). Decoding subject-driven cognitive states with whole-brain connectivity patterns. *Cerebral cortex* **22**, 158–165.

Shirer WR, Ryali S, Rykhlevskaia E, Menon V, Greicius MD (2012b). Decoding subject-driven cognitive states with whole-brain connectivity patterns. *Cerebral cortex* **22**, 158–165.

Sisodia SS, Koo EH, Beyreuther K, Unterbeck A, Price DL (1990). Evidence that β -amyloid protein in Alzheimer's disease is not derived by normal processing. *Science*

Slachevsky A (2000). The FAB: Frontal Assessment Battery at bedside

Spasov S, Passamonti L, Duggento A, Liò P, Toschi N, Alzheimer's Disease Neuroimaging Initiative (2019). A parameter-efficient deep learning approach to predict conversion from mild cognitive impairment to Alzheimer's disease. *NeuroImage* **189**, 276–287.

Spillantini MG, Bird TD, Ghetti B (1998). Frontotemporal dementia and Parkinsonism linked to chromosome 17: a new group of tauopathies. *Brain pathology (Zurich, Switzerland)* **8**, 387–402.

Spires-Jones TL, Hyman BT (2014). *The Intersection of Amyloid Beta and Tau at Synapses in Alzheimer's Disease*. *Neuron*

Stefaniak J, O'Brien J (2016a). Imaging of neuroinflammation in dementia: a review. *J Neurol Neurosurg Psychiatry* **87**, 21–8.

Stefaniak J, O'Brien J (2016b). Imaging of neuroinflammation in dementia: a review. *J Neurol Neurosurg Psychiatry* **87**, 21–8.

Suridjan I, Pollock BG, Verhoeff NP, Voineskos AN, Chow T, Rusjan PM, Lobaugh NJ, Houle S, Mulsant BH, Mizrahi R (2015). In-vivo imaging of grey and white matter neuroinflammation in Alzheimer's disease: a positron emission tomography study with a novel radioligand, [18F]-FEPPA. *Mol Psychiatry* **20**, 1579–87.

Talakad Lohith, Idriss Bennacef, Zhizhen Zeng, Marie Holahan, Michel Koole, Koen Van Laere, Cyrille Sur, Arie Struyk AW and EH (2016). Preclinical evaluation and first-in-human dosimetry of [18F]MK-6240, a new PET tracer for in vivo quantification of human neurofibrillary tangles. *J Nucl Med*

Thies W, Bleiler L, Alzheimer's Association (2013). Alzheimer's disease facts and figures. *Alzheimer's & Dementia*

Thurfjell L, Lötjönen J, Lundqvist R, Koikkalainen J, Soininen H, Waldemar G, Brooks DJ, Vandenberghe R (2012). Combination of biomarkers: PET [18F]flutemetamol imaging and structural MRI in dementia and mild cognitive impairment. *Neurodegenerative Diseases*

Torralva T, Roca M, Gleichgerrcht E, López P, Manes F (2009). INECO Frontal Screening (IFS): a brief, sensitive, and specific tool to assess executive functions in dementia. *Journal of the International Neuropsychological Society: JINS* **15**, 777–786.

Tsvetanov KA, Henson RNA, Tyler LK, Razi A, Geerligs L, Ham TE, Rowe JB (2016a). Extrinsic and intrinsic brain network connectivity maintains cognition across the lifespan despite accelerated decay of regional brain activation. *Journal of Neuroscience* **36**, 3115–3126.

Tsvetanov KA, Henson RNA, Tyler LK, Razi A, Geerligs L, Ham TE, Rowe JB (2016b). Extrinsic and intrinsic brain network connectivity maintains cognition across the lifespan despite accelerated decay of regional brain activation. *Journal of Neuroscience* **36**, 3115–3126.

Turkheimer FE, Banati RB, Visvikis D, Aston JA, Gunn RN, Cunningham VJ (2000). Modeling dynamic PET-SPECT studies in the wavelet domain. *Journal of Cerebral Blood Flow and Metabolism: Official Journal of the International Society of Cerebral Blood Flow and Metabolism* **20**, 879–893.

Turkheimer FE, Edison P, Pavese N, Roncaroli F, Anderson AN, Hammers A, Gerhard A, Hinz R, Tai YF, Brooks DJ (2007). Reference and target region modeling of [11C]-(R)-PK11195 brain studies. *J Nucl Med* **48**, 158–67.

Uludağ K, Roebroek A (2014). General overview on the merits of multimodal neuroimaging data fusion. *NeuroImage* **102**, 3–10.

in t' Veld BA, Ruitenberg A, Hofman A, Launer LJ, van Duijn CM, Stijnen T, Breteler MM, Stricker BH (2001). Nonsteroidal antiinflammatory drugs and the risk of Alzheimer's disease. *N Engl J Med* **345**, 1515–21.

in 't Veld BA, Ruitenberg A, Hofman A, Launer LJ, van Duijn CM, Stijnen T, Breteler MMB, Stricker BHC (2001). Nonsteroidal Antiinflammatory Drugs and the Risk of Alzheimer's Disease. *New England Journal of Medicine*

Vermeiren C, Motte P, Viot D, Mairet-Coello G, Courade JP, Citron M, Mercier J, Hannestad J, Gillard M (2018). The tau positron-emission tomography tracer AV-1451 binds with similar affinities to tau fibrils and monoamine oxidases. *Movement Disorders*

Villegas-Llerena C, Phillips A, Garcia-Reitboeck P, Hardy J, Pocock JM (2016). Microglial genes regulating neuroinflammation in the progression of Alzheimer's disease. *Curr Opin Neurobiol* **36**, 74–81.

Villemagne VL, Ong K, Mulligan RS, Holl G, Pejoska S, Jones G, O'Keefe G, Ackerman U, Tochon-Danguy H, Chan JG, Reininger CB, Fels L, Putz B, Rohde B, Masters CL, Rowe CC (2011). Amyloid Imaging with 18F-Florbetaben in Alzheimer Disease and Other Dementias. *Journal of Nuclear Medicine*

V.L. V, S. F, M.T. F-T, R.S. M, G. J, O. P, J. H, Y. K, C.L. M, K. Y, C.C. R, N. O (2012). *In vivo tau imaging with PET. Neurobiology of Aging*

Walker MP, Ayre G a., Cummings JL, Wesnes K, McKeith IG, O'Brien JT, Ballard CG (2000). The clinician assessment of fluctuation and the one day fluctuation assessment scale: Two methods to assess fluctuating confusion in dementia. *British Journal of Psychiatry* **177**, 252–256.

Wang MM, Miao D, Cao XP, Tan L, Tan L (2018). Innate immune activation in Alzheimer's disease. *Ann Transl Med* **6**, 177.

Warren JD, Rohrer JD, Hardy J (2012). *Disintegrating Brain Networks: From Syndromes to Molecular Nexopathies. Neuron*

Wedderburn C, Wear H, Brown J, Mason SJ, Barker RA, Hodges J, Williams-Gray C (2008). The utility of the Cambridge Behavioural Inventory in neurodegenerative disease. *Journal of neurology, neurosurgery, and psychiatry* **79**, 500–3.

Weingarten MD, Lockwood AH, Hwo SY, Kirschner MW (1975). A protein factor essential for microtubule assembly. *Proceedings of the National Academy of Sciences of the United States of America*

Whitfield-Gabrieli S, Nieto-Castanon A (2012). Conn: a functional connectivity toolbox for correlated and anticorrelated brain networks. *Brain Connectivity* **2**, 125–141.

Wiley CA, Lopresti BJ, Venneti S, Price J, Klunk WE, DeKosky ST, Mathis CA (2009). Carbon 11-labeled Pittsburgh Compound B and carbon 11-labeled (R)-PK11195 positron emission tomographic imaging in Alzheimer disease. *Arch Neurol* **66**, 60–7.

Wisniewski HM, Barcikowska M, Kida E (1991). Phagocytosis of beta/A4 amyloid fibrils of the neuritic neocortical plaques. *Acta Neuropathol* **81**, 588–90.

Wisse LEM, Butala N, Das SR, Davatzikos C, Dickerson BC, Vaishnavi SN, Yushkevich PA, Wolk DA (2015). Suspected non-AD pathology in mild cognitive impairment. *Neurobiology of Aging*

Xia C-F, Arteaga J, Chen G, Gangadharath U, Gomez LF, Kasi D, Lam C, Liang Q, Liu C, Mocharla VP, Mu F, Sinha A, Su H, Szardenings AK, Walsh JC, Wang E, Yu C, Zhang W, Zhao T, Kolb HC (2013). [(18)F]T807, a novel tau positron emission tomography imaging agent for Alzheimer's disease. *Alzheimer's & dementia : the journal of the Alzheimer's Association* **9**, 666–76.

Xu L, Groth KM, Pearlson G, Schretlen DJ, Calhoun VD (2009). Source-based morphometry: The use of independent component analysis to identify gray matter differences with application to schizophrenia. *Human brain mapping* **30**, 711–724.

Yaqub M, van Berckel BNM, Schuitemaker A, Hinz R, Turkheimer FE, Tomasi G, Lammertsma AA, Boellaard R (2012). Optimization of supervised cluster analysis for extracting reference tissue input curves in (R)-[(11)C]PK11195 brain PET studies. *Journal of Cerebral Blood Flow and Metabolism: Official Journal of the International Society of Cerebral Blood Flow and Metabolism* **32**, 1600–1608.

Yokoi T, Watanabe H, Yamaguchi H, Bagarinao E, Masuda M, Imai K, Ogura A, Ohdake R, Kawabata K, Hara K, Riku Y, Ishigaki S, Katsuno M, Miyao S, Kato K, Naganawa S, Harada R, Okamura N, Yanai K, Yoshida M, Sobue G (2018). Involvement of the Precuneus/Posterior Cingulate Cortex Is Significant for the Development of Alzheimer's Disease: A PET (THK5351, PiB) and Resting fMRI Study. *Frontiers in Aging Neuroscience* **10**

Yokokura M, Terada T, Bunai T, Nakaizumi K, Takebayashi K, Iwata Y, Yoshikawa E, Futatsubashi M, Suzuki K, Mori N, Ouchi Y (2016). Depiction of microglial activation in aging and dementia: Positron emission tomography with [11C]DPA713 versus [11C](R)PK11195. *J Cereb Blood Flow Metab*

Zhang ZG, Li Y, Ng CT, Song YQ (2015). *Inflammation in Alzheimer's Disease and Molecular Genetics: Recent Update. Archivum Immunologiae et Therapiae Experimentalis*